Doctoral Dissertation

High Performance Communication for Future Wireless Ultra-dense Networks

YU YU

Supervisor: Associate Professor Yuto LIM

School of Information Science
Japan Advanced Institute of Science and Technology

March, 2018

Abstract

In the past decade, one remarkable trend is the explosive growth of new generation mobile devices, such as smartphones, tablets and wearable smart devices. Moreover, such smart devices are relentless penetrating our daily life, not only into communication, but also into photography, travel (navigation), entertainment, social network, office working, action payment, safety, health care, etc. To satisfy all these different needs, the fifth generation of wireless system (5G) is under developing, which aims to achieve higher capacity, allows a higher density of mobile broadband users, supports ultra-reliable, low latency and massive machine communication since 2020. Depend on the development of wireless systems, the network is changing from homogeneous network to heterogeneous networks (HetNets), and will inevitably move to ultra-dense networks (UDNs). However, there are several key problems need to be solved in UDNs, such as, how to achieve best energy-efficient; how to manage the wireless interference; and how to success low latency communication in execution. This dissertation investigates the related techniques and 5G protocol protocol stack to fulfill these key capabilities to realize high performance communication for future wireless UDNs.

The purpose of this dissertation is that to propose a high performance dense communication (HPDC) framework by focusing on energy-efficiency, low interference and low latency for wireless ultra-dense networks. The HPDC framework should support the protocol stack of 5G and beyond. Therefore, by using D2D communication, multihop fashion, and multi-RAT techniques, three key schemes, which are dense-aware adaptive transmit power control (DATPC) scheme, dense-aware adaptive carrier sense threshold (DACST) scheme, and dense-aware low-latency communication control (DLLCC) scheme will be proposed for future wireless UDNs. Besides of that, I will also propose some novel components to support these schemes in HPDC framework, such as spectrum sensing scheme, e.g., interference-based sensing, etc.; transmission (spectrum) sharing, e.g., concurrent transmission, sequential transmission, and mix of above two transmissions. More detail work is recalled briefly as below.

A dense-aware adaptive transmit power control (DATPC) scheme is needed to maximize end-to-end throughput with minimized the total interference power and reduce the total energy consumption. The core of the DATPC scheme is consensus transmit power control algorithm. It is the first distributed TPC algorithm that supports multiple flow traffics in D2D communication with multihop fashion for ultra dense situation. This scheme should be implemented into open wireless architecture (OWA) layer for 5G and beyond. Furthermore, based on the proposed DATPC scheme, the link to transmission sharing scheme for maximization also need to be discussed. The advantage of DATPC scheme is that different with centralized control, this is the space-division based distributed control scheme. Thus, DATPC scheme can be easily implemented on any devices.

To enrich DATPC scheme in ultra-dense networks, a dense-aware adaptive carrier sense threshold (DACST) scheme is necessary to achieve better network performance. The DACST scheme should cooperate with DATPC scheme to achieve higher user experienced data rate with dramatic improvements of energy efficiency for UDNs. Similar with DATPC scheme, the DACST scheme should also be implemented into OWA layer and also be linked with network layer. In addition, for the evaluation, not only based on simulation results, emulation results or results of real world test are essential. Thus, an advanced Starmesh emulator over the StarBED testbed is designed to further verify the performance evaluation of the proposed DATPC and DACST schemes. Due to the real devices (hardware specification) used for the emulation level evaluation, DACST scheme might not achieve its best performance. But, on the whole, the evaluation results should prove that the proposed DATPC and DACST schemes do increase the energy-efficiency and mitigate the interference level for UDNs.

Besides, a dense-aware low-latency communication control (DLLCC) scheme is necessary to solve the high latency problem, which is caused by end-to-end retransmission. The DLLCC scheme should be implemented into open transport layer with the function of multipath TPC. In mobile and wireless networks, controlling data delivery latency is one of open problems due to the stochastic nature of wireless channels, which are inherently unreliable. This scheme opens an opportunity to explore how the current best-effort throughput-oriented wireless services could be evolved into latency-sensitive enablers of

new mobile applications such as remote three-dimensional (3D) graphical rendering for interactive virtual/augmented-reality overlay. The general system design is based on (i) spatially diverse data delivery over multiple paths with uncorrelated outage likelihoods; and (ii) forward packet-loss protection (FPP), creating encoding redundancy for proactive recovery of intolerably delayed data without end-to-end retransmissions. Analysis and evaluation are based on traces of real life traffic, which is measured in live carrier-grade long term evolution (LTE) networks and campus WiFi networks, due to no such system/environment yet to verify the importance of spatial diversity and encoding redundancy. Analysis and evaluation reveal the seriousness of the latency problem and that the proposed FPP with spatial diversity and encoding redundancy can minimize the delay of re-ordering. Moreover, a novel FPP effectiveness coefficient is proposed to explicitly represent the effectiveness of FPP implementation.

The proposed HPDC framework is evaluated by simulation in MATLAB, emulation with proposed StarMesh emulator, and using real-world data traffic traces. All of the results indicates that the proposed framework do significantly increase energy efficiency, mitigate the violent interference and achieve low-latency communication for high performance communication.

The main contributions of our work are:

- Identify and revisit the problems of ultra-dense network in near future
- To deal with the dense problem, this dissertation point out three main sub-problems and contribute three different scheme to solve them
  - DATPC scheme operates a distributed manner for WUDNs that takes into account the spatial reuse and reduces the system overhead by sharing information with only adjacent nodes. Moreover, the feasibility and complexity of the DATPC scheme are well-triggered by a novel consensus coefficient.
  - DACST scheme revisits the carrier sense threshold for WUDNs and also enhances a TPC to improve the efficiency and effectiveness of power transmission by maximizing the user experienced data rate for a highly dense indoor environments.
  - DLLCC scheme significantly enables the encoding redundancy for a proactive

recovery of intolerably delayed data. In addition, the spatial diversity creates a novel way for high quality of service provision rather than traditional ACK-based retransmission. This scientific approach can also be applied to the time-critical of CPS and/or IoT applications.

Keywords: High performance communication, ultra-dense networks, dense-aware adaptive transmit power control, consensus transmit power control, dense-aware adaptive carrier sense threshold, dense-aware low-latency communication control, spatial diversity, encoding redundancy

Acknowledgments

First of all, the author takes this opportunity to express most sincere gratitude to his mother, who gives him the life, gives him great love and fully understanding through all these years, which is his strongest motivation to continue his study and pursue his life goals.

The author wishes to express his sincere gratitude to his principal supervisor Associate Professor **Yuto LIM** and Professor **Yasuo TAN** of Japan Advanced Institute of Science and Technology for their constant encouragement, inspiring instruction and patient guidance throughout this research endeavor.

The author also would like to thank Associate Professor **Razvan BEURAN** of Japan Advanced Institute of Science and Technology, who used to be a technical staff at StarBED research center of the National Institute of Information and Communications Technology (NICT), gives him insightful comments on his research. Also thanks to all of the staffs in StarBED, who give him useful knowledge that help him to finish his emulation experiments at StarBED.

The author would like to thank NOKIA® Bell Labs for giving him the opportunity to internship as a researcher, also thanks to Dr. **Stepan KUCERA** for his technical expertise and dedicated support, which help the author to complete his minor research.

The author also would like to express his gratitude to the member of examination committee of his doctoral dissertation, Dr. **Bing Zhang**, of NICT, for his valuable comments and suggestions to improve the quality of this thesis.

In addition, the author would like to express to his gratitude to Fostering ICT Global Leader Course of Japan Advanced Institute of Science and Technology for providing him financial support for this work. Also thanks to Professor **Masato AKAGI** and Professor **Satoshi TOJO** for their technical and financial support.

Last but not least, the author wishes to appreciate all members of "Tan and Lim Lab" for their help and cooperation.

Contents

List of Figures

List of Tables

List of Abbreviations

3D	3 Dimensions
3D-BF	3D-Beamforming
3GPP	3rd Generation Partnership Project
3G	3rd Generation wireless systems
4G	4th Generation wireless systems
5G	5th Generation wireless systems
5G NR	5G New Radio
AAS	Active Antenna System
ACI	Adjacent-Channel Interference
ACK	ACKnowledgment
AODV	Ad hoc On-Demand Distance Vector
APs	Access Points
AR	Augmented Reality
ASE	Area Spectral Efficiency
AWGN	Additive White Gaussian Noise
BS	Base Stations
BTS	Base Transceiver Station
CAGR	Compound Annual Growth Rate
CCI	Co-Channel Interference
CDF	Cumulative Distribution Functions
CDMA	Code Division Multiple Access
CoA	Care of Address
C-RAN	Cloud Radio Access Network
CSMA/CA	Carrier-Sense Multiple Access with Collision Avoidance
CT	Concurrent Transmission

CTPC	Consensus Transmit Power Control
D2D	Device-to-Device
DACST	Dense-aware Adaptive Carrier Sense Threshold
DATPC	Dense-aware Adaptive Transmit Power Control
DASH	Dynamic adaptive streaming over HTTP
DL	DownLink
DLLCC	Dense-aware Low-Latency Communication Control
DR-DC	Device Relaying with Device Controlled
DSSS	Direct-Sequence Spread Spectrum
DTPC	Distributed Transmit Power Control
DTX	Discontinuous Transmission
EE	Energy Efficiency
eMBMS	Evolved Multimedia Broadcast/Multicast Service
EMI	ElectroMagnetic Interference
eNodeB	E-UTRAN node B
FA	Foreign Agent
FBMC	Filterbank Based Multi Carrier
FD	Full Duplex
FDD	Frequency-Division Duplex
FOFDM	Flash Orthogonal Frequency Division Multiplexing
FPP	Forward Packet-loss Protection
FTP	File Transfer Protocol
GB	GigaBytes
GFDM	Generalized Frequency Division Multiplexing
GPS	Global Positioning System
HARQ	Hybrid Automatic Repeat reQuest
HPDC	High Performance Dense Communication
HSPA	High Speed Packet Access
HTTP	HyperText Transfer Protocol

HWMP	Hybrid Wireless Mesh Protocol
ICI	Inter-Carrier Interference
ICIC	Inter-Cell Interference Coordination
ICT	Information and Communication Technology
IDMA	Interleave-Division Multiple Access
IEEE	Institute of Electrical and Electronics Engineers
IETF	Internet Engineering Task Force
IMT	International Mobile Telecommunications
IoT	Internet of Things
IP	Internet Protocol
IPv4	Internet Protocol version 4
IPv6	Internet Protocol version 6
ISI	InterSymbol Interference
IT	Information Technology
JAIST	Japan Advanced Institute of Science and Technology
LDS	Low-Density Spreading
LMA	Local Mean Algorithm
LMST	Local Minimum Spanning Tree
LTE	Long Term Evolution
LTS	Long-Term Support
LWA	LTE WLAN Aggregation
LWIP	LTE WLAN radio level integration with IPsec tunnel
M2M	Machine to Machine
MAC	Media Access Control
MBB	Mobile BroadBand
MBH	Mobile BackHaul
Mbps	Megabits per second
MBSFN	Multimedia Broadcast multicast service Single Frequency Network
MC	MacroCell

MCCH	Multicast Control CHannel
MCS	Modulation and Coding Scheme
MEC	Mobile Edge Computing
MFH	Mobile FrontHaul
MIMO	Multiple-Input Multiple-Output
MMP	Max-Min Power
MS	Mobile Station
MTCH	Multicast Traffic CHannel
MTU	Maximum Transmission Unit
MUD	MultiUser Detection
MU-MIMO	Multiple User MIMO
Multi-RAT	Multiple RAT
MWNs	Multihop Wireless Networks
NAV	Network Allocation Vector
NFV	Network Function Virtualization
NICT	National institute of Information and Communications Technology
OFDM	Orthogonal Frequency-Division Multiplexing
OFDMA	Orthogonal Frequency-Division Multiple Access
OLSR	Optimized Link State Routing Protocol
OSI	Open Systems Interconnection reference model
OTP	Open Transport Protocol
OWA	Open Wireless Architecture
PC	Personal Computer
PDCP	Packet Data Convergence Protocol
PDMA	Pattern Division Multiple Access
PIC	Parallel Interference Cancellation
PR	Proportional faiR
QoE	Quality of Experience
QoS	Quality of Service

RAN	Radio Access Network
RAT	Radio Access Technologies
RH	Radio Head
RLC	Radio Link Control
RR	Round Robin
RRH	Remote Radio Head
RRM	Radio Resource Management
RSSI	Received Signal Strength Indicator
RTT	Round-Trip-Time
SACK	Selective ACKnowledgment
SC	Small Cell
SCMA	Sparse Code Multiple Access
SDN	Software Defined Networking
SIC	Successive Interference Cancellation
SINR	Signal-to-Interference-plus-Noise Ratio
SON	Self Organizing Networks
ST	Sequential Transmission
TCP	Transmission Control Protocol
TDD	Time-Division Duplex
TDMA	Time Division Multiple Access
TPC	Transmit Power Control
WLAN	Wireless Local Area Network
WWRF	World Wide Radio Forum
UDN	Ultra-Dense Networks
UDP	User Datagram Protocol
UDN	Ultra-Dense Networks
UE	User Equipment
UFMC	Universal Filtered Multi-Carrier
UL	UpLink

USB	Universal Serial Bus
VNI	Visual Networking Index
VoIP	Voice over Internet Protocol
VR	Virtual Reality
XCST	miX of Concurrent and Sequential Transmission
XOR	binary eXclusive OR

List of Symbols

Chapter 3 & 4

d_0	reference distance (m)
d_{ij}	distance between node i and node j (m)
α_1	distance power loss coefficient of log-distance pathloss model
W_{ij}	wall attenuation from node i to node j
X_σ	shadowing attenuation
α_2	distance power loss coefficient of ITU pathloss model
L_f	floor penetration loss factor (dB)
w	number of floors between transmitter and receiver
f	frequency (MHz)
G_{ij}	channel gain from node i to node j (dB)
η_j	thermal noise of node j
$SINR_{ij}$	SINR from node i to node j
Γ	value depends on the choice of coding and modulation parameters and the BER requirement
P_i	transmit power of node i (Watt)
P_{max}	maximum transmit power
η_j	thermal noise of node j
$\mathcal{I}$	the set of interfering nodes
$\mathcal{N}$	the set of neighbor nodes
R_{ij}	achievable rate from node i to node j
B	channel bandwidth (Hz)
x	the set of transmitting nodes and relaying nodes
y	the set of receiving nodes and relaying nodes
n	total number of nodes in a network

R^s	shared link rate
M	total number of flows
m	total number of nodes in a flow
$R_{F(z)}$	end-to-end flow rate of of *zth* flow
$U^x_{F(z)}$	user experienced data rate of source node x_z
$\bar{U}$	average user experienced data rate
ψ_i	energy efficiency of node i
ψ	energy efficiency of the overall network
O	target rate for CTPC
C	consensus coefficient
ϕ	network scale coefficient

Chapter 5

δ_{ooo}	delay of out-of-order
L	the number of parallel links
ζ	protection percentage
ρ	link percentage
FE	effectiveness coefficient
R	effective transmission rate
r	payload data rate
D_r	delay of re-ordering
B_d	delayed block size
σ	standard deviation
D_{min}	reduced delay

Chapter 1

Introduction

In the past decade, the field of wireless communications was revolutionary changed, which lead the information technology (IT) to information and communication technology (ICT). One remarkable trend is that the explosive growth of new generation mobile devices such as smart watches, smartphones, and tablets. Moreover, such smart devices are relentless penetrating our daily life, not only into communication, but also into photography, travel (navigation), entertainment, social network, office working, action payment and health. Smart devices will also support other key features such as augmented reality (AR), seamless voice control and three dimensions (3D) screen & holography in near future. However, current wireless and mobile communication technologies such as 3rd generation of wireless systems (3G), long term evolution (LTE) and WiFi can not satisfy those future key features. Thus, the 5th generation of wireless systems (5G) which aims to achieve higher capacity, allow a higher density of mobile broadband users, and support device-to-device, ultra reliable, low latency and massive machine communications since 2020. In this chapter, the future forecast of mobile devices and data traffic, requirements and problems towards and beyond 2020; and some key features of 5G are discussed. For example, ultra-dense network, device-to-device (D2D) communication and multi-radio access technologies (RAT) are introduced. This dissertation focus on three key problems of 5G and beyond wireless systems, especially for future wireless ultra-dense networks, which are energy-efficient communication, low-interference communication and low-latency communication. A stat-of-the-art framework is proposed with three key schemes to solve these problems from Open Wireless Architecture (OWA) layer to Open Transport Protocol

(OTP) layer.

1.1 Future Forecast

1.1.1 The Growing Demand of Mobile Devices and Connections Growth

Cisco® Visual Networking Index (VNI) [1] forecasts some of the major global mobile data traffic projections and growth trends from 2016 to 2021. It also introduces the trends of the mobile network through 2021. Some of the eye-catching trends are listed as follows:

- Monthly global mobile data traffic will be 49 exabytes by 2021, and annual traffic will exceed half a zettabyte (ZB)
- Mobile will represent 20 percent of total Internet Protocol (IP) traffic by 2021
- The number of mobile-connected devices per capita will reach 1.5 by 2021
- The average global mobile connection speed will surpass 20 Mbps by 2021
- The total number of smartphones (including tablets) will be over 50 percent of global devices and connections by 2021
- Smartphones will surpass four-fifths of mobile data traffic (86 percent) by 2021
- 4th generation wireless systems (4G) traffic will be more than three-quarters of the total mobile traffic by 2021
- Over three-fourths (78 percent) of the world's mobile data traffic will be video by 2021

The ever changing mix and growth of wireless devices that are accessing mobile networks worldwide is one of the primary contributors to global mobile traffic growth[1]. In 2016, global mobile devices and connections grew to 8.0 billion. Globally, mobile devices and connections will grow to 11.6 billion by 2021 at a compound annual growth rate (CAGR) of 8 percent (see 1-1). Also, there will be 8.3 billion handhold or personal mobile-ready devices and 3.3 billion M2M connections (e.g., global positioning system

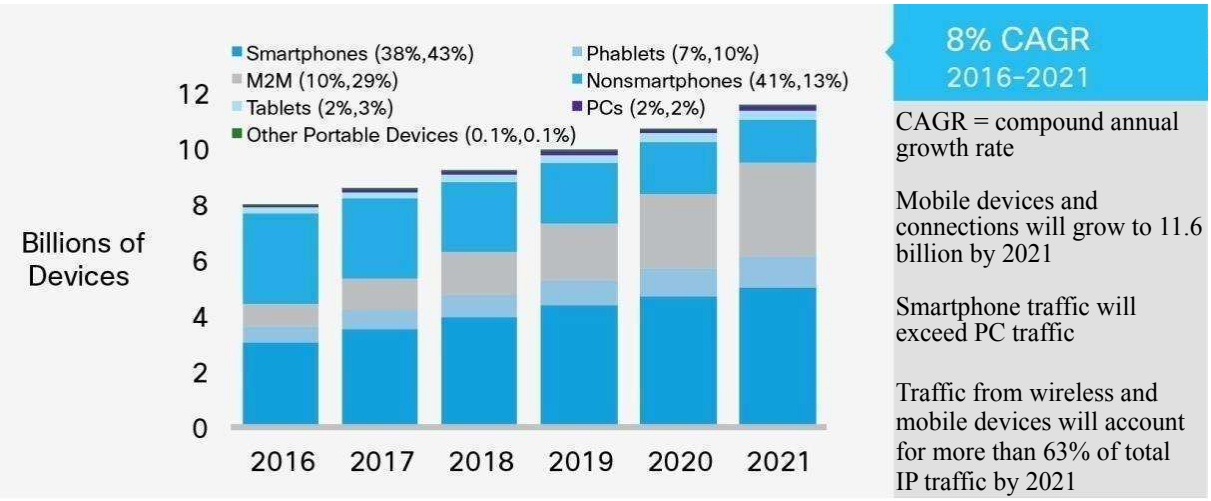

Figure 1-1: Global mobile devices and connections growth from 2016 to 2021

(GPS) in cars, asset tracking systems in shipping and manufacturing sectors, or medical applications making patient records and health status more readily available, etc.) These trends directly change the density of existing wireless networks.

Besides that, global mobile data traffic will increase sevenfold between 2016 and 2021. Smartphone traffic will exceed personal computer (PC) traffic, and mobile network connection speeds will increase threefold by 2021. Thus, 5G will take an important role from 2020. [1] also show that 5G will be 0.2 percent of connections (25 million), but 1.5 percent of total traffic by 2021. 5G connection will generate 4.7 times more traffic than the average 4G connection.

1.1.2 Key Capabilities and Challenges for Future Wireless Networks

Before the introduction of 5G, the requirements towards 2020 should be discussed. [1] shows that the average smartphone will generate 6.8 GB of traffic per month by 2021, a fourfold increase over the 2016 average of 1.6 GB per month. The international mobile telecommunications (IMT) vision [2] also describes growth in traffic, technological trends, potential user and application trends, and spectrum implications to provide guidelines on the framework and the capabilities for IMT of 2020 and beyond. Figure 1-2 illustrates some examples of envisioned usage scenarios for IMT of 2020 and beyond. Basically, it can be divided into three use cases:

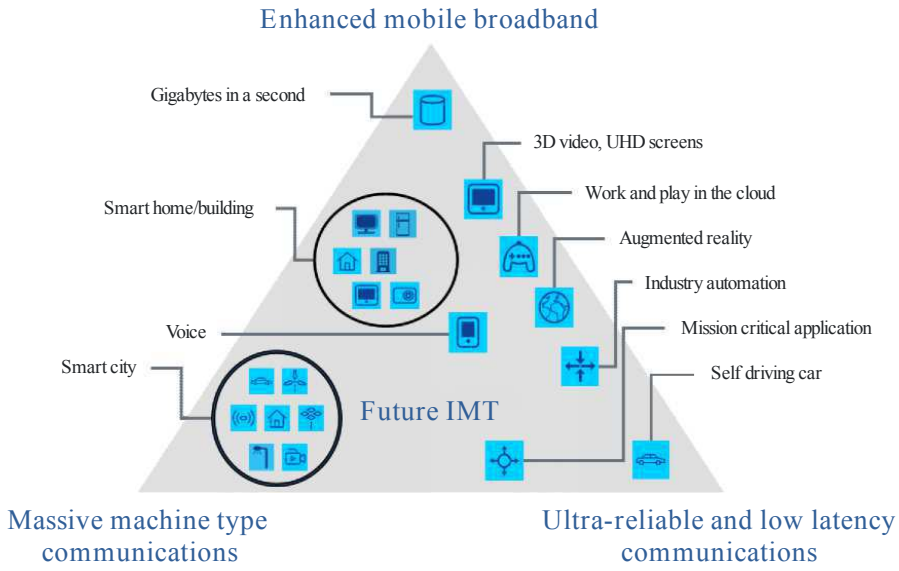

Figure 1-2: Usage scenarios of IMT for 2020 and beyond

- Enhanced Mobile Broadband

  Mobile Broadband addresses the human-centric use cases for access to multi-media content, services and data. This use case will come with new application areas and requirements in addition to existing Mobile Broadband applications for improved performance and an increasingly seamless user experience. For example, for an area with high user density, very high traffic capacity is needed, while the requirement for mobility is low, such as 8K, 3D holography, AR, etc.

- Ultra-reliable and low latency communications

  This use case has stringent requirements for capabilities such as throughput, latency and availability to satisfy low transmission error and low round-trip-time (RTT). Some examples include wireless control of industrial manufacturing or production processes, remote medical surgery, distribution automation in a smart grid, self-driving, transportation safety, etc.

- Massive machine type communications

  This use case is characterized by a very large number of connected devices typically transmitting a relatively low volume of non-delay-sensitive data. Devices are required to be low cost, and have a very long battery life. This is the infrastructure of Internet of Things (IoT).

Figure 1-3 illustrated eight parameters of key capabilities and the importance of each

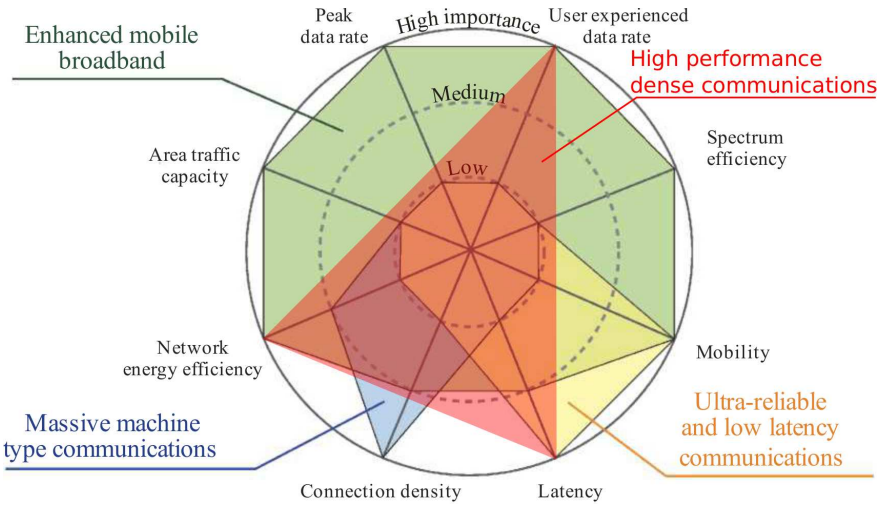

Figure 1-3: The importance of key capabilities in different usage scenarios

key capabilities for the above three use cases by using an indicative scaling in three steps as "high", "medium" and "low". ITU-R introduced the importance of each key capability for the usage scenarios "enhanced Mobile Broadband", "ultra-reliable and low latency communication", and "massive machine-type communication".

In this dissertation, our focus is on future wireless ultra-dense networks. As we known, wireless end users put more emphasis on its experienced data rate rather than peak data rate or area traffic capacity. Due to most of the wireless devices are battery-based equipments, the energy consumption or EE is another key impact factor. Besides, latency is also key impact factor for high quality of experience (QoE). Thus, following these vital requirements of an end user, the novel high performance dense communication (red triangle parts in Fig. 1-3) is defined as the basic capabilities for the future wireless UDNs. The challenge here is that how to trade-off the satisfying above key capabilities and growing cost. Also the efficiency, scalability and diversity will become the key design criteria [3]. These key capabilities and challenges are continuously encouraging industry, research and standardization organizations to move forward with high momentum to the new revolution of 5G.

1.1.3 5G Wireless System

Before we introduce 5G, first, let us review the mobile wireless systems from 1G to 5G with their features (see Table 1.1).

5G is viewed for providing communication and data services using all possible access

solutions and core network switching rather than a new radio access technology. As shown in Figure 1-3, 5G aims to achieve higher capacity, allow higher density of mobile broadband users and support device-to-device, ultra reliable, and massive machine communications [3]. The key technologies to achieve key capabilities are list as follows:

- Enhanced air interface technology
  - Filtered orthogonal frequency division multiplexing (FOFDM) [4]
  - Filter bank based multi carrier modulation (FBMC) [5]
  - Pattern division multiple access (PDMA) [6]
  - Sparse code multiple access (SCMA) [7]
  - Interleave-division multiple access (IDMA) [8]
  - Low-density spreading (LDS) [9]
  - 3D-beamforming (3D-BF)[10]
  - Active antenna system (AAS) [11]
  - Massive multiple-input multiple-output (MIMO) [12]
  - Network MIMO [13]
  - Time-division duplex (TDD) - Frequency-division duplex (FDD) cooperation
- Network layer technology
  - Software defined networking (SDN) [14]
  - Network function virtualization (NFV) [15]
  - Cloud radio access network (C-RAN) [16]
  - Self organizing networks (SON) [17]
- Enhanced mobile broadband technology
  - Multihop or D2D
  - Small cell (SC) [18]
  - Dynamic adaptive streaming over HTTP (DASH) [19]

  - Evolved multimedia broadcast/multicast service (eMBMS) [20]

- Technology to enhance the communication of a large scale of devices
  - Machine to machine (M2M) [21]

- High reliability and low latency communication technology
  - Universal filtered multi-carrier (UFMC) [22]
  - Generalized frequency division multiplexing (GFDM) [23]
  - Multi-RAT
  - Network Coding

- Network energy efficiency technology
  - Power control
  - Interference management
  - Discontinuous transmission (DTX)

- Terminal technology
  - Full duplex (FD)
  - improvements of chip, battery, and display

- Privacy and security technology

- Rate improvement technology
  - Carrier aggregation
  - IMT-WLAN
  - Advanced physical layer techniques
  - Network densification

1.2 Research Problems and Motivations

Among these techniques in 5G, this dissertation investigates the potential ways to achieve high performance dense communication for future wireless ultra-dense networks. The high performance dense communication includes three parts of problems to solve, which includes energy-efficient, low interference, and low latency communication. The intention is to find the research-based knowledge for the possibility of practical implementation in near future wireless technologies.

1.2.1 Research Problem

As we mentioned, to achieve high performance communication for future wireless networks for end users, the 5G technologies should satisfy all kinds of real social scenarios. However, ITU only defined three usage scenarios. These would solve most of the usage for mobility, sparse and usual environments. For dense environment, there is no research try to solve the issues to achieve high performance communication (see Fig. 1-4). This dissertation give brightly definition of future wireless ultra-dense networks, and list all of the issues to achieve high performance dense communication. These will be introduced in the following subsections.

1.2.2 Vision of Future Wireless Ultra-dense Networks

ABI research concludes that "more than 80% of all traffic originating or terminating indoors", and anticipates in-building mobile data traffic to grow by more than 600% by 2020, which means will reach 53 exabytes per month worldwide in 2020. Users will expect a satisfactory end-user experience in the presence of a large number of concurrent users, for example in a crowd with a high traffic density per unit area and a large number of handsets and machines/devices per unit area. Examples are audio-visual content to be provided concurrently across an entire cell or infotainment applications in shopping malls, stadiums, open air festivals, or other public events that attract a lot of people. This includes users who use their phone while in unexpected traffic jams, or when traveling in public transportation systems, as well as professionals working in organizations such as police, fire brigades, and ambulances to exploit the public communication networks

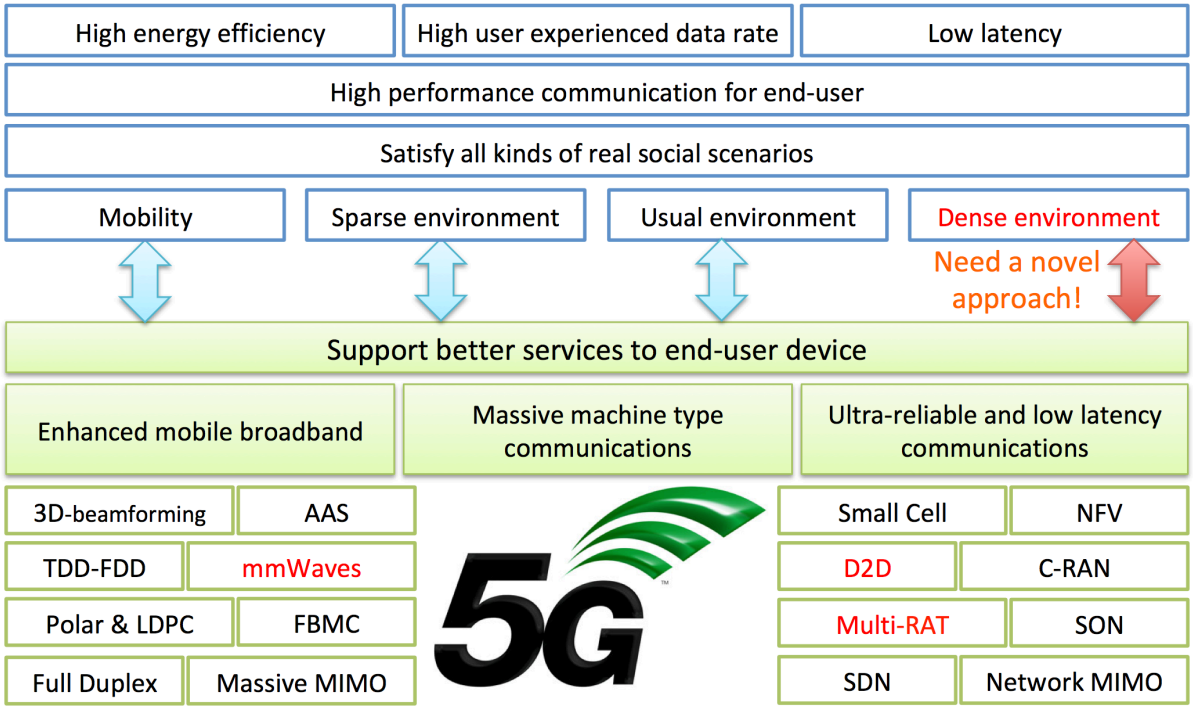

Figure 1-4: Novel approach is necessary for the future wireless networks

in crowded environments and machine-centric devices. To solve this problem with scarce spectrum resources, the only way is to improve the spectrum reuse per unit area. With this high level spectrum reuse, the network density will increase beyond imagination.

Ultra-dense Networks (UDNs) address the high traffic demands via infrastructure densification. UDNs are orders of magnitude denser than today, assuming, for instance, several access nodes per room indoors and an access node on each lamppost outdoors, which of course raises severe interference and mobility challenges, and increased pressure on cost per access node. Ultra-Dense Networks can be defined as those networks where there are more cells than active users [24–26]. In other words, the density of access points is much greater than the density of users. Another definition of UDNs was solely given in terms of the cell density, irrespective of the users density. Ding et al. [27] provided a quantitative measure of the density at which a network can be considered ultra-dense ($\geq 10^3$ cells/km2). For the future wireless UDNs, these kind of definition of UDNs is not accurate because too much focus on cells. With the D2D communication, the devices should also be recognized as density factor. However, the network densification cannot continue endlessly.

In this dissertation, the more appropriate definition of UDNs from the user point

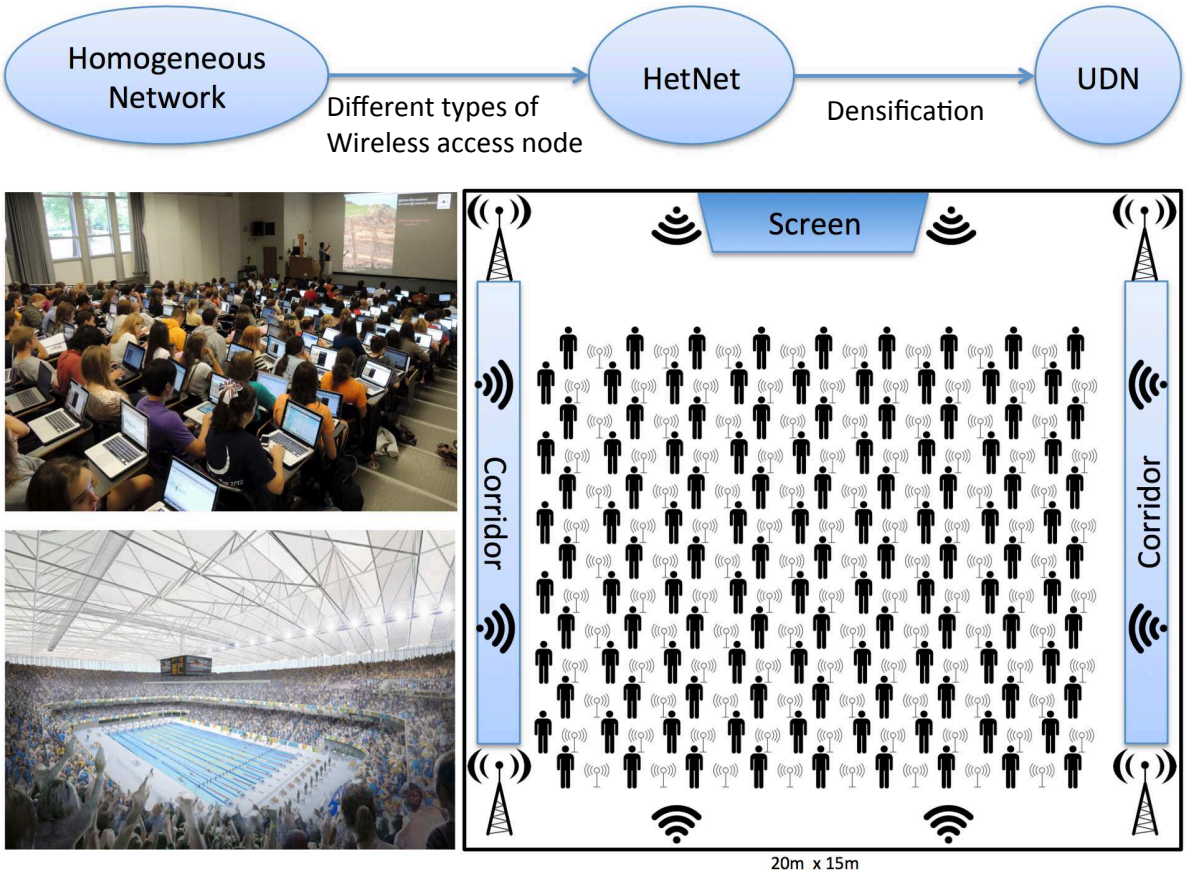

Figure 1-5: An example of future wireless ultra-dense network for indoor environment

of view is described. Let the distance between every two wireless devices, e.g., APs, UEs, etc., is λ. If $0.1 \leq \lambda \leq 10$ in meters, then the network environment is recognized as UDNs, similar to the defination on [28]. Here, the value "0.1 meter" represents the minimum distance between two devices. The value "10 meters" is an average value that is calculated as the average density of wireless devices in the metropolis such as Tokyo, Shanghai, or New York, etc. Figure 1-5 is an example of future wireless ultra-dense network for indoor environment.

The key research issues in future wireless UDNs are list as follows:

- Energy-efficient communication issue
- Interference management issue
- Spectrum sharing issue
- Resource management issue
- User association issue

Three key research issues will be discussed respectively in the following subsections.

1.2.3 Energy-efficient Communication

With the explosive growth of traffic, wireless applications and mobile data connections with high demand for QoS, more energy is consumed in ICT. As depicted in Figure 1-6, almost 5% of the total worldwide electricity consumption is consumed in ICT at 2012 and will increase with lower to 4% and higher to 10% CAGR [29]. Vary with the increasing electricity consumption, there is still a great gap with battery technologies.

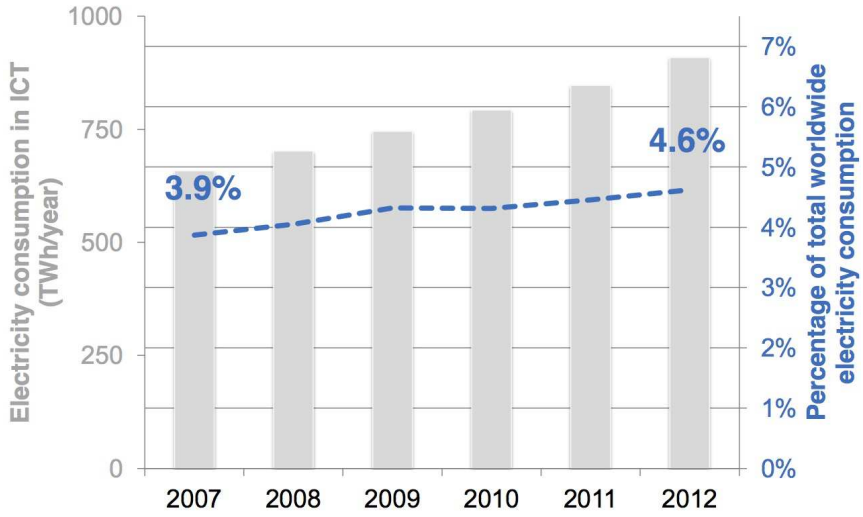

Figure 1-6: Electricity consumption in ICT and Percentage of total worldwide electricity consumption

Therefore, energy-efficient communication have been paid increasing attention under the background of limited energy resource and environmental-friendly transmission behaviors [30]. The definition of energy efficiency (EE) of the network is defined as the ratio between the total network throughput and the total network power consumption[31]. [32] numerically showed that there is an unavoidable network energy requirements when network getting dense by the cell size. As the network will become ultra-dense wireless network, which means the access points is greater than the number of UE, the major energy consumption component will be the idling and backhauling power, as UE itself in the D2D communication networks.

The requirements of EE is that to achieve $10^3\times$ traffic increase with half electricity consumption by today. In order to enhance the requirements, energy consumption should

be considered in the protocol design in medium access control (MAC) layer, or in OWA layer for 5G. The energy efficiency of a network can be improved by both reducing RF transmit power and saving circuit power. If a sleep mode is introduced, the energy-efficient can be further enhanced. To enhance energy efficiency, the traffic variation characteristic of different users should be well exploited for adaptive resource management. Examples include discontinuous transmission (DTX), base station and antenna muting, and traffic balancing among Multi-RAT. In this dissertation, an transmit power control algorithm on OWA layer is introduced to solve the bottleneck problem in multihop fashion ultra-dense D2D communication networks and strongly improve the energy efficiency ratio.

1.2.4 Interference Management

The definition of interference in wireless network is that interference is anything that modifies, or disrupts a signal as it travels along a channel between a transmitter and a receiver. It can be classified as follows:

- Electromagnetic interference (EMI), disturbance that affects an electrical circuit due to either electromagnetic induction or electromagnetic radiation emitted from an external source
- Co-channel interference (CCI), also known as crosstalk, is from two different radio transmitters using the same frequency
- Adjacent-channel interference (ACI), interference caused by extraneous power from a signal in an adjacent channel
- Intersymbol interference (ISI), distortion of a signal in which one symbol interferes with subsequent symbols
- Inter-carrier interference (ICI), caused by doppler shift in OFDM modulation

Interference is identified as one of the major bottlenecks limiting the throughput in a wireless system. Unlike the wired medium, the broadcast and multiple-access nature of the wireless medium ensures that every transmitter is heard by every neighboring receiver. The signal transmitted by a user is interference to all the neighboring users who operate on the same frequency spectrum. Since our objective is to support large numbers of users

with multihop D2D communication while providing the highest possible data rates using limited spectrum in UDNs, the interference level rise dramatically. it is imperative that we understand the best ways to handle interference in wireless networks.

For the interference management, one kind of the key technologies is inter-cell interference coordination (ICIC) techniques. ICIC present a solution by applying restrictions to the radio resource management (RRM) block, improving favorable channel conditions across subsets of users that are severely impacted by the interference, and thus attaining high spectral efficiency. However, inter-cell coordination increase the overhead in UDNs, thus, non-centralized control which means distributed control is preferred to solve our research issues. In the current market, technologies such as WiFi or Bluetooth provide some D2D communication functionality. However, these work in unlicensed band, and the interference is uncontrollable. Thus, an distributed interference management is necessary for each device in UDNs. In this dissertation, we propose an adaptive RSSI management scheme with spatial reuse to management the interference and additionally lead great improvement of the EE and network throughput.

1.2.5 Low-latency Communication

The requirement of low-latency and high reliable communications is an important emerging area which current wireless technologies cannot support. Basically, low-latency communication can be divided into two parts, user-centric and machine-centric communication. For user-centric communication, users expect the experience of instantaneous connectivity wherein applications need to exhibit "flash" behavior without waiting times: a single click and the response is perceived as instantaneous, such as a few millisecond (ms). This requirement cannot be achieved by the current 4G technology. Flash behavior will be a key factor for the success of cloud services, virtual reality (VR) and AR applications. The low latency and high reliability communication that supports such behavior thus becomes an enabler for the future development of new applications, e.g. in e-health, safety, office, entertainment, and other sectors. On another hand, the design of new applications for machine-centric communication is envisaged based on M2M communication with real-time constraints. For example, real-time traffic control optimization, emergency and disaster response, smart grid, efficient industrial communications, etc.

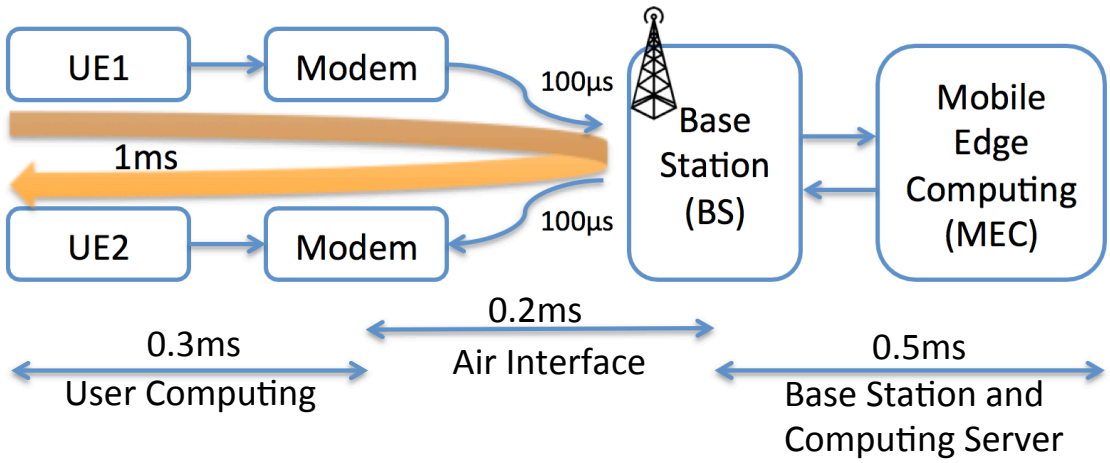

Figure 1-7: Latency budget of communication between two UE

The requirement of network latency in 5G is less than 1ms for the end-to-end communication [2]. In order to achieve this requirement, it is necessary to analyze the whole chain between the end points in the networks. As depicted in Figure 1-7, a possible latency budget of communication between two user equipment (UE) is provided. The UE data is provided to the embedded system that controls the air interface, the the data passes through the UE protocol stack, the terminal and base station's physical layer, the base station's protocol stack, eventually the Mobile edge computing (MEC) [33] processing stack and then goes back through the same reverse chain. As we know, the MEC can greatly reduced the latency than UE communicate with the core network. However, most of the time is still used between base station and mobile edge computing server (0.5ms in Figure 1-7). When the long distance communication occurs, the intolerable latency is also occur between the base station to core network parts. Thus, if some of the packets is lost or delayed during this period, retransmission is the only way to achieve reliable communication. However, under Multi-RAT in 5G, which means the user can communicate with multiple access network (LTE, WiFi, etc.), an new low latency communication scheme based on spatial diversity and encoding redundancy is proposed on open transport protocol (OTP) layer in this dissertation.

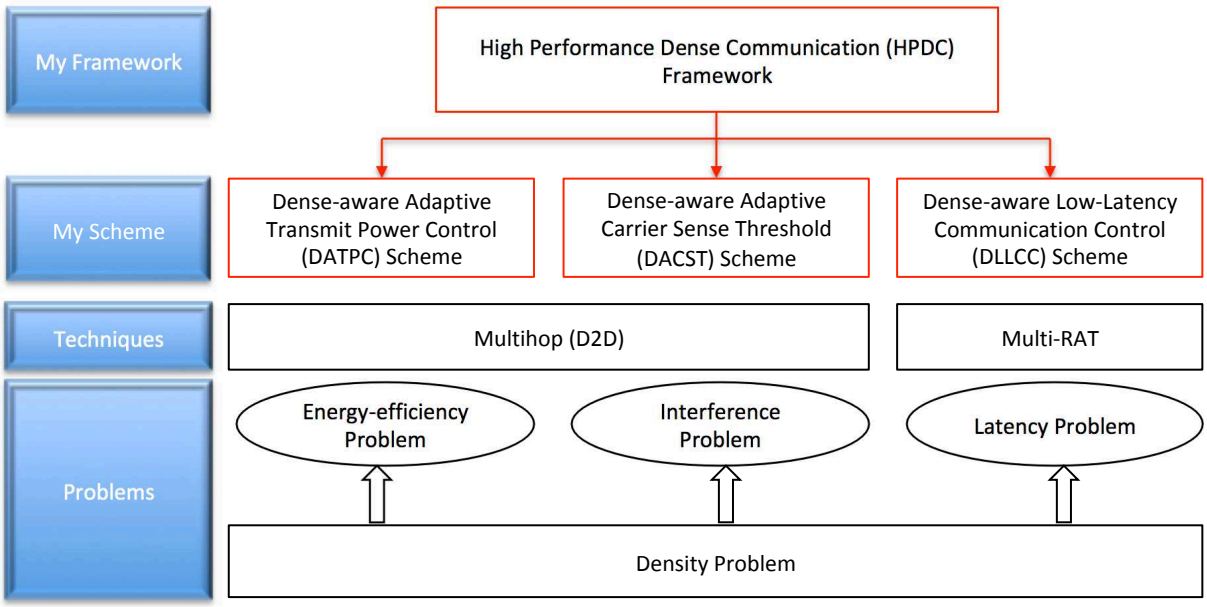

Figure 1-8: Proposed conceptual framework for future wireless ultra-dense networks

1.3 Dissertation Vision and Objectives

The vision of this research is to realize a high performance communication for future ultra-dense wireless network.

To accomplish this vision, the author proposes a high performance dense communication framework by focusing on energy-efficient, low interference and low latency for ultra-dense wireless network (see Fig. 1-8).

The research objectives are summarized as follows:

- To present a dense-aware adaptive transmit power control scheme (DATPC) for energy-efficient communication problem between open wireless architecture (OWA) and lower network layer (Material related to this objective appears in published papers [3], [8], [9], [11] and in an as yet unpublished paper [2])
- To propose a dense-aware adaptive carrier sense threshold scheme (DACST) for low interference management problem between OWA and lower network layer (Material related to this objective appears in published papers [6], [7], [10] and in an as yet unpublished paper [2])
- To introduce a dense-aware low-latency communication control scheme (DLLCC)

which includes spatial diversity and encoding redundancy approaches, to solve the low latency communication problems in open transport protocol layer (Material related to this objective appears in published papers [1], [4])

1.4 Structure of the Dissertation

The remainder of this dissertation is organized as follows:

- Chapter 2. High Performance Dense Communication Framework
  In Chapter 2, some of the key technologies for the future wireless networks, especially for ultra-dense networks will be introduced. To propose the high performance dense communication framework, the 5G protocol stack is also be analyzed. Follow the protocol stack, two components, which are spectrum sensing and spectrum sharing, are introduced for the proposed framework. At the end of chapter 2, the overview of proposed high performance dense communication framework is explained.

- Chapter 3. Dense-aware Adaptive Transmit Power Control Scheme
  The proposed DATPC scheme that incorporates consensus transmit power control (CTPC) algorithm with full concurrent transmission to maximize end-to-end throughput, minimize the total interference power and reduce the total energy consumption is described in this chapter. Based on the DATPC, the spectrum sharing scheme is also be analyzed through simulation.

- Chapter 4. Dense-aware Adaptive Carrier Sense Threshold Scheme
  In Chapter 4, a dense-aware adaptive carrier sense threshold (DACST) scheme is proposed, which incorporates proposed realistic interference model and auto CST fallback algorithm. Through changing the CST, the network topology would be optimized, DATPC scheme would achieve better performance. In addition, an advanced StarMesh emulator over the StarBED testbed is used to further verify the performance evaluation of the proposed DATPC and DACST schemes.

- Chapter 5. Dense-aware Low-Latency Communication Control Scheme
  The dense-aware low-latency communication control (DLLCC) scheme in LTE and WiFi using spatial diversity and encoding redundancy is discussed in Chapter 5. The

general scheme design is based on (i) spatially diverse data delivery over multiple paths with uncorrelated outage likelihoods; and (ii) forward packet-loss protection (FPP), creating encoding redundancy for proactive recovery of intolerably delayed data without end-to-end retransmissions.

- Chapter 6. Conclusion and Future Work

  Chapter 6 summarizes the dissertation and draws some future trends.

Table 1.1: Main features from 1G to 5G

Technology	**1G**	**2G/2.5G**	**3G**	**4G**	**5G**
Deployment	1970/1984	1980/1999	1990/2002	2000/2010	2014/2015
Bandwidth	2 Kbps	14 – 64 Kbps	2 Mbps	200 Mbps	> 1Gbps
Technology	Analog Cellular	Digital Cellular	Broadband CDMA/IP Technology	Unified IP and Seamless Combination of LAN/ WAN/ WLAN/ PAN	4G +WWWW
Service	Mobile telephony	Digital voice, short messaging	Integrated high quality audio, video and data	Dynamic information access variable devices	Dynamic information access, variable devices with AI capabilities
Multiplexing	FDMA	TDMA CDMA	CDMA	CDMA	CDMA
Switching	Circuit	Circuit for access network and air interface	Packet except for air interface	All packet	All packet
Core Network	PSTN	PSTN	Packet Network	Internet	Internet
Handoff	Horizontal	Horizontal	Horizontal	Horizontal and Vertical	Horizontal and Vertical

Chapter 2

High Performance Dense Communication (HPDC) Framework

2.1 Introduction

In this chapter, some of the key technologies for the future wireless networks, especially for ultra-dense networks will be introduced. To propose the high performance dense communication framework, the 5G protocol stack is also be analyzed. Follow the protocol stack, two components, which are spectrum sensing and spectrum sharing, are introduced for the proposed framework. At the end of this chapter, the overview of proposed high performance dense communication framework is explained.

2.2 Related Key Technologies for the proposed HPDC

In this dissertation, we only focus on several kinds of new technologies which are changing the current network evolution (see Fig. 1-8), which are device-to-device (D2D) communication, multihop wireless networks and Multi-radio Access Technologies (RAT).

2.2.1 D2D Communication

Due to the scare spectrum resource, spectrum reuse per unit are became the core issue to improve the rate outage. Two efficient technologies are small cell under the cellular netowrk and D2D communication to efficiently reuse spectrum resources. Different with

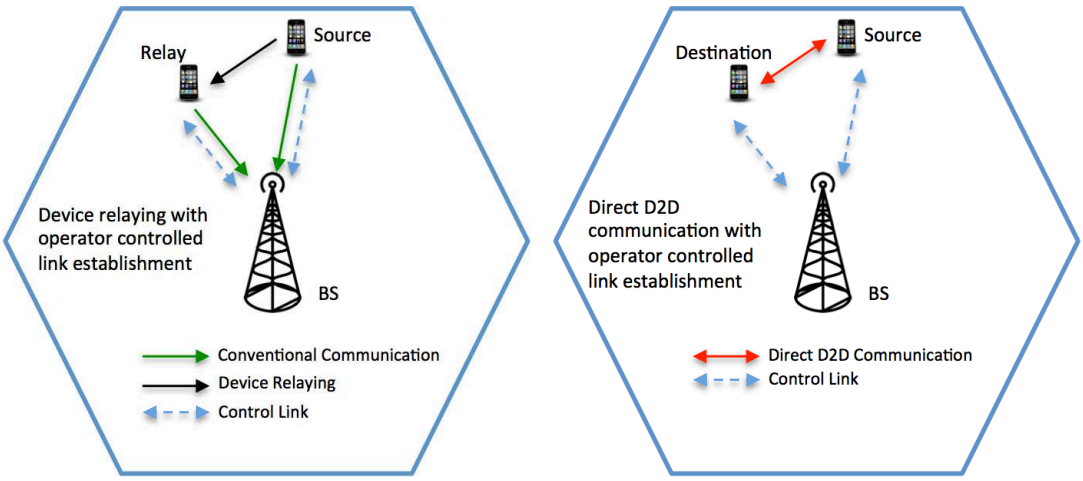

(a) DR-OC (b) DC-OC

Figure 2-1: Device relaying D2D communication

small cell ways, D2D communication is a new paradigm in wireless communication where two nearby devices can direct establish a connection with a minimal intervention of the network [34]. D2D communication can be classified into four main types [35], device relaying D2D communication (see Figure 2-1), and device controlled D2D (see Figure 2-2). These devices are said to be in the device tier because the device connects directly to another or realizes its transmission through the assistance of other device. Also, the D2D communication can be implemented in both licensed bandwidth and unlicensed bandwidth. The difference between them is not only on that who is take charge of create the control link, but also on security and quality of service (QoS). In this research, we mainly focus on the device controlled D2D communication, especially in device relaying with device controlled link establishment (DR-DC) type (see Figure 2-2(a))

There are lots of benefits with D2D communications. For the operators, there are significant performance gains in link reliability, spectral efficiency, system capacity, transmission coverage, and also can reduce the cost significantly. For the end users, it can reduce the power consumption, increased the throughput, and discovery neighboring activities efficiently. Furthermore, D2D communication can be of critical use in natural disasters. In an earthquake or hurricane, an urgent communication network can be set up using D2D functionality in a short time, replacing the damaged communication network and Internet infrastructure.

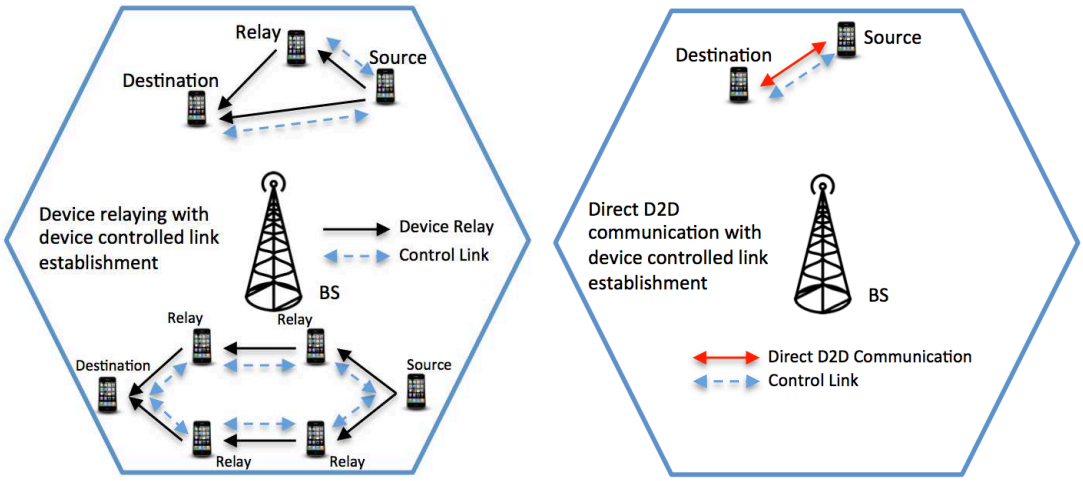

(a) DR-DC (b) DC-DC

Figure 2-2: Device controlled D2D communication

2.2.2 Multihop Wireless Networks

Multihop Wireless Networks (MWNs) is a network of computers or other electronic equipments that are connected by wireless communication links. The difference between MWNs and traditional wireless networks is that all the nodes work cooperatively to send the packets to its destination in MWNs. That means a node will send packets to a neighbor node that it can communicate directly (see Figure 2-3). The neighbor node, in its turn, forwards the packets to one of its neighbor nodes and keeps on [36]. This process terminates when the packet reaches its ultimate destination. Each link over which packets are sent is referred to as a hop; the set of links is called path, which is discovered by using a distributed routing algorithm; and the particular characteristic of transmission is called multihop fashion. Due to the multihop fashion, MWNs is introduced as a promising approach for next generation wireless networks to enable cooperative and self-organized communication, even with the absence of infrastructure. Some examples of this architecture are the ad-hoc mode architecture of 802.11, mobile ad hoc networks, wireless multihop network of 802.11, wireless sensor networks, wireless mesh network, vehicular ad hoc networks and D2D communication with multihop fashion.

MWNs also have many challenges. For example, due to the unreliable wireless links, packet loss and dynamic topology, how to determine the routing protocol for sending packets to the intended destination is one of the main challenges. The routing protocol Famous routing protocol such as optimized link state routing protocol (OLSR), Ad hoc on-

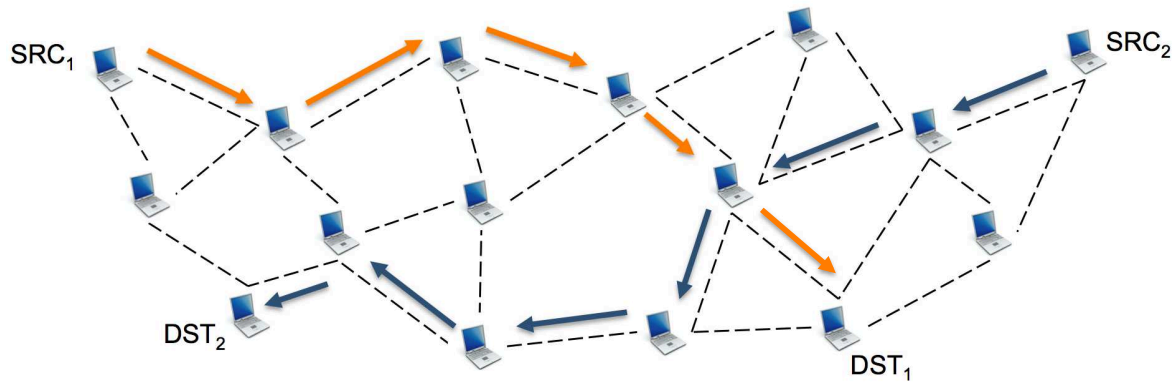

Figure 2-3: An example of multihop wireless networks

demand distance vector (AODV), hybrid wireless mesh protocol (HWMP), etc. Another problem is that the level of congestion at an intermediate node may become an important issue. Because of the location, the intermediate nodes may have high change to relay the others' data packets. In this case, the power consumption of this node is higher than others, also the buffer overflow occurs more frequently. Thus, a power management based routing protocol is necessary.

2.2.3 Multi-RAT

Multi-RAT refers to the coordination between different RATs to provide a high QoS to the end users. With mobile broadband (MBB) growth and evolution of the network, the network is becoming dense and complex, each site can be up to seven bands spectrum, five modes (GSM/UMTS/LTE-FDD/TD-LTE/WiFi), and five layers network architecture (Low-frequency macro coverage layer/high-frequency capacity layer/hotspot Micro capacity layer/indoor Pico layer/WiFi hotspots) [37]. If lack of effective coordination, it cannot effectively use all of the wireless network resources and cannot guarantee user experience. Thus, it can be concluded as the competition between different radio access technologies has come to an end [38] and the cooperation stems as a vital solution beyond the 2020, 5G wireless world. Figure 2-4 shows a typical multi-connectivity deployment scenario for a UE with different 5G radio interfaces (wide area, mmWaves, cmWaves), WLAN, LTE, and WiMAX. We also compared the LTE, 5G and WLAN features in Table 2.1.

Meanwhile, intelligent terminals, pads and other types of UEs spread quickly, and

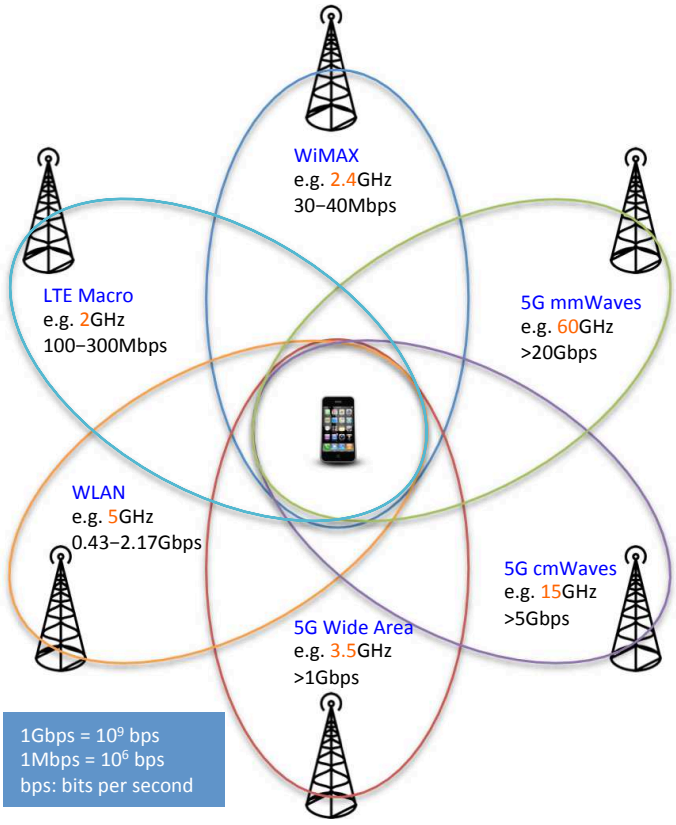

Figure 2-4: Typical Multi-RAT deployment scenario beyond 2020

the service types of MBB increase rapidly. In such a multi-layer/multi-band/multi-mode wireless network, a question on how to improve the utilization efficiency of radio resources, to guarantee quality of experience (QoE) of MBB service, to simplify multi-RAT network management, is a huge challenge of the Single-RAN.

The associated strict performance requirements of the 5G [39] necessitate the exploitation of every single resource. Correspondingly, the abundance of WiFi nodes with comparable rates to the current cellular technology inspires many collaboration techniques where the delay intolerance traffic can be offloaded to the WiFi layer [40]. The RAT selection algorithms and the offloading mechanisms are of a key importance to the fruition of this paradigm [41]. Also, the mobility of the flows across cellular and WiFi access points is challenging, however active investigations are in progress [38, 42, 43]. Moreover, the splitting of data across multiple flows in Multi-RAT has emerged as another challenge. Furthermore, the simultaneous connection to access nodes of different RAT stems as a viable offloading alternative, while different flows with different QoS requirements are carried by the cellular cells or the WiFi access nodes [44].

Table 2.1: Comparison among different RAT

	LTE	**5G**	**WLAN**
Spectrum	Licensed	Licensed	Unlicensed
Multiple	Scheduled	Scheduled (Contention free)	Random access (contention based)
QoS support	Mobile broadband, interactive	Mobile broadband, interactive, ultra-reliable, low latency	Best effort
Carrier frequencies	Below 3.5GHz	Variable, up to mmWave (70GHz)	Below 6GHz
Typical radio deployment	Macro	Small cell, macro	Unplanned small cell
ARPU category	Medium to high	Low to high	Low
Mobility support	Full	Full	Restricted

2.3 5G Network Architecture and Protocol Stack

2.3.1 5G Network Architecture Concept

Figure. 2-5 shows the concept of 5G network architecture. Basically, it has three parts, which are core network, mobile backhaul (MBH) and mobile fronthaul (MFH) [45]. For this research, our focus is mainly about the mobile fronthaul. In Fig. 2-5, there is a radio head (RH) in the MFH. Under RH, there are four remote radio head (RRH). The RH can be recognized as macro-cell base station, and the RRH can be recognized as small cell or pico-cell base station. For macro-cell base station, the range is under 2 kilometers. For small cell or pico-cell base station, the range is normally under hundreds of meters. Under the RRH, there are UEs. Our focus is more on the ultra-dense situation, which can be seen as the UEs or RRH with red shadow. The distance between these UEs are normally less than 10 meters. Also, the number in one RRH is much greater than usual case. In the daily life, this environment can be recognized as classroom, meeting room, stadium, etc.

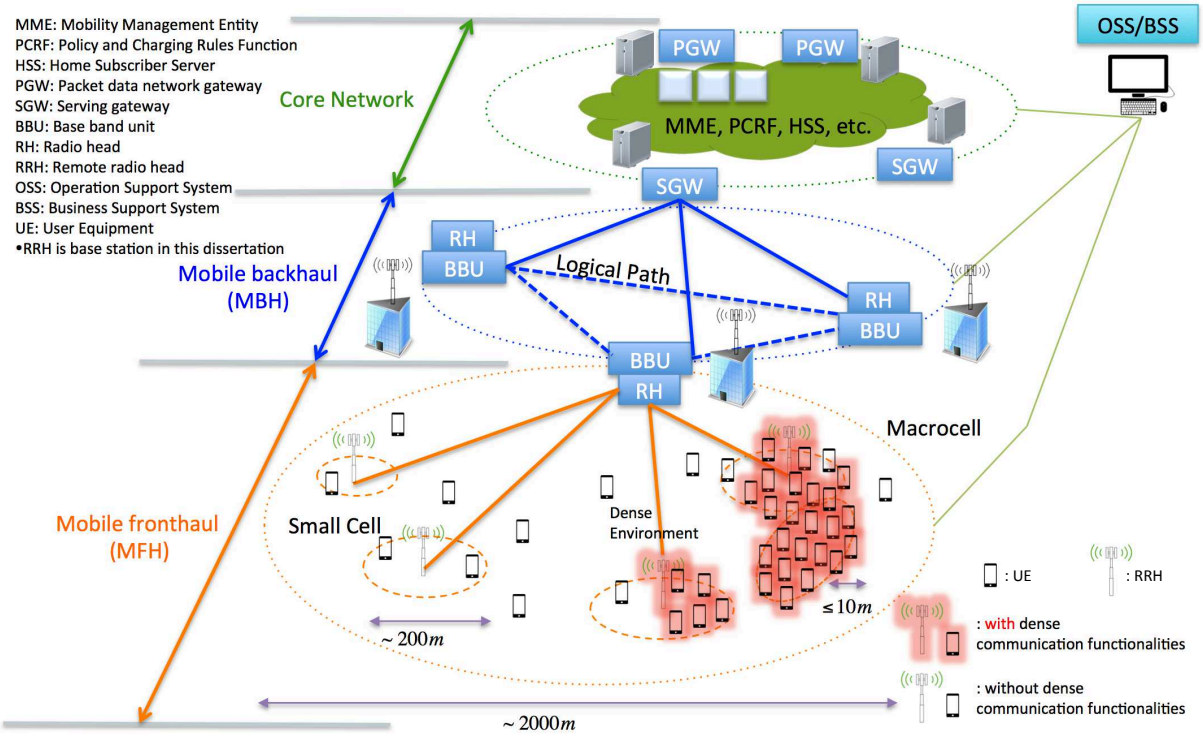

Figure 2-5: 5G network architecture concept

The deployment cost of proposed framework should not cost much, but the implementation of the proposed framework could presumably cost a little more in terms of CPU and memory. The transmit power and carrier sense threshold need to be modified, and the range of them should be extended. These modifications are only performed at the end devices and cooperated RRH. There is no need to do any modification on the mobile backhaul and core network.

2.3.2 5G Protocol Stack

The mobile devices under 5G would have software defined radios and modulation schemes as well as new error-control schemes that can be downloaded from the Internet [46]. The development is seen towards the terminal devices as a focus of the 5G mobile networks. The terminal devices would have access to different wireless technologies at the same time and the devices should be able to combine different flows from different technologies. The vertical handovers should be avoided, because they are not feasible in a case when there are many technologies and many operators and service providers. In 5G, each network will be responsible for handling user-mobility, while the terminal devices would make the

final choice among different wireless or mobile access network providers for a given service [47]. Such choice would be based on open intelligent middle-ware in the mobile phone.

As shown in Figure 2-6, we compared the protocol stack among Open system interconnection reference model (OSI) [48], TCP/IP [49], and 5G.

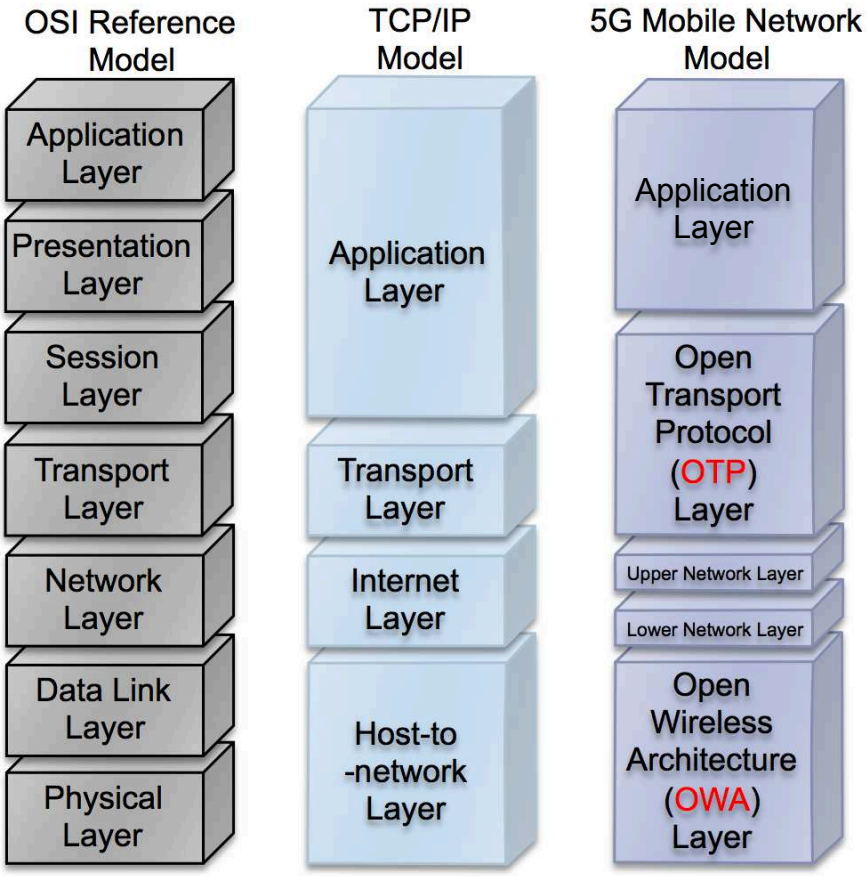

Figure 2-6: Protocol stack for OSI, TCP/IP, and 5G

Open wireless architecture (OWA) Layer

The OWA layer of 5G mobile model, it has the same functions with OSI layer 1 – physical layer and OSI layer 2 – Medium access control (MAC) layer [50]. For TCP/IP, OWA is equal to the host-to-network layer.

Network Layer

The network layer will be Internet Protocol (IP) layer, because there is no competition today on this level. The IP version 4 (IPv4) is worldwide spread and it has several problems such as limited address space and has no real possibility for QoS support per

flow. These issues are solved in IPv6, but traded with significantly bigger packet header. Then, mobility still remains a problem. There is Mobile IP standard on one side as well as many micro-mobility solutions (e.g., Cellular IP, HAWAII etc.). All mobile networks will use Mobile IP in 5G, and each mobile terminal will be Foreign Agent (FA), keeping the Care of Address (CoA) mapping between its fixed IPv6 address and CoA address for the current wireless network. However, a mobile can be attached to several mobile or wireless networks at the same time. In such case, it will maintain different IP addresses for each of the radio interfaces, while each of these IP addresses will be CoA address for the FA placed in the mobile Phone. The fixed IPv6 will be implemented in the mobile phone by 5G phone manufactures.

The 5G mobile phone shall maintain virtual multi-wireless network environment. For this purpose there should be separation of network layer into two sub-layers in 5G mobiles (see Figure 2-6), i.e., Lower network layer (for each interface) and Upper network layer (for the mobile terminal). This is due to the initial design of the Internet, where all the routing is based on IP addresses which should be different in each IP network world wide. The middle-ware between the Upper and Lower network layers shall maintain address translation from Upper network address (IPv6) to different Lower network IP addresses (IPv4 or IPv6), and vice versa.

Open Transport Protocol (OTP) Layer

The OTP layer has the same function of session layer and transport layer of OSI reference model or parts of application layer and transport layer of TCP/IP model.

The mobile and wireless networks differ from wired networks regarding the transport layer. In all TCP versions the assumption is that lost segments are due to network congestion, while in wireless networks losses may occur due to higher bit error ratio in the radio interface. Therefore, TCP modifications and adaptation are proposed for the mobile and wireless networks, which re-transmit the lost or damaged TCP segments over the wireless link only. For 5G mobile terminal devices will be suitable to have transport layer that is possible to be downloaded and installed. Such mobiles shall have the possibility to download (e.g., TCP, UDP, etc. or new transport protocol) version which is targeted to a specific wireless technology installed at the base stations. This is the reason to be

called as open transport protocol.

Application Layer

The application layer of 5G model is equal to the application layer and presentation layer of OSI reference model, or just contains part of current application layer of TCP/IP model.

Regarding the applications, the ultimate request from the 5G mobile terminal is to provide intelligent QoS management over variety of networks. Today, in mobile phones the users manually select the wireless interface for particular Internet service without having the possibility to use QoS history to select the best wireless connection for a given service. The 5G phone shall provide possibility for service quality testing and storage of measurement information in information databases in the mobile terminal. The QoS parameters, such as delay, jitter, losses, bandwidth, or reliability, will be stored in a database in the 5G mobile phone with aim to be used by intelligent algorithms running in the mobile terminal as system processes, which at the end shall provide the best wireless connection upon required QoS and personal cost constraints.

In the future wireless networks there must be a low complexity of implementation and an efficient means of negotiation between the end users and the wireless infrastructure. The Internet is the driving force for higher data rates and high speed access for mobile wireless users. This will be the motivation for an all mobile IP based core network evolution.

2.4 Spectrum Sensing

The goal of spectrum sensing is to determine the status of the spectrum and the activity of the users by periodically sensing the target frequency band. The objective of spectrum sensing is to detect the presence of transmissions from licensed users [51].

Spectrum sensing can be either centralized or distributed. In centralized spectrum sensing, a sensing controller (e.g. access point or base station) senses the target frequency band, and the information thus obtained is shared with other nodes in the system. Centralized spectrum sensing can reduce the complexity of terminal devices, since all the sensing functions are performed at the sensing controller. However, centralized spectrum

sensing suffers from location diversity. In distributed spectrum sharing, unlicensed users perform spectrum sensing independently, and the spectrum sensing results can be either used by individual cognitive radios (i.e. non-cooperative sensing) or shared with other users (i.e. cooperative sensing) [51].

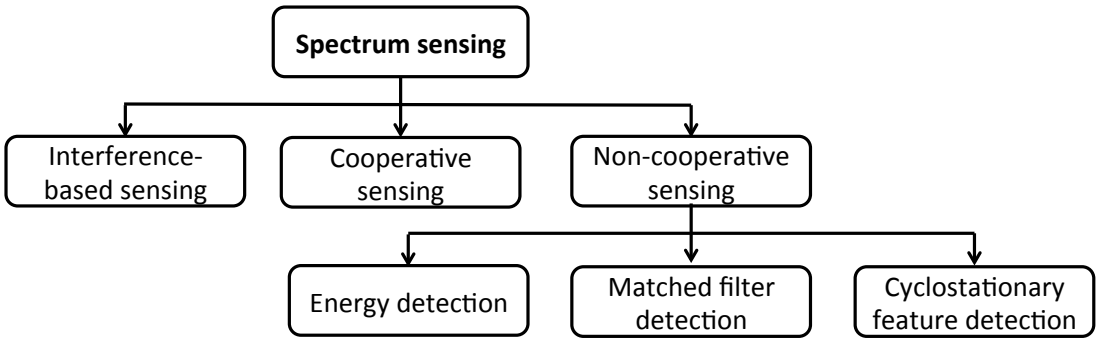

Figure 2-7: Different types of spectrum sensing in the OWA layer

There are three major types of spectrum sensing, namely, non-cooperative sensing, cooperative sensing, and interference-based sensing (see Figure 2-7).

2.4.1 Interference-based Sensing

In this case, the sensing algorithm will measure the noise/interference level (from all sources of signals) at the receiver of the licensed user. This information is used by an unlicensed user to control the spectrum access (e.g. by computing expected interference level) without violating the interference temperature limit. Spectrum analysis is required for the characterization of different spectrum bands in terms of operating frequency, bandwidth, interference, primary user activity, and channel capacity. For example, in the spectrum underlay approach, based on the interference temperature limit at the primary receiver and operating frequency, the permissible transmission power at the cognitive radio can be determined.

A primary medium access control problem for a cognitive radio is the spectrum decision, which deals with the decision of transmission. Spectrum decision takes into account the fact that spectrum sensing could be erroneous. In case of transmission, it considers what modulation and power level to use, how to share the spectrum holes among cognitive radios. Spectrum decisions can be made based on either a local or a global optimization criterion. In case of local optimization, the spectrum access decision is made

in a non-cooperative (i.e. distributed) way and, game theory is a powerful tool to analyze the spectrum sharing problem in a non-cooperative (i.e. competitive) spectrum access scenario.

2.4.2 Cooperative sensing

In cooperative sensing, spectrum sensing information from multiple unlicensed users are exchanged among each other to detect the presence of licensed users. The cooperative spectrum sensing architecture can be either centralized or distributed. Using cooperative exchange of spectrum sensing information, the hidden node problem can be solved and the detection probability can be significantly improved in a heavily shadowed environment. However, this incurs a greater communication and computation overhead compared with non-cooperative sensing.

2.4.3 Non-cooperative sensing

Non-cooperative spectrum sensing is used by an unlicensed user to detect the transmitted signal from a licensed user by using local measurements and local observations. The model for signal detection at time t can be described as

$$x(t) = \begin{cases} n(t), & H_0, \\ h * s(t) + n(t), & H_1 \end{cases}$$

where $x(t)$ is the received signal of an unlicensed user, $s(t)$ is the transmitted signal of the licensed user, $n(t)$ is the additive white Gaussian noise (AWGN), and h is the channel gain. H_0 and H_1 are defined as the hypotheses of not having and having a signal from a licensed user in the target frequency band, respectively.

The three different methods in non-cooperative sensing are as follows:

- *Matched filter detection or coherent detection:* Matched filter detection is generally used to detect a signal by comparing a known signal with the input signal. A matched filter will maximize the received SNR for the measured signal. Therefore, if the information of the signal from a licensed user is known (e.g. modulation and

packet format), a matched filter is an optimal detector in stationary Gaussian noise.

- *Transmitter energy detection:* In the case of energy detection, the output signal from a bandpass filter is squared and integrated over the observation interval. A decision algorithm compares the integrator output with a threshold to decide whether a licensed user exists or not. In general, the energy detection performance deteriorates when the SNR decreases. Therefore, energy detection is susceptible to the uncertainty of noise power, and can only detect the presence of the signal but cannot differentiate the type of signal (e.g. signals from secondary users sharing the same channel with the primary user).

- *Cyclostationary feature detection:* A signal is cyclostationary if the autocorrelation is a periodic function. With this periodic pattern, the transmitted signal from a licensed user can be distinguished from noise, which is a wide-sense stationary signal without correlation. In general, cyclostationary detection can provide a more accurate sensing result and it is robust to variations in noise power.

In order to improve the overall performance of spectrum sensing, multiple detection methods can be integrated in a single unlicensed system.

2.5 Spectrum Sharing (Transmission Sharing)

Access to shared and unlicensed spectrum will extend 5G in multiple dimensions - such as more capacity, higher spectrum utilization, new deployment scenarios. It will benefit mobile operators with licensed spectrum but also opens the doors to those without licensed spectrum – such as cable operators, enterprise or IoT verticals – to take advantage of the 5G New Radio (5G NR) family of technologies [52]. 5G NR is designed to natively support all spectrum types and, through forward compatibility, has the flexibility to take advantage of new spectrum sharing paradigms. This creates opportunities for new innovation to take spectrum sharing to the next level in 5G.

The key spectrum sharing technologies are list as follows [53]:

- Spectrum aggregation (LTE-U/LAA)

- Radio Aggregation (LWA(LTE+WiFi))

- Tiered sharing (CBRS, LSA)
- Standalone Unlicensed (MulteFire)

Besides of these technologies, we also proposed three transmission sharing technologies for high performance communication. We introduce them into the follow subsections.

2.5.1 Concurrent Transmission (CT)

Concurrent transmission is a form of transmission in which several transmissions are executed during overlapping time periods – concurrently – instead of sequentially (one completing before the next starts). Assuming massive MIMO and full duplex technologies are used, multiple transmissions would be on transmitting at the same time.

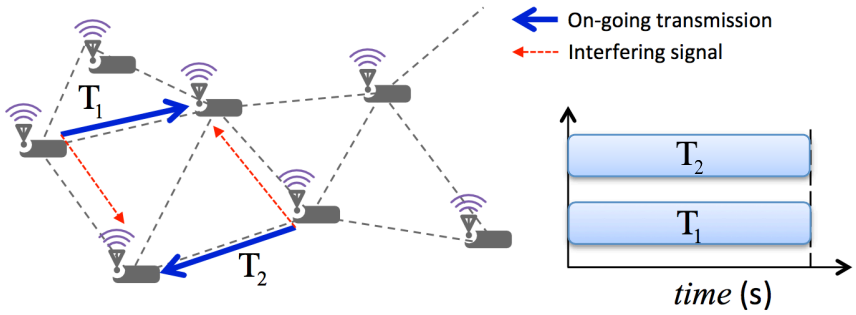

Figure 2-8: An Example of a concurrent transmission

As shown in Figure 2-8, concurrent transmission T_1 and T_2 exist and they are on-going at the same time. The problem of concurrent transmission is the interference issue. In the figure, the blue thick arrows represent the on-going signal, meantime, the transmitting nodes also disrupt the other nodes that are not their receivers (the red thin arrows). In UDN, the interference is rapidly increase because they are near with each other. On the other hand, if the network is sparse, which mean the distance between any two devices is not near, thus, the concurrent communication would lead significant throughput growth.

2.5.2 Sequential Transmission (ST)

Sequential transmission is a form of transmission in which several transmissions are executed sequentially. It is similar to the time-division multiple access (TDMA), which is a channel access method for shared medium netowrks that allows several users to share the

same frequency channel by dividing the signal into different time slots. The TDMA and sequential transmission is quite different. TDMA dividing the signal into different time slots for all of the potential transmitting nodes, even some of them not transmit all the time. However, sequential transmission is a kind of scheduling method that only support the current transmitting nodes to transmit their data packets sequentially.

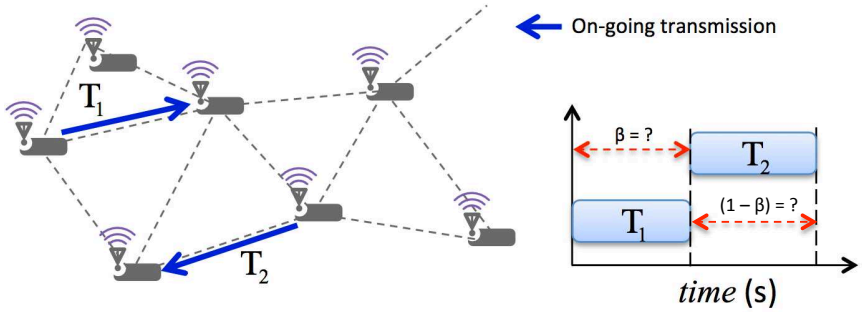

Figure 2-9: An Example of a sequential transmission

In this case, there is no interference between nodes because at one time slot, only one transmitter is transmit data packets, the rest nodes are keep silent, which means no transmission. As shown in Figure 2-9, T_1 and T_2 are transmit in different time slots. The problem here is that how to optimally balance the transmissions? Simply the problem, what is the best value of β to reach the optimization network capacity?

2.5.3 Mix of Concurrent and Sequential Transmission (XCST)

For the above transmission methods, they have their advantages and disadvantages respectively. In this subsection, we propose a transmission method namely mix of concurrent and sequential transmission to take the advantages of both concurrent transmission and sequential transmission to achieve the optimal network capacity.

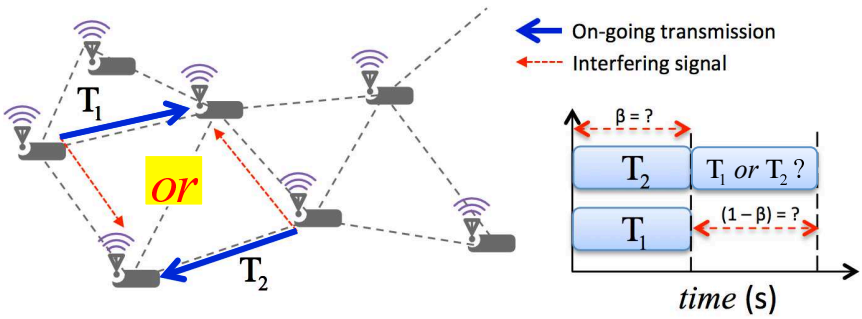

Figure 2-10: An Example of a mix of concurrent and sequential transmission

As shown in Figure 3-17, concurrent and sequential are combined to maximize the capacity at the give time slot [54]. Here, how to calculate the best value of β and who takes more time slots for the transmission would be the key issues for the optimization.

2.6 High Performance Dense Communication (HPDC) Framework

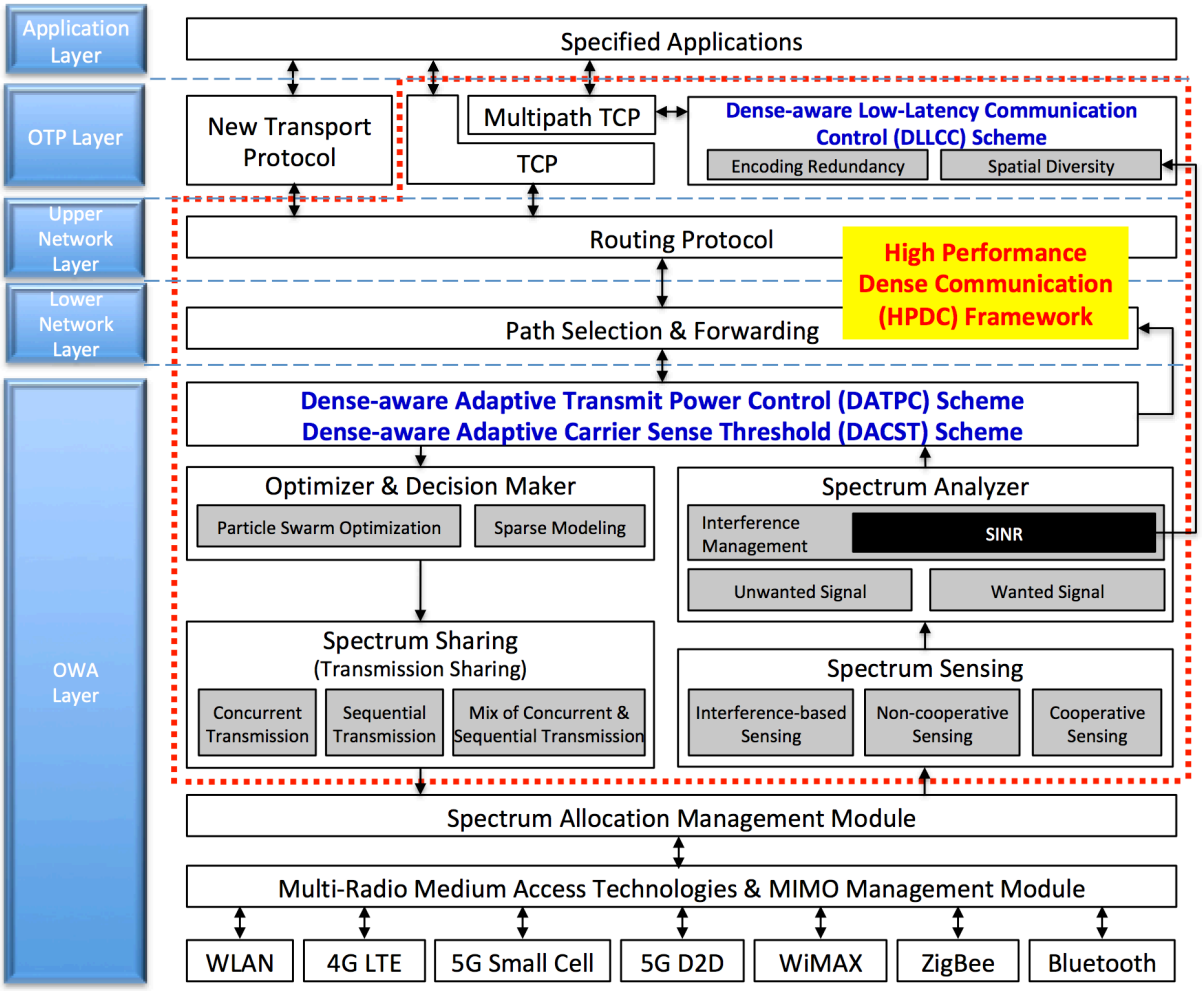

Figure 2-11: Block diagram of HPDC framework

A conceptual framework is developed for high performance communication in future wireless ultra-dense networks. In the near future, no technology will be able to provide alone the high demand of fast and reliable communication due to the very high increasing requirements of wireless and industrial communication. The network should be flexible in integration to work with other technologies. This framework is conceptualized based

on the combination of the future potential network technologies such as D2D, MWN, and Multi-RAT to support the new requirements. This framework is an important concept aiming for the future 5G because it depicts very core parts of future wireless networks to be able to provide the high-rate with low-energy, low interference, low latency, and high reliable services to future wireless devices and machines. This framework is called high performance dense communication (HPDC) framework for future wireless ultra-dense networks. The block diagram of HPDC is shown in Figure 2-11.

As shown in Figure 2-11, the red dotted line is the proposed framework under the latest 5G protocol stack. We already introduced the spectrum sensing scheme and spectrum sharing scheme in this chapter. The rest parts are introduced in follow chapters. This framework represents three scheme to achieve the requirements of high performance communication. They are dense-aware adaptive transmit power control scheme, dense-aware adaptive carrier sense threshold scheme, and dense-aware low-latency communication control scheme.

2.6.1 Dense-aware adaptive transmit power control scheme

A dense-aware adaptive transmit power control scheme is proposed for high user experienced data rate with low energy consumption at the OWA layer. This scheme exploits the benefit of transmit power control as an opportunity for energy efficient operation. Moreover, the scheme combines the spectrum analyzer scheme, optimizer and decision maker scheme and spectrum sharing scheme to increase the user experienced data rate and optimize the whole network capacity with low energy consumption.

2.6.2 Dense-aware adaptive carrier sense threshold scheme

We extend our work with a dense-aware adaptive carrier sense threshold scheme to achieve low interference in ultra-dense networks. The proposed DACST scheme works between the OWA layer and network layer. This scheme exploits the benefit of CST as an opportunity for topology control and interference management operation because only change the transmit power is not enough for the ultra-dense networks. The proposed DACST scheme can reduce the interference to lead significant user experienced data rate improvement. Moreover, the scheme combines the spectrum analyzer scheme (spatial reuse part), opti-

mizer and decision maker scheme and path selection and forwarding scheme to increase the network capacity and with low interference level.

2.6.3 Dense-aware low-latency communication control scheme

Only the high data rate and high energy efficiency can not satisfies all of the requirements of high performance communication for future wireless ultra-dense networks. Low latency and high reliable communication is another key issues. Thus, a dense-aware low-latency communication control scheme is proposed to achieve low latency communication at OTP layer. Multi-RAT and multipath TPC are the trend of future wireless network, under this situation, how to use these technologies to achieve low latency is an interest research issues. We proposed spatial diversity and encoding redundancy approaches to achieve low latency. Moreover, an novel forward packet-loss protection effectiveness coefficient is proposed to explicitly represent the effectiveness of the implementation.

2.6.4 Assumptions and Constraints

Here are some assumptions listed as follows for the proposed HPDC framework.

- 5G existing protocol stack can be integrated with minimum modification
- Spectrum from different wireless technologies can be used
- The range of transmit power and carrier sense threshold must be extended
  - Carrier sense threshold : minimum maintain -96 dBm, maximum from -65 dBm to -30 dBm
  - Transmit power: minimum from -1 dBm to -40 dBm, maximum maintain 23 dBm

Also, there are three constraints are listed as follows:

- Low mobility only (dense environment does not allow high mobility)
- Device with below 4G technology cannot be used
- Device with static transmit power and carrier sense threshold cannot be used

Besides, the proposed HPDC framework can be implemented on both UEs and BSs. Channel allocation, routing protocol, and security are beyond the scope of this dissertation.

2.7 Summary

This chapter presents some key technologies for the future wireless networks, especially for ultra-dense networks. To propose the high performance dense communication framework, we analyzed the 5G architecture and protocol stack. Follow the stack, we introduced two components of the framework, which are spectrum sensing and spectrum sharing. The proposed HPDC framework with three key schemes are also described in this chapter.

Chapter 3

Dense-aware Adaptive Transmit Power Control Scheme

In this chapter, we propose a dense-aware adaptive transmit power control (DATPC) scheme that incorporates consensus transmit power control (CTPC) algorithm with concurrent transmission to maximize user experienced data rate, minimize the total interference power and reduce the total energy consumption. As we know, the key factor of influencing the network capacity performance is the effect of interference power of receiving nodes, which is obtained from the other transmitting nodes in D2D communication network with multihop fashion or in MWNs that are simultaneously using the same channel. Minimizing total interference power can improve overall network capacity and reduce total energy consumption. The user experienced data rate, totol energy consumption, interference level and energy-efficient ratio are the main metrics for the performance evaluation. We set up a simulation to further analyze the performance of these scheme by some scenarios which include the varying number of nodes and flows. Based on the DATPC, the spectrum sharing scheme uses mix of concurrent and sequential transmission can provides a better average capacity. Moreover, the ITU pathloss model [55] is used for 60 GHz frequency for ultra-dense networks.

3.1 Problem Statement

Recently, the number of wireless devices has increased tremendously. In 2009, the world wide radio forum (WWRF) offered a vision for future wireless communication called, “7 trillion wireless devices serving 7 billion people by 2017" [56]. As a result of 7 trillion wireless devices, wireless network is the real ubiquitous network around our daily life. However, most wireless communication devices, such as laptops, tablet PCs and smart-phones, are battery-based equipments. Therefore, one very important issue for these devices is the reduction of the energy consumption.

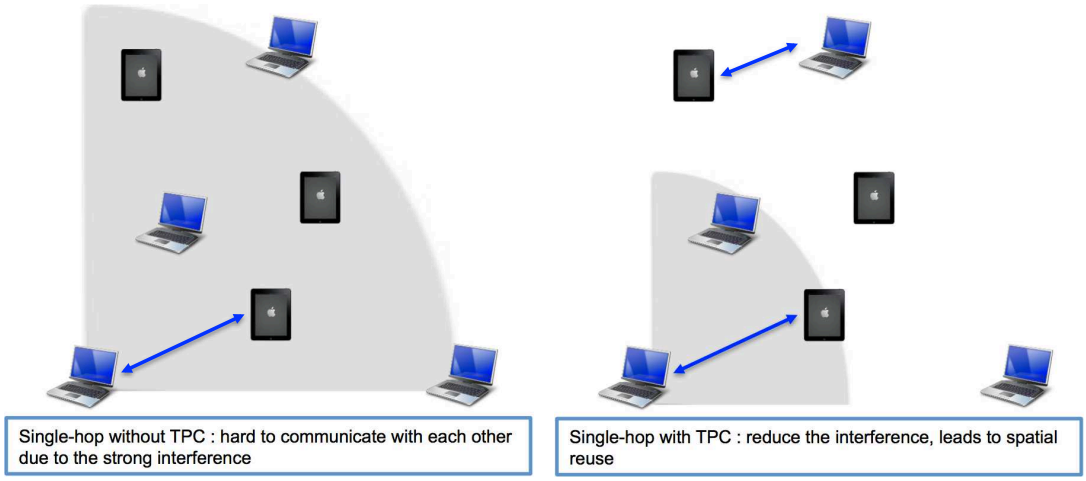

(a) High transmit power with wide transmission range

(b) Low transmit power with Simultaneous communication

Figure 3-1: Transmit power control can active more simultaneous communication links

Wireless devices normally are battery dependent with low radio frequency power, therefore the communication range would be limited. In traditional wireless networks, each node has a wider transmission range and consumes more energy than the nodes using multihop fashion (see Figure 3-1(a)). As a result of the transmission range, the simultaneous communications are limited in traditional wireless networks. Transmit power control (TPC) is a technical mechanism used in radio communications to reduce the power of a radio transmitter to the minimum necessary to maintain the link with a certain quality. Decreasing the transmit power of each node can limit the transmission range of each node, not only numbers of simultaneous communications could be increased, but also the battery capacity of each wireless devices could support for longer time (see Figure 3-1(b)). The advantage of TPC is that it improves the performance of network, such as

user experienced data rate, network capacity, and etc.

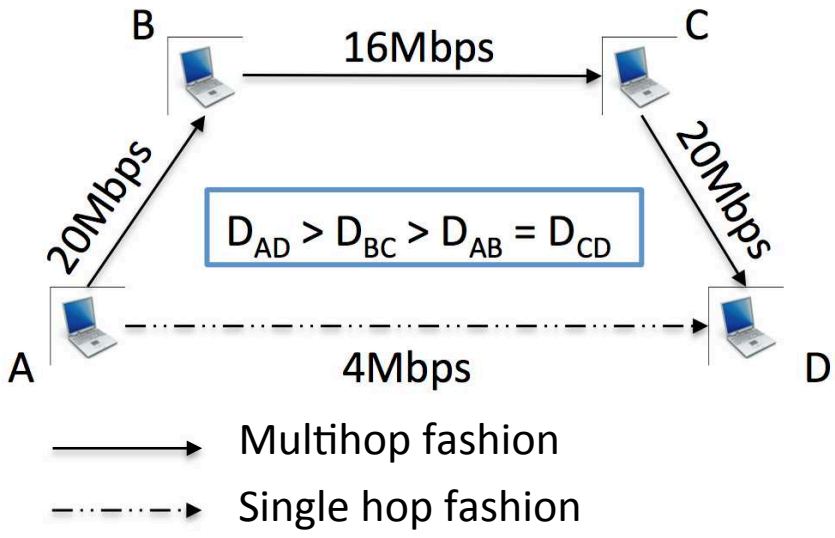

(a) Multihop fashion increase the user experienced data rate

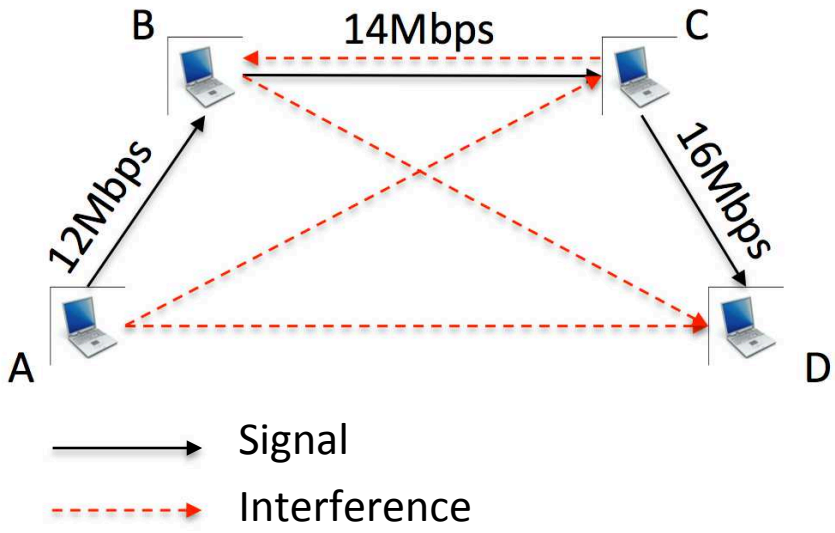

(b) Simultaneous communication with interference in MWNs

Figure 3-2: Bottleneck problem in MWNs with simultaneous communication

When the transmit power reduced, rather with previous single hop to deliver the packet form a source node to a destination node, deliver the packet via other intermediate nodes can achieve higher user experienced data rate. As shown is Figure 3-2(a), the D in box means the distance between two nodes.

With single hop, $Rate^{s}_{(AD)}$ =4 Mbps

With multihop fashion, $Rate^{m}_{(AD)} = \frac{\min\left\{Rate_{(AB)}, Rate_{(BC)}, Rate_{(CD)}\right\}}{\sum timeslots} = \frac{16}{3}$ =5.3 Mbps

Under multihop wireless environments, excessive reductions in transmit power in-

creases the number of transmission hops. This increases the network traffic load and induces additional interference in the multihop network. In Figure 3-2(b), when the node A, B, C are doing the transmission at the same time, they are interfered with each other, which lead the link rate decrease, but the user experienced data rate is increased.
$Rate^{m'}_{AD} = \min\left\{Rate'_{(AB)}, Rate'_{(BC)}, Rate'_{(CD)}\right\}$ =12 Mbps
The problem is that 12 Mbps is the optimized end-to-end rate from the source node to the destination node or not, the answer is no. Transmit power control can also adjust the interference level, which can achieve higher user experienced data rate to optimize the network capacity.

Therefore, the trade-off between the transmit power reduction and the number of transmission hops is extremely significant, which means a suitable TPC algorithm can maximize the network performance.

3.2 Background and Motivation

3.2.1 Related Works

Typical TPC algorithms in wireless networks are used for the sensor networks, such as: local mean algorithm (LMA) [57], and local minimum spanning tree (LMST) [58]. LMA is a typical power control algorithm that gives emphasis to the power conservation while keeping the connectivity of the sensor network. It mainly focuses on network lifetime rather than other performance metrics. In LMST, each node builds its local minimum spanning tree independently and only keeps on-tree nodes that are one hop away as neighbors in the final topology. This algorithm is used for dynamic wireless ad-hoc network with limited mobility. The topology under LMST has a small average node degree (close to the theoretical bound), and a small average radius. However, the free space model used in this algorithm is a primitive prototype that would be enhanced. Other TPC algorithm such as max-min power (MMP) algorithm aims for objective to maintain the best possible modulation and coding scheme (MCS) of each link while decreasing the transmission power as much as possible. However, each link with the best possible MCS does not lead to optimized capacity of the whole network. The study in [59] proposed a distributed transmit power control (DTPC) algorithm for maximizing user experienced data rate in

wireless multihop networks. It is shown that DTPC improves the user experienced data rate performance for the single flow existing networks. Moreover, it is known that there are limitations of TPC for indoor wireless local area networks [60].

3.2.2 Motivation

The proposed DTPC in [59] does not consider at all the issue of multi-flow traffics in various multihop wireless network topologies. First, the DTPC is modified to support the multi-flow traffics. Then, the modification of DTPC leads to the proposed of CTPC algorithm and its consensus coefficient to maximize the average user experienced data rate by controlling the transmit power that is similar to DTPC algorithm.

In this chapter, the routing protocol, scheduling, fairness and others are not considered for the motivation to observe the aftermath of TPC algorithm on the network performance of the MWNs.

Another motivation is to introduce a network emulator for the MWNs. Normally, other algorithms and routing protocols were evaluated by network simulators. But the network emulator cannot only support the real-time execution, but also provide better result reliability. The proposed CTPC algorithm has been evaluated under both simulation and emulation. For the emulation, the advanced wmediumd [61] has been implemented on large scale network emulation testbed, which is called StarBED [62][63]. This emulator is called StarMesh Emulator.

3.3 System Model

In this section, the system model and assumption issues are described.The system model is based on QOMET [64]. The system model is defined as follows:

- Outdoor/indoor (Frequency = 2.5 GHz) channel gain (in decibels) between node i and node j is depend on log-distance pathloss model, PL_0 is assumed as Friis free space model

$$PL_{ij} = PL_o + 10 \cdot \alpha_1 \cdot \log_{10}\left(\frac{d_{ij}}{d_0}\right) - W_{ij} + X_\sigma \tag{3.1}$$

  where $PL_o = 20 \cdot \log_{10}(d_0)$

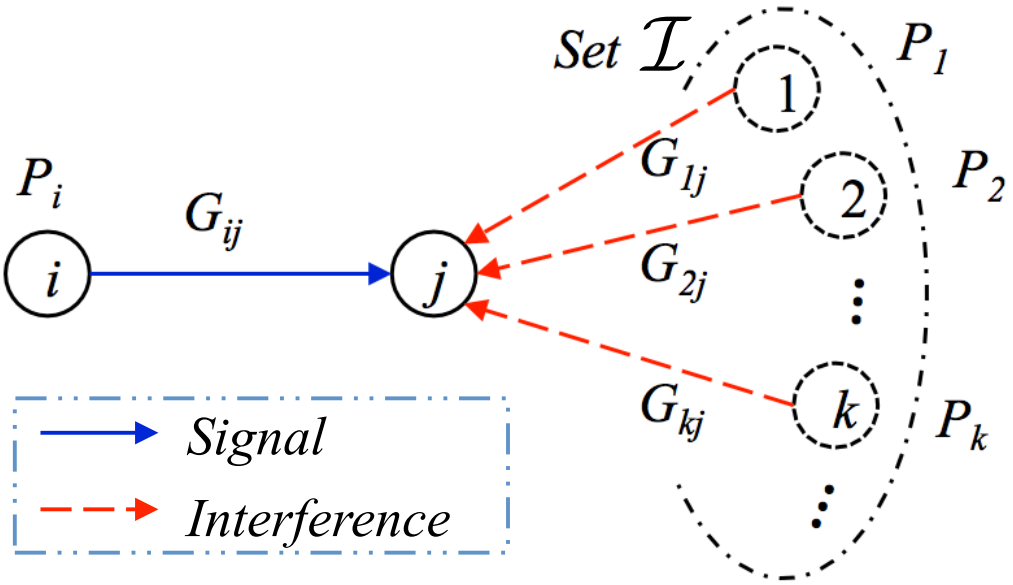

Figure 3-3: All of the other transmitting nodes are recognized as interfering nodes to receiver node j

- Indoor (Frequency = 60 GHz) channel gain (in decibels) between node i and node j is formulated with ITU site-general models [55]. Here, $PL(d_0)$ is the pathloss at d_0 (dB) and L_f is the floor penetration loss factor. Thus, the channel gain is

$$PL_{ij} = PL(d_0) + \alpha_2 \cdot \log_{10}\left(\frac{d_{ij}}{d_0}\right) + L_f(w) \tag{3.2}$$

  where $PL(d_0) = 20 \cdot \log_{10} f - 28$, for a reference distance d_o at 1 meter. Also, if the frequency value is 60 GHz or more, it is assumed propagation within a single room or space, and do not include any allowance for transmission through walls. Under this assumption, the $L_f = 0$ dB for $w = 0$

- Power ratio (no unit) between node i and node j is

$$G_{ij} = \frac{1}{10^{\left(\frac{PL_{ij}}{10}\right)}} \tag{3.3}$$

- Signal to interference and noise ratio (no unit) from node i to node j is

$$SINR_{ij} = \frac{G_{ij}P_i}{\eta_j B + \sum_{k\in\mathcal{X},k\neq i} G_{kj}P_k} \tag{3.4}$$

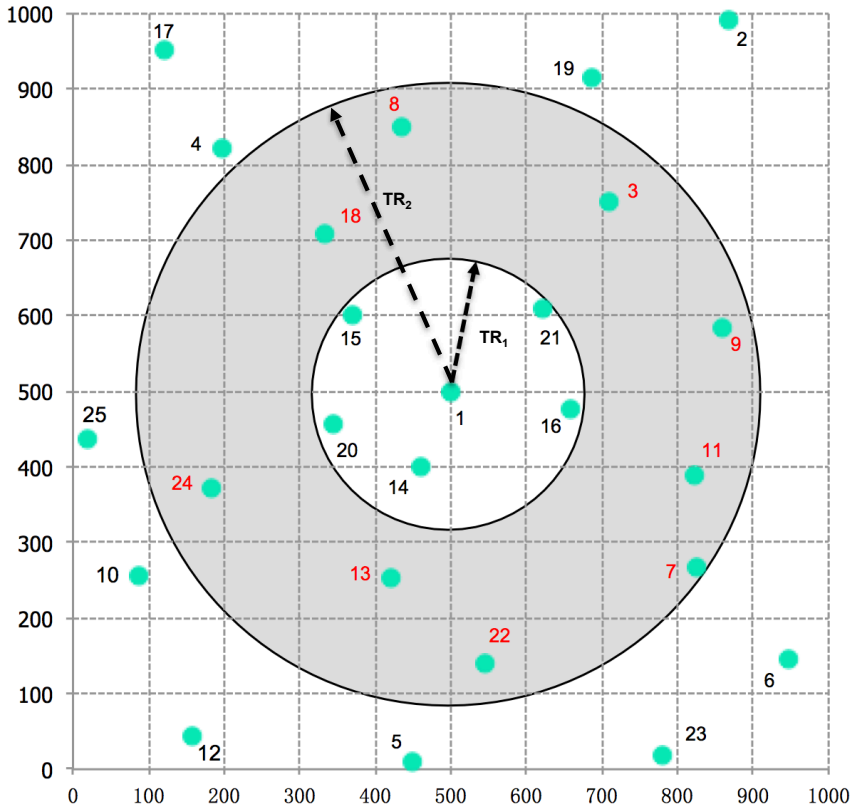

Figure 3-4: 2-hop neighbor interference model

where k denotes the interfering node. E.g., in Fig. 3-3, the interfering nodes are demonstrated in the right side, which are belong to the set $\mathcal{I}$.

- Rate of transmission (bit/s) from node i to node j is

$$R_{ij} = B\log_2\left(1 + \frac{1}{\Gamma} SINR_{ij}\right) \tag{3.5}$$

3.3.1 2-hop Interference Model

In this chapter, the interference model is defined as that the total interference power level of a node k is accumulated from all the two-hop interference neighbor nodes. This model modifies by assuming the interferers [65], which are located out of the 2-hop range are no interference effect. Based on this model, all the nodes that are transmitting data to other neighbor nodes are considered as interference nodes if and only if the nodes are in the area that between one-hop neighbor range and two-hop neighbor range (see Figure 3-4). This interference model can be the worst case when all the transmitting nodes in

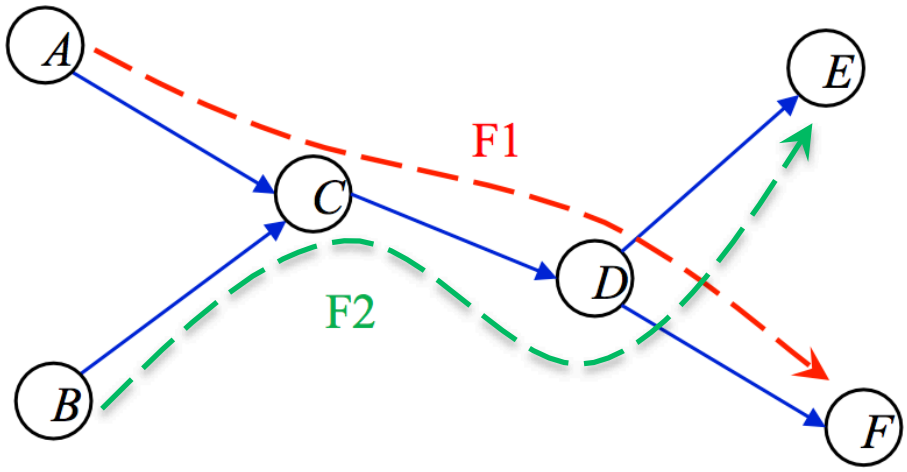

Figure 3-5: An example of shared link situation.

the aforementioned area have been the interference nodes.

3.3.2 Shared Link Situation

For D2D communication, the cross talking always exist. An example of cross talking is shown in Fig. 3-5. There are two flows, one is from node A to node F, the other one is from node B to node E. For sparse environment, due to the single hop transmission cannot deliver packets from the source node to destination node or the interference is greater than the signal at the receiver, multihop transmission is one way to mitigate the interference. For dense environment, the proposed dense-aware adaptive carrier sense threshold scheme (in Chapter 4) can prevent the cross talking by the topology control.

Another important thing is shared link situation. After the topology control, if a link is shared by multiple flows, then the link rate should be divided by the total number of flows, i.e., $R^s_{CD} = \frac{R_{CD}}{2}$ in Fig. 3-5.

3.3.3 Definitions of Key Capabilities

This research aims to achieve the best user experienced data rate with higher energy efficiency. Consider a local ultra-dens network with n nodes. All of the communication is in one channel, which experiences same flat fading and *additive white Gaussian noise* (AWGN). There are x transmitting nodes, i.e., transmitter and relay nodes, and y receivers, which also including the relay nodes. All of the $n_{i,i\in x}$ interfere with $n_{j,j\in y}$, where $(j \neq i)$. The transmit power allocation of transmitting nodes is denoted by vector

$P = [P_1, P_2, \cdots, P_x]$.

User experienced data rate:

When multi-flow exists, one link might be shared with multiple concurrent transmission flows (see Fig. 3-5). Thus, the shared link rate is defined as

$$R_{ij}^{s} = \frac{R_{ij}}{\epsilon_{ij}} \tag{3.6}$$

where ϵ_{ij} is the total number of flows that sharing the link rate from node i to node j. Due to the consideration of D2D communication with multihop fashion, the end-to-end flow rate is restricted by the lowest link rate, which is defined as

$$R_{F(z)} = \min\{R_{12}^{s}, R_{23}^{s}, \cdots R_{(m-1)(m)}^{s}\} \tag{3.7}$$

where $z \in M$, m is the total number of nodes in z th flow.
Let the z th flow is from source node x_z to its destination node y_z with $m-2$ relay nodes. The user experience data rate of source node x_z is define as

$$U_{F(z)}^{x} = R_{F(z)} \tag{3.8}$$

Thus, the definition of average user experience data rate ($\bar{U}$) is

$$\bar{U} = \frac{\sum_{z=1}^{M} (U_{F(z)}^{x})}{M} \tag{3.9}$$

where M is the total number of transmitting flows.

Energy-Efficiency:

Note that as in [66], both transmission power and circuit power are be calculated for the EE communication. Circuit power represents average energy consumption of each device electronics, and transmit power is used for data transmission. In this paper, the proposed algorithm only controls the transmit power. Circuit power does not influence the achievable rate due to all of the nodes are assumed to be active. Thus, the EE is

defined as

$$\psi_i = \frac{U^i_{(}F(z))}{\sum_{k=1}^{m-1} \frac{P_k}{\epsilon_{k(k+1)}} \times t_k} \tag{3.10}$$

where $i \in x$, U_i is given by Equation (3.8); $m-1$ is total hops from the source node to destination node of flow z; t is the total time for transmission and $0 \leq P_k \leq P_{max}$. The solution to Equation (3.10) is different from the existing power allocation schemes in general, which maximize throughput with power constraints. The transmit power control in ultra-dense networks with multihop D2D communication to optimize the overall network EE is also different from traditional power control scheme that emphasize network throughput improvement. Consequently, the EE of the overall network can be defined as

$$\psi = \sum_{i=1}^{M} \psi_i \tag{3.11}$$

Different with centralized EE control scheme with single hop transmission , which means the ratio of sum network throughput to sum network power consumption, i.e., $\sum_{i=1}^{x}(R_i)/\sum_{i=1}^{x}(P_i)$, transmit power and EE of different nodes are not shared. Thus, the definition is based on summation of distributed EE with multihop transmission.

3.4 Proposed Dense-aware Adaptive Transmit Power Control Scheme

In this section, the proposed sense-aware adaptive transmit power control scheme is described (see Figure 3-6). Proposed DATPC comprises various components such as spectrum sensing (described in 2.4), spectrum analyzer, DATPC core part (consensus TPC algorithm), optimizer and decision maker spectrum sharing (described in 2.5) and spectrum allocation management module.

The DATPC scheme is a scheme that adjust the best transmit power for the packet transmission with consensus transmit power control algorithm. The best transmit power is calculated from the average signal-to-interference-plus-noise ratio (SINR) with 2-hop neighbors' shared information. If the current SINR is equal to the average SINR, then use this transmit power to transmit data packets. If not, re-calculate the new SINR then share

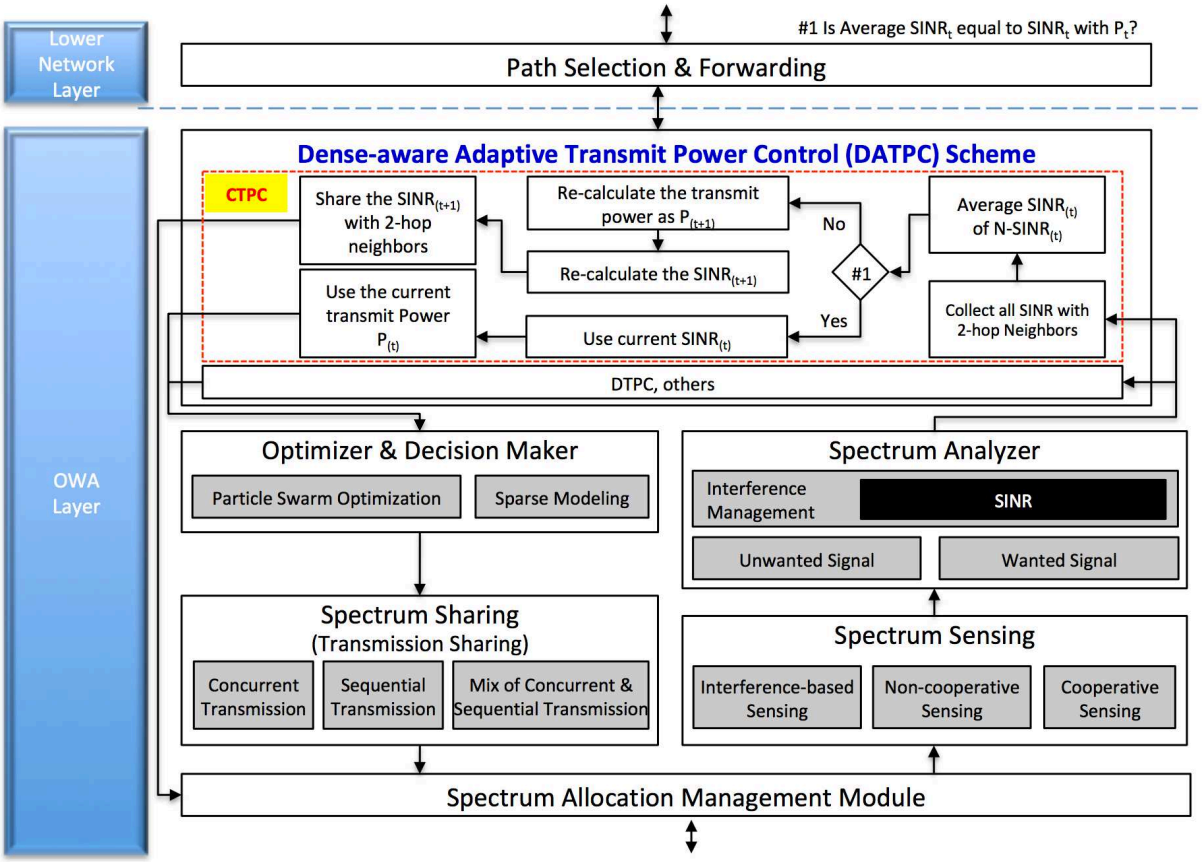

Figure 3-6: Dense-aware adaptive transmit power control scheme

the information with 2-hop neighbors through spectrum allocation management module.

Here, the proposed DATPC scheme can employ proposed CTPC algorithm, and also can employ other power control algorithms, e.g., DTPC. The proposed CTPC is for the purpose of high performance dense communications, which has been described in Fig. 1-3. For other requirements, such as IoT devices, which requires low power and low throughput, the DTPC may achieve better performance than CTPC.

The detail explanation of DATPC is in the follow subsections.

3.4.1 Spectrum Analyzer

This subsection is describe the key support component, which is spectrum analyzer. Based on the spectrum sensing, especially with interference-based sensing, the unwanted signal (interference) and wanted signal can be measured. From these information, the interference management would calculated the SINR form its neighbor nodes with system model (described in Section 3.3). Then share the information to DATPC scheme.

3.4.2 Consensus TPC algorithm

The core of the DATPC is the consensus TPC algorithm. In MWNs, when multi-flow situation exists, the proposed CTPC algorithm is defined as two steps. First step, maximizing the minimum link rate of each flow. Because the user experienced data rate between a source and destination is restricted by the lowest link rate. So maximum the minimum link rate could increase the user experienced data rate. Second step, calculating the average rates of all existing flows to make all link rates converge on the calculated average rates by adjusting the transmit power of each node. In addition, adjustment of consensus coefficient can achieve the margin of user experienced data rate.

$$\begin{aligned} R'_{F(z)} &= \max_{P} \quad \min\{R^s_{12}, R^s_{23}, \dots R^s_{(m-1)(m)}\} \\ O &= \max_{P} \quad \Big(mean\{R'_{f(1)}, R'_{f(2)}, \dots R'_{F(z)}\}\Big) \times C \\ & \qquad P = [P_1, P_2, \dots P_n] \quad 0 \le P_i \le P_{max} \end{aligned} \tag{3.12}$$

Algorithm 1 Consensus TPC Algorithm

01: **Definition**: t is timeslots, C is consensus coefficient
02: **Input**: Initialize $P_i(0) = P_{max}$
03: **Output**: Transmit power for timeslot t
04: **Begin**
05: Measure $SINR_{ij}(t)$
06: Calculate $R^s_{ij}(t)$ or $SINR^s_{ij}(t)$
07: Share $R^s_{ij}(t)$ or $SINR^s_{ij}(t)$ with neighbor nodes
08: Calculate next target rate of each flow $R'_{F(z)}(t+1)$ where

$$R'_{F(z)}(t+1) = mean\{R^s_{ij}(t)\}$$

09: Calculate next target rate of all flows $O(t+1)$ where

$$O(t+1) = mean\{R'_{F(z)}(t+1)\}$$

10: Calculate $O'(t+1) = O(t+1) \times C$
11: **If** $O'(t+1) = R^s_{ij}(t)$
12: $P_i(t+1) = P_i(t)$
13: Set $t \leftarrow t+1$. Go to step 17
14: **else**
15: Calculate $P_i(t+1)$ from $O'(t+1) \times \epsilon_{ij}$
16: Set $t \leftarrow t+1$. Go to step 4
17: **End**

Algorithm 1 reveals the proposed consensus TPC algorithm, which operates based on

the time slot and observes the following steps:

1. All the transmitting nodes set the initial transmit power to the maximum transmit power P_{max}.

2. The transmitting node i which using the transmit power decided for the time t to sends the packet to its receiving node j.

3. Upon the receiving packet, the receiving node j measures its $SINR_{ij}$ and feeds it back to its transmitting node i.

4. Based on the $SINR$ feedback, the transmitting node i calculates its current link rate $R_{ij}(t)$, and then calculate its R^s_{ij} with its ϵ_{ij}.

5. Each transmitting node shares the information of R^s_{ij} with its neighbouring nodes. As a sharing method, the overhearing technique can be used[67].

6. The next target rate of each flow $R_{F(z)}(t+1)$ is determined as the average value of the recognized adjacent link rates of each flow, as follows:

$$R'_{F(z)}(t+1) = mean\{R^s_{ij}(t)\} = \frac{1}{m}\sum\nolimits_{ij\in\{awarelinks\}} R^s_{ij}(t) \tag{3.13}$$

   where m is the total number of aware links of z^{th} flow.

7. The next target $O(t+1)$ is determined average value of aware flows, as follows:

$$O(t+1) = mean\{R'_{F(z)}(t+1)\} = \frac{1}{M}\sum\nolimits_{z\in\{awareflows\}} R'_{F(z)}(t+1) \tag{3.14}$$

   where M is the total number of aware flows.

8. Update the next target $O'(t+1)$ as follows:

$$O'(t+1) = O(t+1) \times C \tag{3.15}$$

9. If the next target rate $O'(t+1)$ is the same as the current target rate $R^s_{ij}(t)$, the $P_i(t)$ is decided as the final transmit power and the iteration ends. Otherwise, from

(4), the next transmit power $P_i(t+1)$ is calculated to obtain the next target rate $O'(t+1) \times \epsilon_{ij}$, as follows:

$$P_i(t+1) = \min\left\{ \frac{\left(2^{(\frac{O(t+1)\times\epsilon_{ij}}{B})} - 1\right)\left(I_j(t) + \eta_j B\right)}{G_{ij}}, P_{max} \right\} \tag{3.16}$$

where $\frac{I_j(t)+N_j(t)}{G_{ij}}$ is derived from the $SINR_{ij}$, and $I_j(t) = \sum_{k\in\mathcal{X},k\neq i} G_{kj}P_k$. Then, the operation continues from Step 2).

3.5 Numerical Simulation

In this section, the proposed DATPC scheme is evaluated compare with no TPC algorithm and DTPC algorithm in the MATLAB simulation environment. Here, the routing protocol is not focused.

3.5.1 Simulation Scenarios and Parameters

Two scenarios exist multi-flow in the MWNs to be used to evaluate the two TPC algorithms and also without TPC algorithm. The topologies are shown in Figure 3-7 and Figure 3-8.

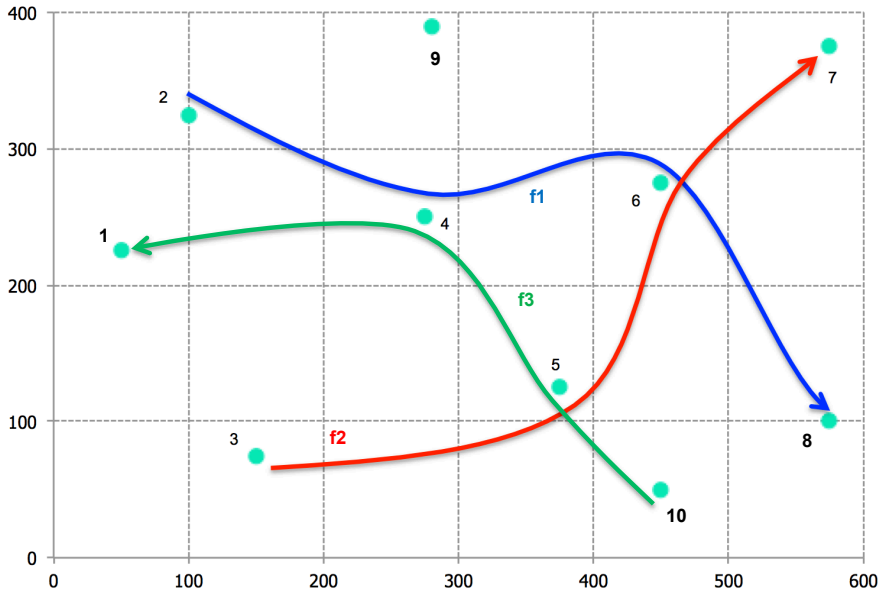

Figure 3-7: Network topology of 10 random nodes

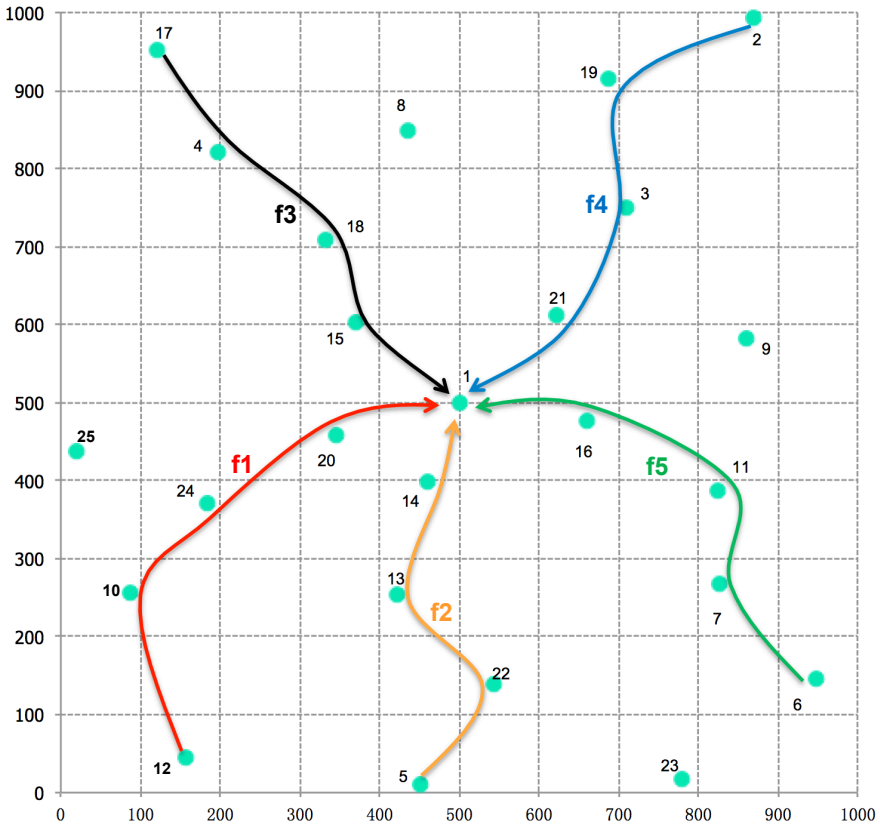

Figure 3-8: Network topology of 25 random nodes

In Figure 3-7, there are 10 random nodes in 400 m × 600 m area. In the topology, 3 different flows exist, and the average hop of this topology is 3.

In Figure 3-8, there are 25 random nodes and only one destination node in 1000 m × 1000 m area. In this topology, 5 flows exist, and the average hop of this topology is 4.

Network scale (ϕ) is changed to verify the CTPC algorithm and interference model. For example, the original network size of 25 nodes topology is identified as sparse network, which means $\phi = 1$. The coverage area of 100 m × 100 m is identified as ultra-dense network, which means ($\phi = 0.1$). In ultra-dense scenarios, the distance between every two neighbor nodes in each flow is less than 15 meters.

The system parameters are list in TABLE. 3.1. Network simulation operates on the premise that intermediate node can transmit and receive the data packets simultaneously without self-interference. Here, the frequency is considered as less than 5 GHz.

Table 3.1: Parameters for simulation and emulation

Parameter	Value
Minimum distance between nodes (d_0)	10 m
Maximum transmit power (P_{max})	0.2 Watt
Attenuation constant (α_1)	3.5
Wall attenuation (W_{ij})	0 dB
Shadowing parameter (X_σ)	8 dB
Noise level (η)	–120 dBm
Channel bandwidth (B)	10 MHz
Value depends on the choice of coding and modulation parameters, and the BER requirement (Γ)	1
Maximum distance of one-hop neighbor	231 $\times\phi$
Maximum distance of two-hop neighbor	400 $\times\phi$
Consensus coefficient (C)	$1 \sim 2$

3.5.2 Performance Metrics, Results and Discussion

Performance Metrics

For the performance metrics, we only focus on average transmit power and average user experienced data rate. We compare them with no TPC algorithm, DTPC and CTPC. Also, we show the influence with network scale (ϕ) and consensus efficient. For the network scale, we modified interference model also changes vary with the network scale as $\phi = 0.01, 0.1, 0.6 - -1.2$ of the original network size (600 m $\times$ 400 m of 6 nodes scenario and 1000 m $\times$ 1000 m of 25 nodes scenario). For the consensus coefficient *(C)* changes from 1 to 2 every 0.05.

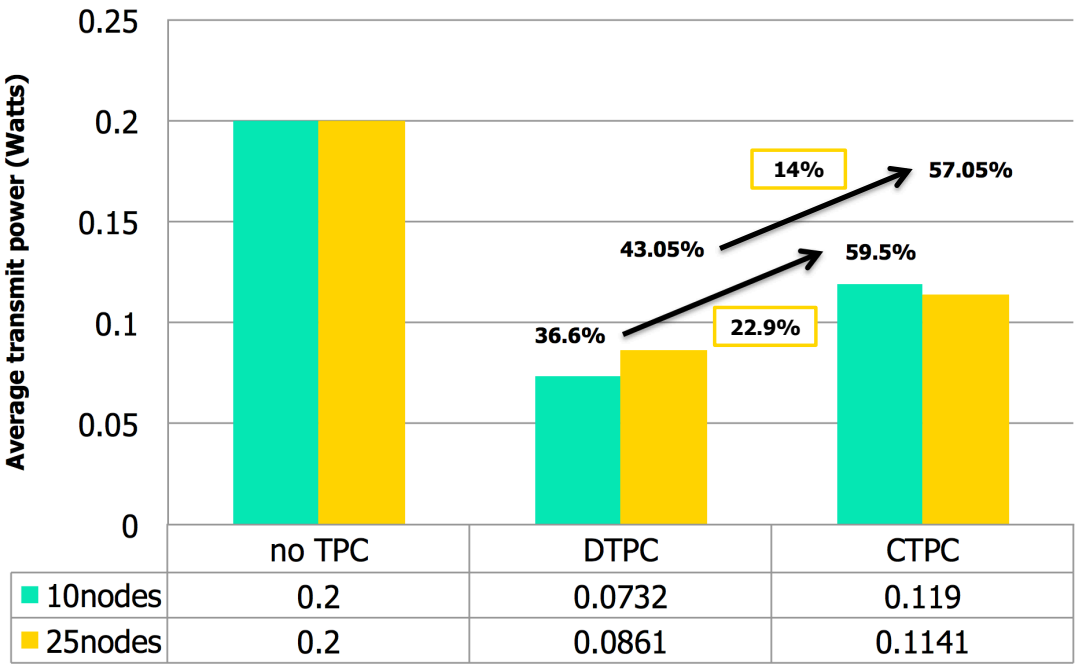

Figure 3-9: The performance of the average transmit power without TPC, with DTPC, and with CTPC

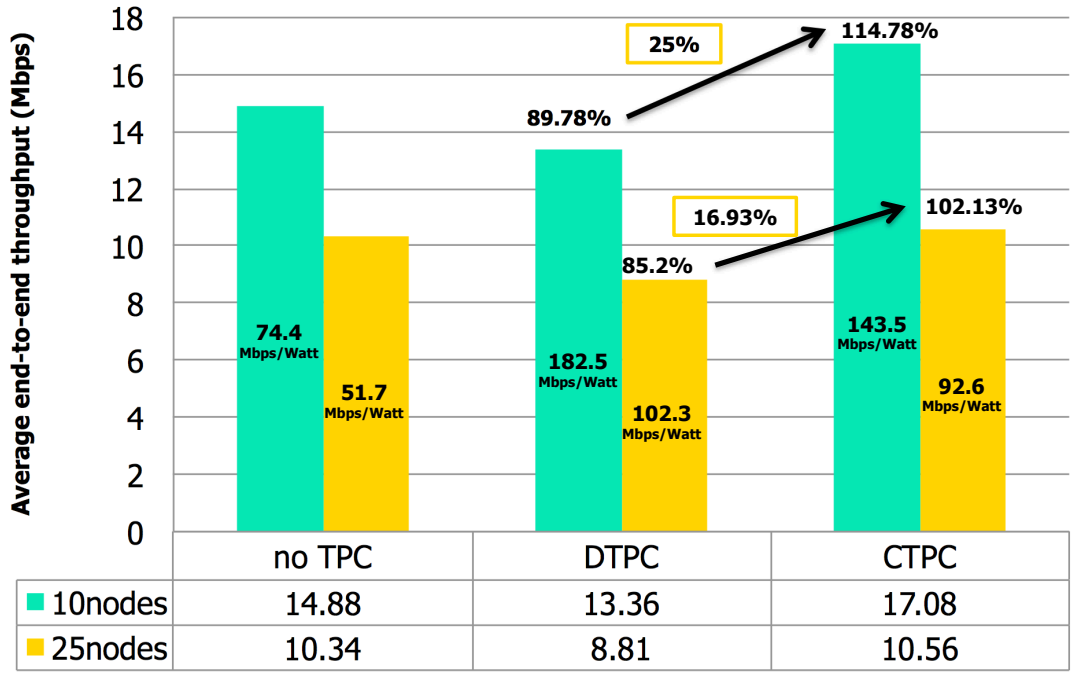

Figure 3-10: The performance of the average user experienced data rate without TPC, with DTPC, and with CTPC

Comparison results among no TPC, DTPC and CTPC

Figure 3-9 shows the average transmit power by using DTPC, CTPC and without using TPC algorithm. Compare with no TPC situation, using TPC algorithm leads significant

energy saving. Figure 3-10 shows the average user experienced data rate by using DTPC, CTPC and without using TPC algorithm. Compare with no TPC situation, only CTPC algorithm improve the user experienced data rate with low power consumption. For 10 nodes scenario, DTPC use 36.6% average transmit power to achieve 89.78% of the average user experienced data rate. Although the transmit power decreased, but the throughput also decreased. However, CTPC use around 59.5% average transmit power to achieve 114.78% of the average user experienced data rate. More power consumption used than DTPC, but more user experienced data rate achieved with CTPC. 25 nodes scenario also had the similar results. Figure 3-9 also indicates that the interference among nodes decreases sharply. As mentioned, the model of interference used in this chapter is the worst case, even though under this condition, the CTPC also shows its superiority.

Influence of Network Scale

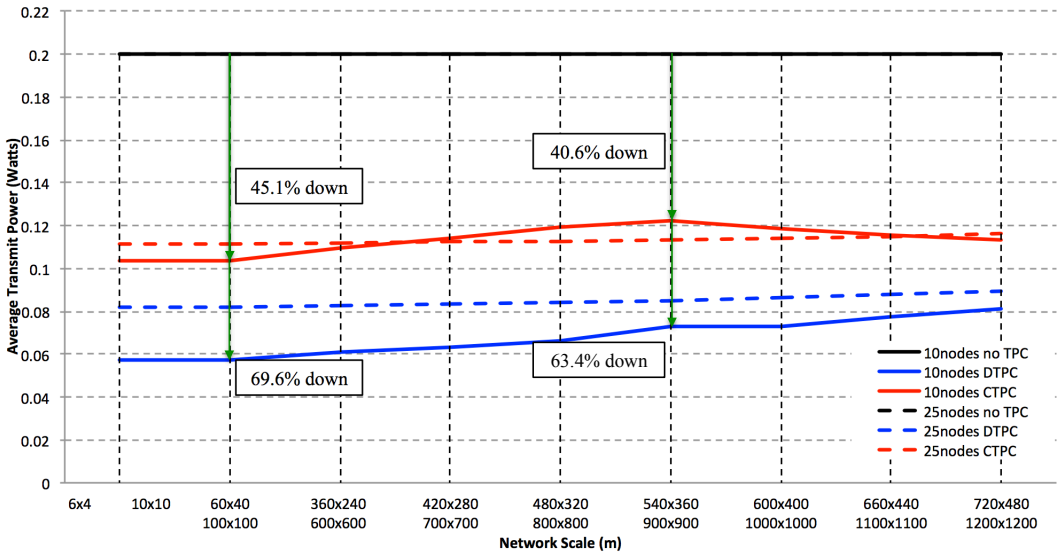

Figure 3-11: Influence of network scale on average transmit power

Figure 3-11 and 3-12 show us that the influence of network scale on average transmit power and average user experienced data rate. When network scale ϕ changes from 0.01 to 1.2, the user experienced data rate decrease at the same time, the transmit power doesn't change so much. The reason is that the interference model also changes the 1-hop distance and 2-hop distance, which means the interferes unchanged vary with network scale. Thus, in this situation, the interferes for a specified node doesn't change. So the interference level also doesn't change. Only the user experienced data rate change

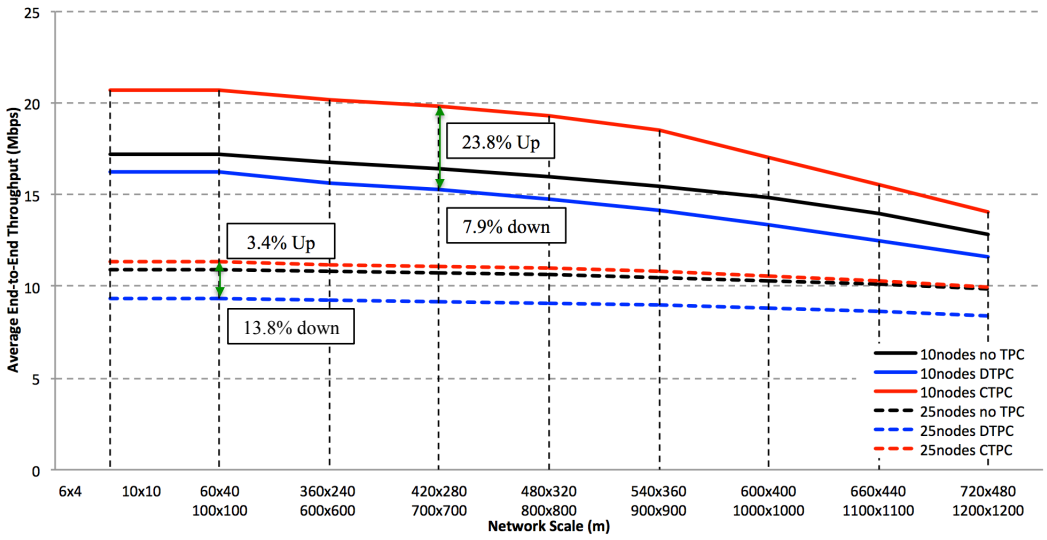

Figure 3-12: Influence of network scale on average user experienced data rate

because the distance between nodes changed. Through the pathloss model, short distance will bring high channel gain. So, in dense environment, the user experienced data rate is high.

Form this two figures, we notice that the interference model used in this chapter is too simple. Thus, we propose an spatial reuse interference management model in next chapter with carrier sense threshold to evaluate proposed DATPC scheme more accurately.

Influence of consensus coefficient

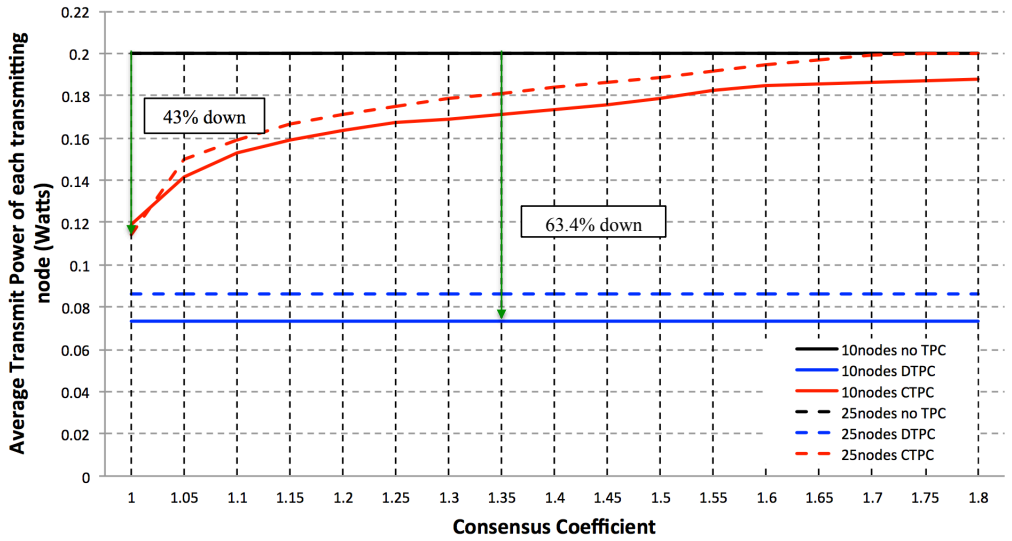

Figure 3-13: Influence of consensus coefficient on average transmit power

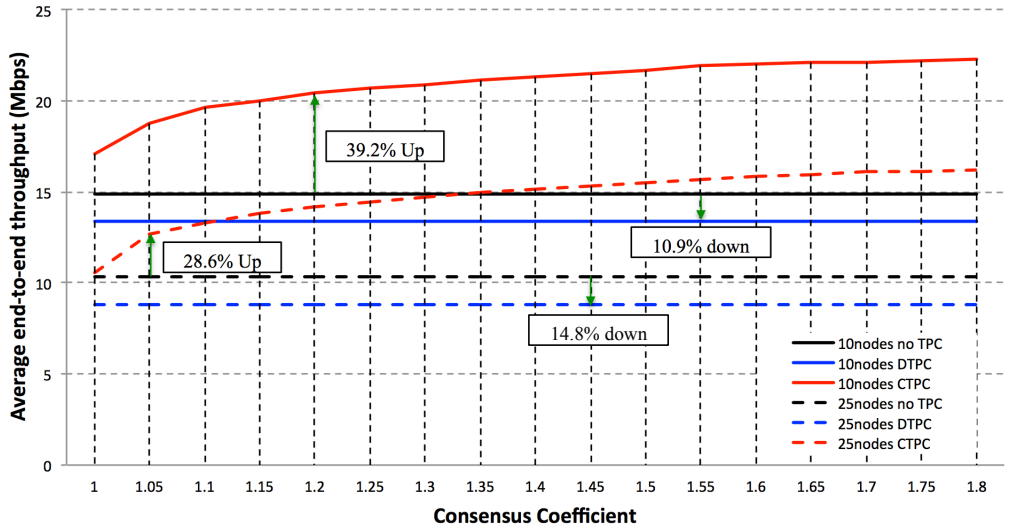

Figure 3-14: Influence of consensus coefficient on average user experienced data rate

Figure 3-13 and 3-14 show us that the influence of consensus coefficient on average transmit power and average user experienced data rate.

Figure 3-13 shows that when the consensus coefficient changes from 1.0 to 1.2, the average transmit power changes sharply, and from 1.2 to 2(1.8) it changes slowly. Figure 3-14 shows the similar results that when the consensus coefficient changes from 1.0 to 1.2, the average user experienced data rate changes sharply, and from 1.2 to 2(1.8) it changes slowly. Thus, the consensus coefficient between 1.0 to 1.2 should be the best value to maximum user experienced data rate with acceptable transmit power reduction.

3.6 Quantitative Comparison of Spectrum Sharing

In this section, we first use two different scenarios to do the explain the comparison of proposed spectrum sharing transmission methods. Then the quantitative results is analyzed.

3.6.1 Simulation Scenarios and Parameters

Two kinds of simulation scenarios is used to evaluate the spectrum sharing transmission method. Figure 3-15(a) is big gap of interference level topology. In this topology, there are two data flows exist, and the interference level of them are quite different. Figure 3-15(b) is similar interference level topology. Due to the two flows are nearly parallel,

compare to Figure 3-15(a) the interference is much similar. The system parameters are list in TABLE. 3.1.

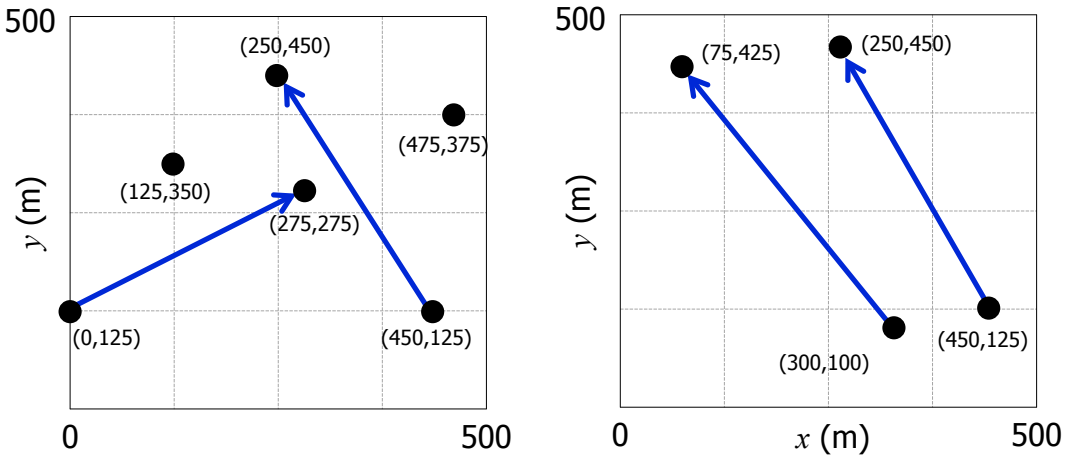

(a) Big gap of interference level topology (b) Similar interference level topology

Figure 3-15: Two scenarios with different topology

3.6.2 Results and Discussion

Results for big gap of interference level topology

The simulation results of Figure 3-15(a) are showed on Figure 3-16. In the Figure, the blue solid line represents signal, and the red dotted line represents interference. Figure 3-16(a) indicates that the network capacity can achieve to 8.16 Mbps under concurrent transmission. $R'_{45} = 1.95$ Mpbs is quite smaller than $R'_{12} = 6.21$ Mbps. The reason is that there is a great gap of interference level between the two flows, which means node 5 receive more interference from node 1 than receive signal from node 4.

Figure 3-16(b) reveals that the network capacity can achieve to 12.90 Mbps under sequential transmission. The best value of β =0.39. Or simply to calculate the average is 12.09 Mbps.

Figure 3-16(c) demonstrates that the network capacity can achieve to 12.96 Mbps under the mix of concurrent and sequential transmission. The best value of β =0.61. We notice that during the concurrent transmission period, the data rate of R'_{45} and R'_{12} is equal. The results is optimized with DATPC scheme with CTPC algorithm. Thus, under DATPC, the network capacity can achieve to 9.68 Mbps only. Thus, only the CTPC is not enough to optimize the network capacity.

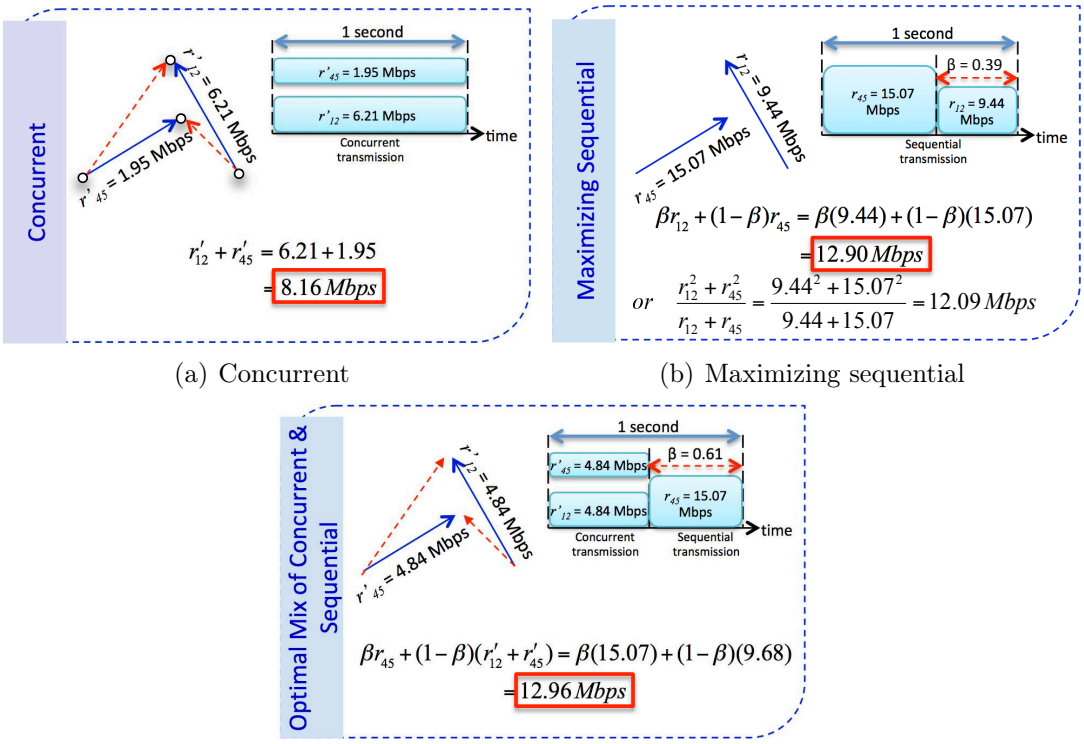

(a) Concurrent (b) Maximizing sequential

(c) Optimal mix of concurrent and sequential

Figure 3-16: Results of spectrum sharing on big gap of interference level topology

Results for similar interference level topology

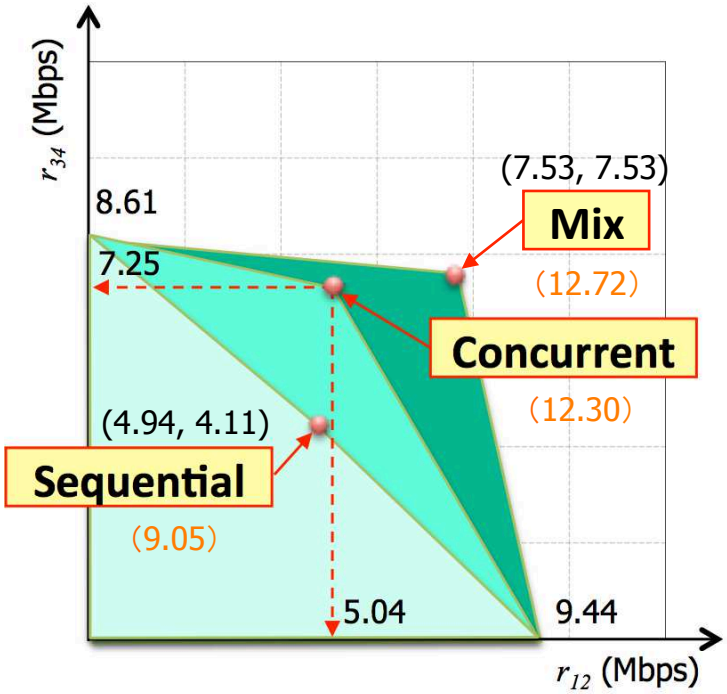

Figure 3-17: Results of spectrum sharing on similar interference level topology

The simulation results of Figure 3-15(b) are showed on Figure 3-16. Under the sequential transmission, the network capacity only can achieve 9.05 Mbps. Under the concurrent transmission with CTPC algorithm, the network capacity can achieve to 12.30 Mbps. However, under the mix of concurrent and sequential transmission, the network capacity can achieve to 12.72 Mbps.

Discussion

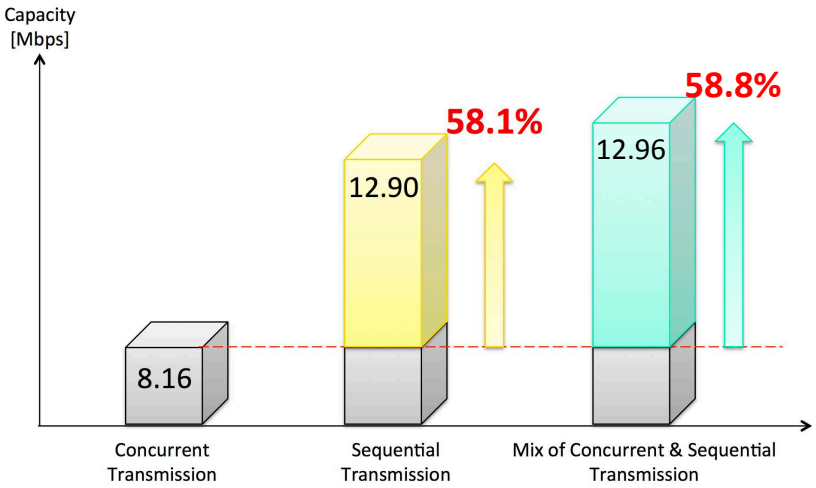

(a) Big gap of interference level topology

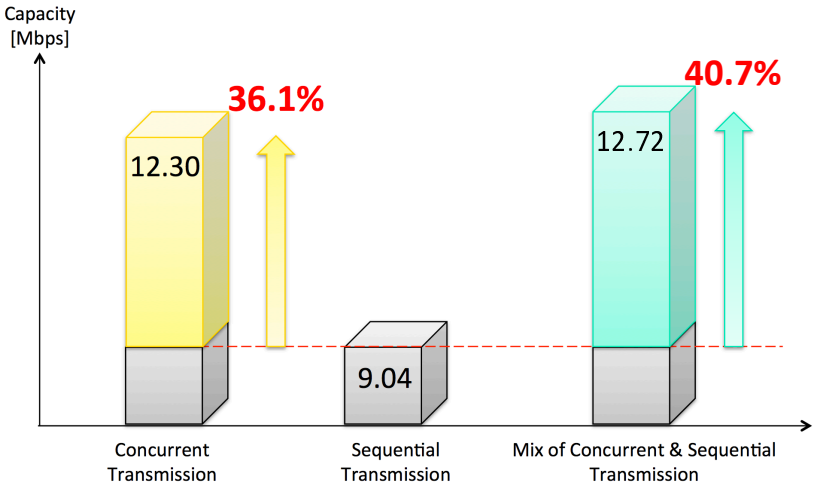

(b) Similar interference level topology

Figure 3-18: Comparison results of spectrum sharing scheme with specific scenarios

Figure 3-18 concludes the results of Figure 3-16 and Figure 3-17 with column chart. For conclusion, Figure 3-18 demonstrate that for both scenarios, mix of concurrent and sequential transmission with DATPC scheme can achieve the optimal network capacity.

The sequential transmission or concurrent transmission shows their advantages and disadvantages vary with different scenarios.

Quantitative Comparison with random Scenarios

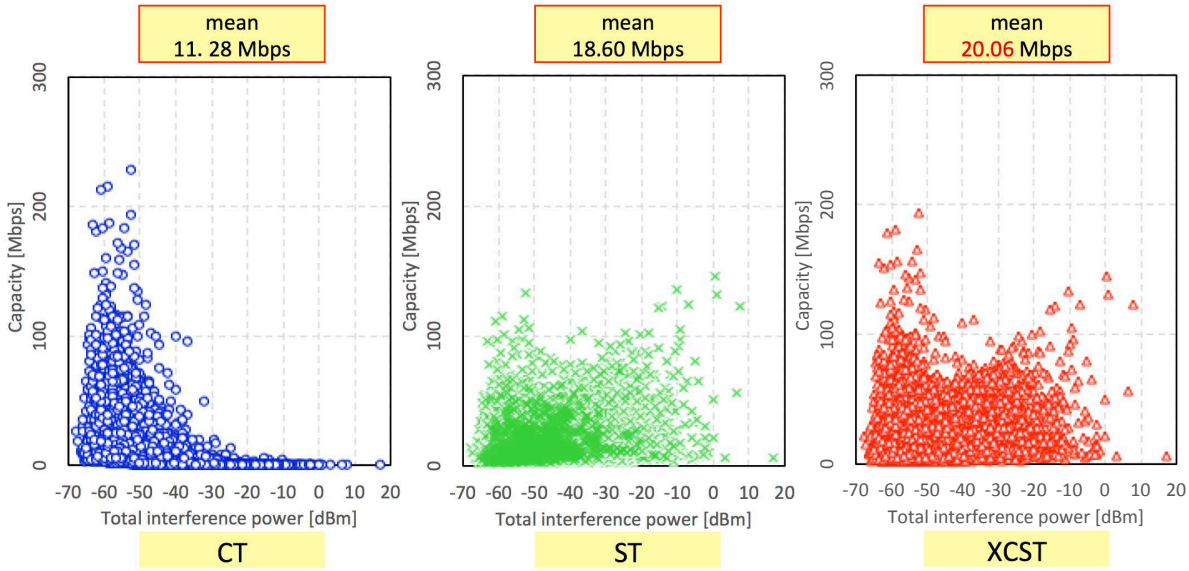

Figure 3-19: Quantitative comparison results of spectrum sharing with random scenarios

Figure 3-19 is the quantitative comparison results of spectrum sharing with random scenarios. The random scenarios means 4 random nodes with 2 pair communication in 500 m $\times$ 500 m area. Under the same setting of system model and parameters, 10000 times simulation are performed to analyze the effect of CTPC on CT, ST, XCST. Fig. 3-19 indicates that the average capacity of CT is 11.28 Mbps; average capacity of ST is 18.60 Mbps, and average capacity of XCST is 20.06 Mbps. Consequently, XCST increased capacity by 77% over CT, and 11.1% over ST.

3.7 Summary

In this chapter, the CTPC algorithm had been presented to leverage the drawbacks of DTPC when the multi-flow exists in the multihop wireless networks. The simulation results reveal that the CTPC algorithm can accomplish the average user experienced data rate up to about 114% and also exhibits its superiority compared to others regardless of the size of network density. The problem is that the 2-hop interference model is too simple,

thus we will introduce the reality interference model, and spatial reuse based CTPC with scheduling is proposed in the next chapter. Also, the parameter of consensus coefficient with reality interference model can celebrate the iterations of proposed DATPC scheme. Moreover, through the simple scenarios, it can be conclude that mix of concurrent and sequential always provides a better average capacity with CTPC algorithm. Also, in next chapter, further research work will be conducted to investigate the performance and implementation issue of the CTPC when the emulation testbed, called StarBED is used.

Chapter 4

Dense-aware Adaptive Carrier Sense Threshold Scheme

In this chapter, we propose a dense-aware adaptive carrier sense threshold (DACST) scheme that incorporates the proposed realistic interference model and auto CST fallback algorithm. As we showed in Chapter 3, a realistic interference model is necessary because the interference level is much higher in wireless UDNs. Only change the transmit power may not have much progress for user experienced data rate and overall energy efficiency. Even the transmit power is very small, still it will bring greater interference level than signal level due to large number of devices in a small area. Through changing the CST, the network topology would be optimized, DATPC scheme would achieve better performance. An spatial reuse based CTPC with scheduling is proposed for analyzed the interference model. In addition, an advanced Starmesh emulator over the StarBED testbed is used to further verify the performance evaluation of the proposed DATPC and DACST schemes. Both the simulation and emulation results reveal that the proposed scheme enables all the traffic flows to accomplish the maximum average end-to-end throughput. At the same time, the total interference power and the total power consumption are decreasing.

4.1 Problem Statement and Motivation

4.1.1 Problem Statement

Increase in system capacity and data rates can be achieved efficiently in a wireless system by getting the transmitter and receiver closer to each other. In our defined future wireless UDNs, the distance between transmitter and receiver are less than 10 meters. In this case, the unplanned deployment of APs or mass mobile devices with D2D communication will lead terrible interference with each other. The fundamental limits of capacity and achievable data rates mainly depends on the interference. Thus, the interference management become a key issue for wireless UDNs.

To cope with the technical challenges including interference management faced in wireless UDNs, researchers have suggested a variety of solutions. These solutions vary depending on the physical layer technology and the specific scenarios considered. In this research, we mainly focus on co-tier interference. Normally, we can cancel the interference or avoid the interference by several technologies, such as time-division based interference management, frequency-division based interference management, code-division based interference management and space-division based interference management.

- Time-division based interference management means set different time slots for users to do the communication. On each time slot, only one transmitter is sending data packets. The other transmitters are into the network allocation vector (NAV) mode. The NAV virtual carrier sensing mechanism is a prominent part of the carrier-sense multiple access with collision avoidance (CSMA/CA) MAC protocol used with IEEE 802.11 WLANs. The limitation of time-division based interference management is that we cannot divide the time into ultra tiny slots, thus, the number of UEs inside a small area is much greater than the limitation of time-division, it does not work well. Moreover, the fairness of time-division interference management is not good.

- For frequency-division based interference management, we can use the different frequency to transmit data packets, although there will be ICI among different transmitters, but the receiver has the filtration component to filter the unwanted signal. However, the spectrum is scarce, which means the use of possibility with frequency is limited. For wireless UDNs, only the frequency-division based interference is not

enough.

- For the third one is the code-division based interference management. It can be easily understand as different language between UEs. For example, indoor environment like meeting room, there are 100 audiences with 100 mobile devices, some of them speak Japanese, some of the speak Chinese, some of them speak Chinese, and so on. In this case, the English speaker talk with each other, the Chinese speaker and Japanese speaker would not be particularly affected. At the same time, they can speak Chinese or Japanese with other friends. However, the efficient and useful "language" (code) is limited. Thus, this also need to cooperative with other interference management.

- The last fashion of interference management is space-division. Only in future wireless UDNs, it will be widely used. 5G mobile networks will be focused in utilizing the given position of the mobile station (MS) in relation to base transceiver station (BTS) in order to focus all MS Radio frequency power to the BTS direction and vice versa, thus enabling power savings for the Mobile Operator, reducing MS SAR index, reducing the EM field around base stations since beam forming will concentrate RF power when it will be used rather than spread uniformly around the BTS, reducing health and safety concerns, enhancing spectral efficiency, and decreased MS battery consumption.

4.1.2 Motivation

In space domain, spatial reuse can optimize user experienced data rate and EE in wireless UDNs. Spatial reuse accommodates more concurrent transmission, which gains higher network capacity [68]. However, the increasing number of concurrent transmission would also brings intolerable interference. IEEE 802.11 media access control (MAC) has employed physical carrier sensing to ensure an adequate level of spatial reuse. Under the physical carrier sensing, only the signal strength of an interfere is below the carrier sense threshold (CST) of the receiver, the interfere can do the concurrent transmission. Therefore, increasing the carrier sense threshold (CST) would lead high interference and also lead high fairness of communication (concurrent transmission), and vice versa. The signal

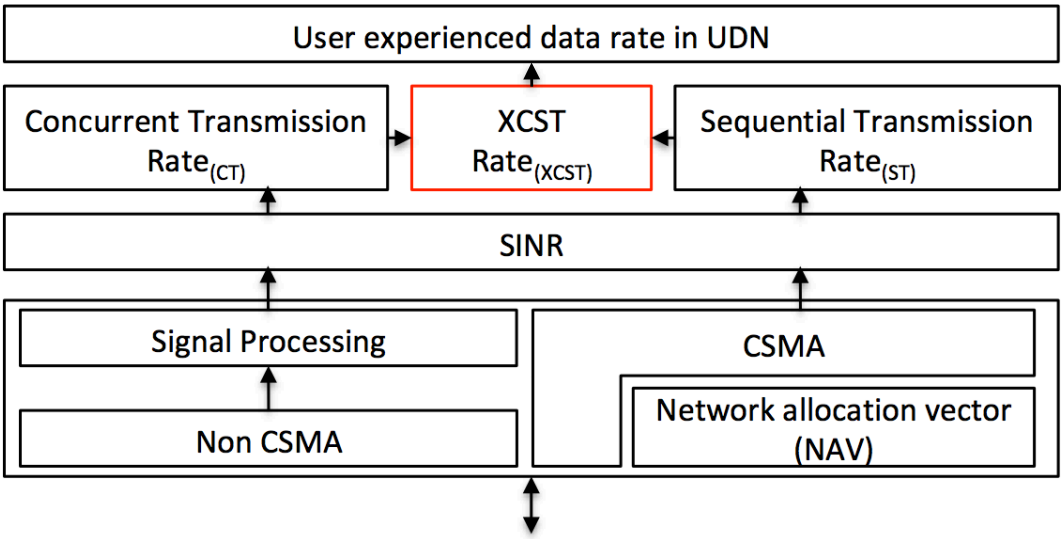

Figure 4-1: Motivation of adaptive CST for XCST optimization

strength is decided by the transmit power and pathloss model on distance. Thus, how to trade-off between CST adjustment and TPC in wireless UDNs is extremely significant, which can optimize the XCST (see Fig 4-1).

4.2 Related Works

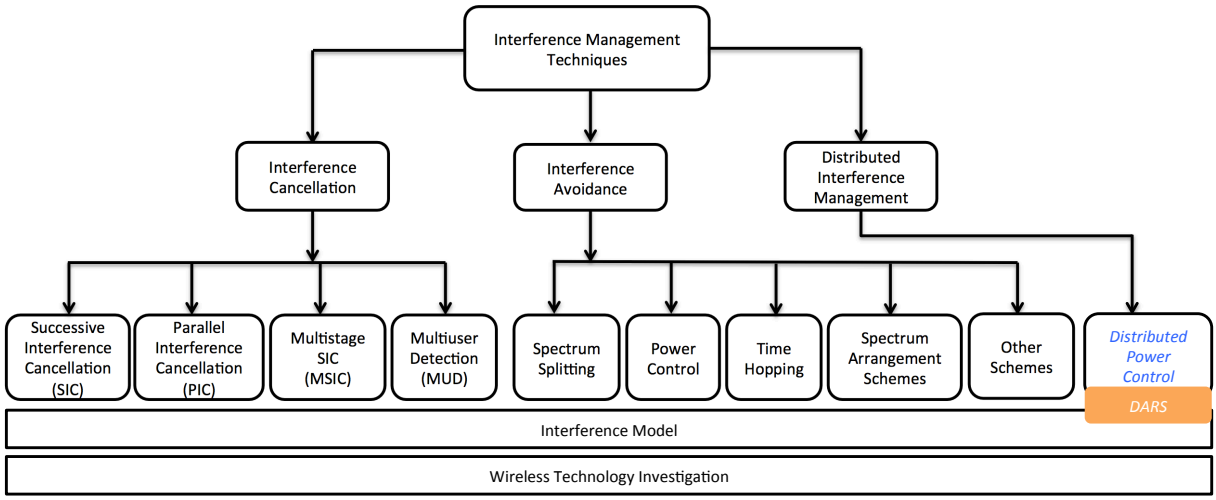

Figure 4-2: Different interference management techniques

Figure 4-2 shows the block diagram of different interference management techniques. Traditional way is normally interference avoidance. Spectrum splitting is mainly to solve the cross-tier interference problems [69]. In some cases, where there is very dense deploy-

ment of small cells, and the cross-tier interference is hard to manage, it is suggested that separate portion of spectrum should be used for the small cell operations [70].

Power control is a key technique in the interference avoidance, especially in dense femtocell deployment. If the transmit power of a femtocell is controlled and optimized, the outdoor macrocell UE can be protected sufficiently. One such technique is proposed in [71], where femtocell network optimization is performed with constraints on the indoor coverage and the interference caused by femtocell BS to the macrocell UEs outside. The optimization problem is formulated as a mixed integer problem and as a result, the maximum transmit power and operational frequency of femtocell is obtained.

For time hopping, a simple technique in [72] provides power control to femtocells to avoid causing interference to nearby macrocell users. It is based on the assumption that the femtocell takes information about macrocell users from the macrocell base station. Once the macrocell user in under interference, the nearby femtocell reduces its transmit power.

For spectrum arrangement schemes, the closed loop power control performs better at the low expense of macrocell throughput. Another solution is provided in [73], where a joint power control, channel management and admission control algorithm is proposed to cope with the co channel interference in the downlink.

Resource allocation is of much importance in OFDMA systems and various schemes have been proposed, such as the Round Robin (RR) and Proportional Fair (PR) schemes [74]. The RR scheme works like a cyclic scheme, each macrocell UE is allocated same time slot. The users are in a kind of queue and the time slot returns to its starting point after going through the queue of users. In the PR scheme, users are given priority based on their needs. A user with a need of higher data rate would be selected first. Results show that the PR schemes perform better than the RR scheme. On the other hand, for a femtocell it is desired to allocate sub channels that reduce the interference and increase the area spectral efficiency (ASE).

For interference cancellation, two classical ways of interference cancellation used extensively in wireless networks are Successive interference cancellation (SIC) and parallel interference cancellation (PIC) [75, 76]. To have a better scheme, we have Multistage SIC, which is smoother trade off between the two techniques [77]. Multiuser detection

(MUD) works on the same principle and identifies the signature of each user. It selects the most probable signal out of K number of users, depending on its observations and channel state information [78, 79].

In this research, we mainly focus on the distributed interference management. In wireless UDNs, the centralized techniques is not the best way for all of the end-users. Providing sufficient knowledge to the small cells is possible through the backhaul network, but this would cause much congestion on the backhaul network. Furthermore, as the number of small cell can be very large, this makes it impractical for the operator to provide large information to the small cell through the backhaul. In this case, distributed schemes are of much importance. In this chapter, the DACST scheme would cooperative with the DATPC scheme to control the topology and management interference, maximizes the user experienced data rate and additionally leads to significant reduction of total energy consumption, which means higher EE.

4.3 Interference models

In wireless UDNs, under the normal CST setting, the DATPC scheme cannot achieve good performance because all the nodes are within the receivers' transmission range. Under this situation, the user would face two cases. One case is the user can experience very high data rate with very low fairness. High data rate is because the very less concurrent transmissions, which means the interference level is low or no interference. Low fairness is because huge amount of nodes would scramble for countable channels. Another one is all of the nodes do the concurrent transmission, which leads the great gap among user experienced data rate. If the distance between one source and its destination is longer than others, then the user experienced data rate would be very small. The reason is because the interference level might be different order of magnitude compared with its signal level. The proposed DACST scheme can prevent the great gap among user experienced data rate (e.g., cross talking). The DATPC scheme with DACST scheme tunes the nodes' transmit powers to maximize the user experienced data rate with high EE.

To let the DACST scheme work, a suitable interference model is needed. Unlike the previous interference model [80], the CST-based realistic interference model is used to define the nodes are within or outside the transmission range of a receiving node. For

the end-to-end throughput in MWNs, we use throughput calculation, which is under the spatial reuse as described in [81].

4.3.1 Realistic Receiver based Interference Model

The interference model is divided into two parts, within parts and outside parts. For within parts, nodes are considered as neighbor nodes. For outside parts, nodes can be considered as interference nodes if and only if they are transmitting packets. The interference level of one receiver is defined as the total interference power of all other transmitting nodes outside of its CST range.

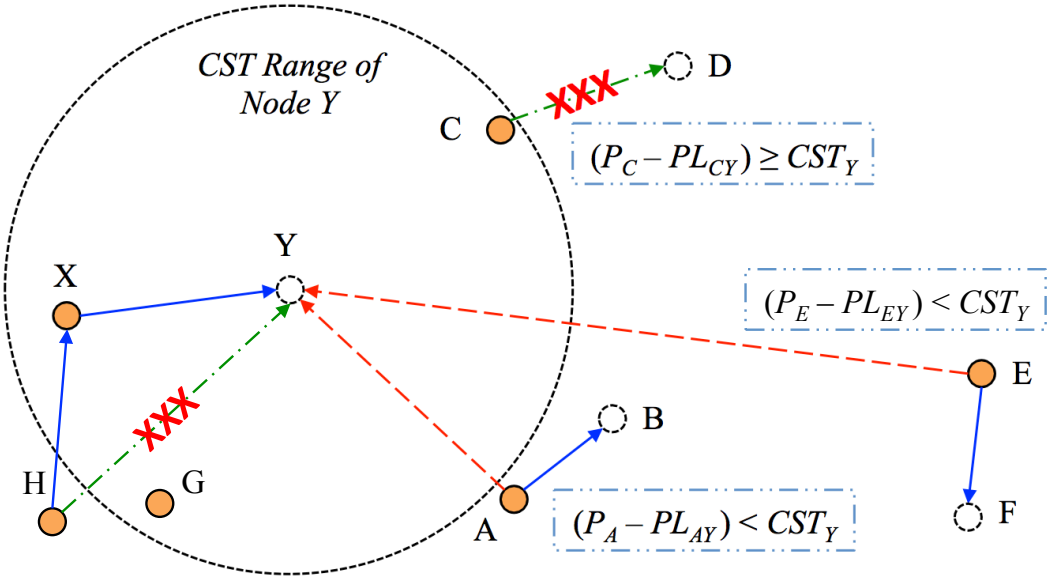

Figure 4-3: Realistic interference model

For example, node X is transmitting with node Y. Depends on the transmit power of node X, node Y has its own CST range. For other concurrent transmission, if the value of $P_C - PL_{CY} \geq CST_Y$, then the node C is considered as within node Y's transmission range. Thus, node C is a neighbor node of node Y, which means C cannot do the concurrent transmission with current P_C. Oppositely, if the value of $P_A - PL_{AY} \leq CST_Y$, then the node A is considered as outside of node A's transmission range. Thus, node A can do the concurrent transmission, which means node A is an interference node of node Y if it transmits packets to its destination node B. Node E is similar to node A. Node E interferes node Y less than node A due to the longer distance. (see Figure 4-3). If node C want to send packets to its destination node D, then node C and node X should share the

resource to do the communication. Here, TDD is used for the spatial reuse calculation due to it is the most easy way to be understood and implemented. Also, node H is in the outside area of node Y. Node H cannot transmit its packets directly to node Y. Node H should recognize node X as its relay node for the transmission. Here, node X is used rather than node G due to node X is transmitting packets to node Y.

4.4 Proposed Dense-aware Adaptive Carrier Sense Threshold Scheme

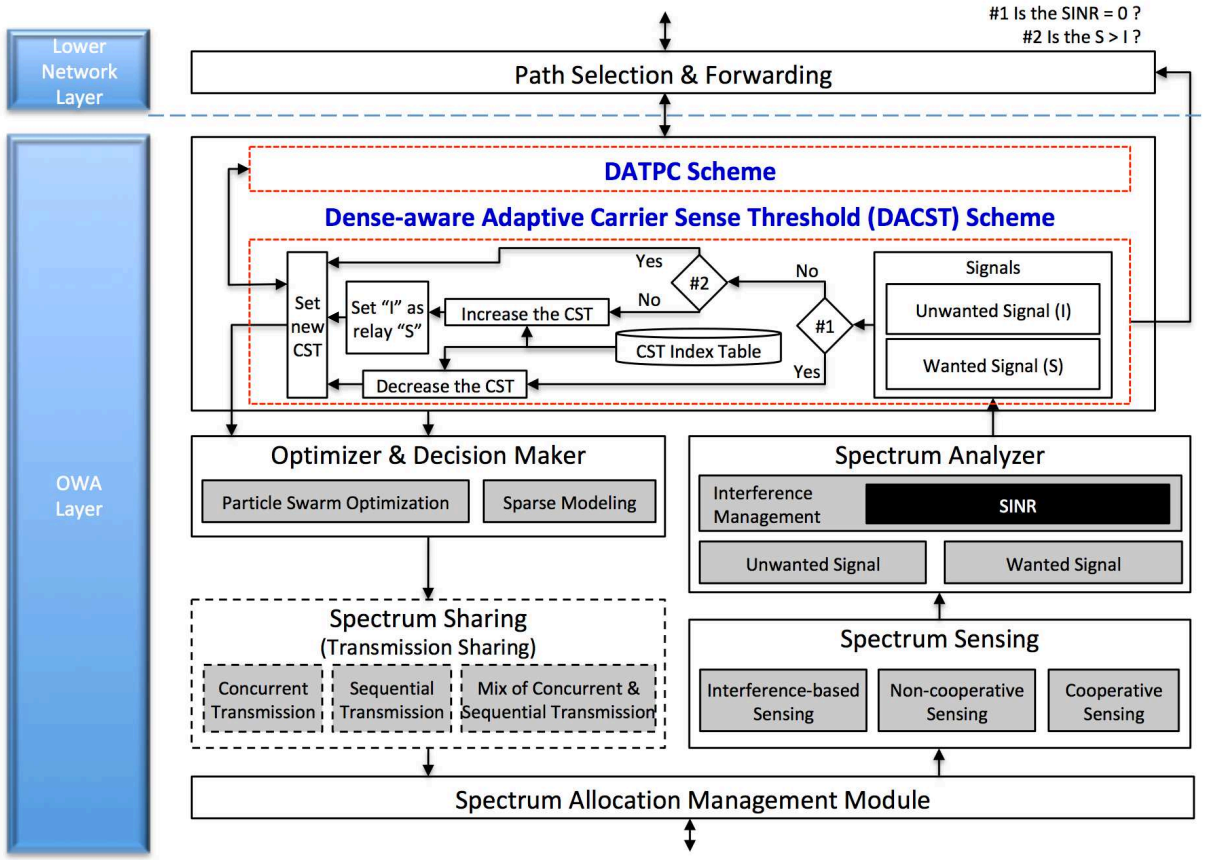

Figure 4-4: Dense-aware adaptive carrier sense threshold scheme

In this section, the proposed DACST scheme is described (see Figure 4-4). Proposed DACST comprises various components such as spectrum sensing (described in 2.4), spectrum analyzer, core parts of adaptive CST algorithm, path selection and forwarding, optimizer and decision maker, spectrum sharing (described in 2.5) and spectrum allocation

Algorithm 2 Adaptive CST Algorithm

01: **Definition**: t is timeslots, In is follow CST index table
02: **Input**: Initialize $CST_j(0) = 1$ (CST_{max})
03: **Ountput**: CST_j for timeslot $t+1$
04: **Begin**
05: Measure $S_{ij}(t), I_(kj)(t)$
06: Calculate $SINR_{ij}(t)$
07: **if** $SINR_{ij}(t) = 0$
08: $CST_j(t+1) = CST_j(t) + In$
09: Set $t \leftarrow t+1$ Go to step 05
10: **else**
11: **if** $S_{ij}(t) \geq I_(kj)(t)$
12: Set $t \leftarrow t+1$ Go to step 19
13: **else**
14: $CST_j(t+1) = CST_j(t) - In$
15: Set i as interference;
16: Set $k = \arg\min_{k \in \mathcal{I}} [I_{(kj)}(t)]$ as signal
17: Set $t \leftarrow t+1$ Go to step 05
18: **endif**
19: **endif**
20: **End**

management module.

The DACST scheme is a scheme that adjust the CST for the data receiving with low interference, path selection and forwarding. First, follow the maximum CST, receive the wanted signal (S) by using the proposed receiver based interference model. If the SINR is equal to 0, which means current CST setting cannot receive the packets from any source nodes. In this case, the CST should follow the CST index table to increase its index number of CST, which means decrease its corresponding dBm value. If the SINR is not equal 0, then go to next step. If the signal level is larger than interference level, then the current value of CST can be recognized as optimal CST for the receiver. Oppositely, if the signal is smaller than interference level, then the receiver recognizes neighbor nodes as relay nodes, then increase its index number of CST. This is the first function of DACST scheme for topology control. This can prevent the high interference communication with proposed DATPC scheme, and help the path selection and forwarding scheme to decide the routing path, increase total number of concurrent transmission.

In some situation, even after the topology control, the neighbor nodes still more than two (grid scenarios). Then the adaptive CST algorithm use sequential transmission to

optimize the network capacity (user experienced data rate). Under transmission sharing scheme, there is two selections for user experienced data rate optimization, which are sequential transmission or concurrent transmission. Here, if the sources are transmitting to the same receiver, then concurrent transmission is used with signal processing technique. If the receiver are different, sequential transmission is used with TDD technique.

4.4.1 Adaptive CST Algorithm

In this subsection, the proposed adaptive CST algorithm is described (see Algorithm 2). The core part of DACST scheme is the ACST algorithm.

4.4.2 Carrier Sense Threshold Index Tables

Carrier Sense Threshold Index Table 1 (CST = Corresponding dBm value)			
1 = -30	2 = -40	3 = -50	4 = -60
5 = -70	6 = -80	7 = -90	

Figure 4-5: Carrier sense threshold reference table for usual environments

Carrier Sense Threshold Table (CST = Corresponding dBm value)			
1 = -30	8 = -51	15 = -72	22 = -93
2 = -33	9 = -54	16 = -75	23 = -96
3 = -36	10 = -57	17 = -78	24 = -99
4 = -39	11 = -60	18 = -81	25 = -102
5 = -42	12 = -63	19 = -84	26 = -105
6 = -45	13 = -66	20 = -87	27 = -108
7 = -48	14 = -69	21 = -90	

Figure 4-6: Carrier sense threshold reference table for ultra-dense environments

Follow the ITU pathloss model with 60 GHz frequency, the CST interval is set as 3

dBm. Large value of interval would lead the convergence faster, relatively, small value of interval would lead high accuracy. The CST range is from -30 dBm to -108 dBm. For ultra-dense environments, the CST is changed from index 1 to index 27 (see Table. 4-6). For usual environment, the CST is adjusted from index 1 to index 7 (see Table. 4-5). Follow the CST index table, the network topology can be optimized.

4.5 Numerical Simulation for usual environment

Based on the system model, interference model, and spatial reuse calculation, network throughput and power consumption of a given MWN can be evaluated. In this section, routing and scheduling algorithms are not focused. We assume that a static routing is used to evaluate DATPC scheme with static CST values.

4.5.1 Scenarios

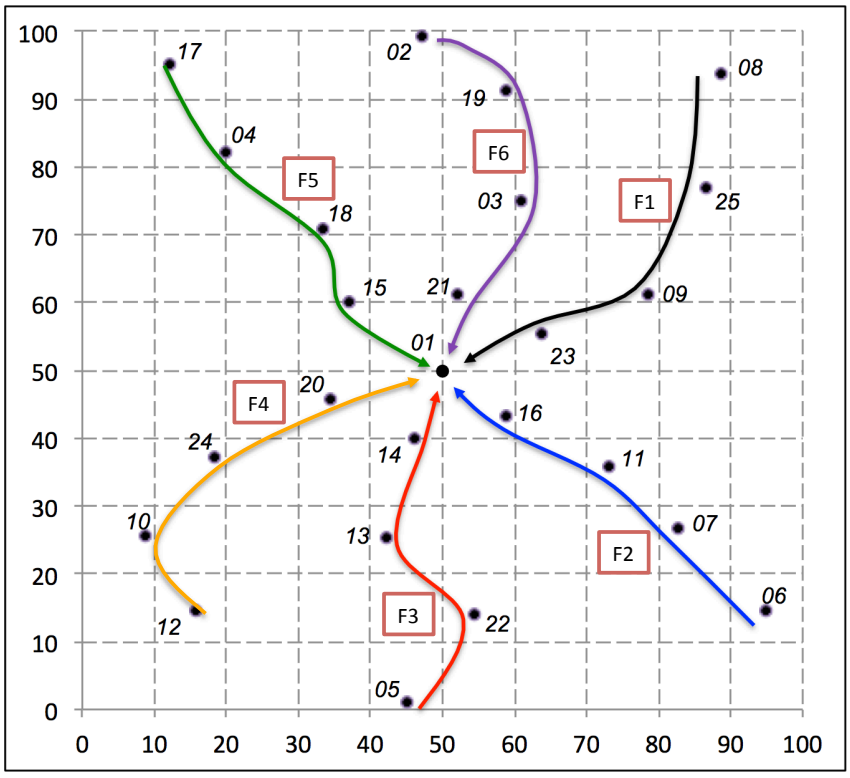

Figure 4-7: Star network topology of 25 nodes

The scenario including multi-flow is used to evaluate the DATPC and DACST schemes.

The topology is depicted in Figure 4-7. 25 nodes scenario has a star topology with the coverage area of 100 m × 100 m. There is only one destination (node 1) with 6 flows, and average hop count is 4. The distance between every two neighbor nodes in each flow is less than 20 m. Node 1 is the destination node that only receive data packets from other transmitters in this topology.

4.5.2 Parameters

The system parameters are listed in TABLE 4.1. Network simulation operates on the premise that the intermediate node can transmit and receive the data packets simultaneously without self-interference.

Table 4.1: Parameters for simulation and emulation

Parameter	Value
Minimum distance between nodes (d_0)	1 m
Maximum transmit power (P_{max})	0.1 Watt
Attenuation constant (α)	4.0
Wall attenuation (W_{ij})	0 dB
Shadowing parameter (X_σ)	8 dB
Noise level (η)	-174 dBm
Channel bandwidth (B)	10 MHz
Value depends on the choice of coding and modulation parameters, and the BER requirement (Γ)	1
Consensus coefficient (C)	Variable
CST†	Variable

In TABLE 4.1, the † mark means that the CST is follow CST index table 1 to adjust its corresponding dBm value in order to find out the transmit power limitation of DATPC

scheme when only DATPC scheme is used to evaluate dense network topology scenario. Here, the frequency is considered as less than 5 GHz.

4.5.3 Influence of CST for Usual Network

Table 4.2: The network performance with different CST of 25 nodes scenario

CST *(dBm)*		-90	-70	-50	-40	-30
CST Range *(m)*		354.8	112.2	35.5	19.9	11.2
$\bar{P}$(Watts)	No DATPC	0.1	0.1	0.1	0.1	0.1
	DATPC	0.0516	0.0473	0.2270	0.0596	N/A
	Propotion *(%)*	51.64	47.32	22.70	59.57	N/A
Minimum P (Watts)		0.0123	0.0040	0.0009	0.0127	N/A
$\bar{U}$ (Kbps)	No DATPC	0.6603	0.6694	10.4014	216.2292	N/A
	DATPC	0.6331	0.7338	43.3738	367.5471	N/A
	Proportion *(times)*	0.95	1.1	4.17	1.7	N/A
EE (bits/Joule)	No DATPC	6.69	6.69	104.01	2162.29	N/A
	DAPTC	12.26	15.51	1910.740	6170.01	N/A

Network performance is analyzed with different CST. While the network scale shrinks from sparse to dense, DATPC scheme does not work well. Because in dense network, the distance between nodes are short, all the nodes with small CST become neighbors, which means all the nodes share the communication medium simultaneously. In TABLE 4.2, the results indicate that either minimum transmit power or CST of the existing hardware specification is required to be changed in order to cope with the dense wireless network topology when power control is applied. The column of "CST = -90" is the normal setting for the UEs, and the results show that only the DATPC scheme reduced the power consumption without improvements of end-to-end throughput. The limitation of current CST is from -65 dBm to -100 dBm. In wireless UDNs, the CST should be changed from -35 dBm to -70 dBm. The column of "CST = -50" shows that when the CST increase, the DATPC works very well (with 22.7% average transmit power to achieve

4.17 times average end-to-end throughput). And if "CST = -40", the DATPC improves much better. However, the column of "CST = -30" shows that there are limitations to set the sensitivity. Through the routing table, which means the settings of CST must make sure that there is at least one neighbor node inside of its range.

4.6 Numerical Simulation for dense environment

In this section, the cooperation of DACST and DATPC is analyzed. Here, the routing protocol is not focused.

4.6.1 UDNs Scenarios

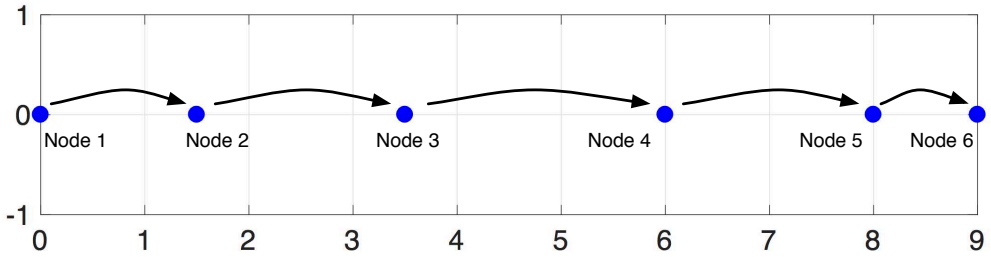

Figure 4-8: 6 nodes chain topology with full communication

One simple scenario with 6 nodes chain topology is used to evaluate the DACST and DATPC schemes. The topology is depicted in Fig. 4-8. The 6 nodes chain topology is follow the definition of wireless UDNs. The average distance between 2 nodes is about 2 meters. There is only one destination (node 6) with 5 flows, which means every nodes except node 6 is transmitting different packets to node 6.

Another scenario with 121 nodes grid topology is also used to evaluate the DACST and DATPC schemes. The topology is depicted in Fig. 4-9. The 121 nodes grid topology is follow the definition of wireless UDNs. The average distance between 2 nodes is about 1 meters. There are 8 destinations (left side nodes near to the access point) with 112 flows, which means every nodes except destination nodes are transmitting different packets.

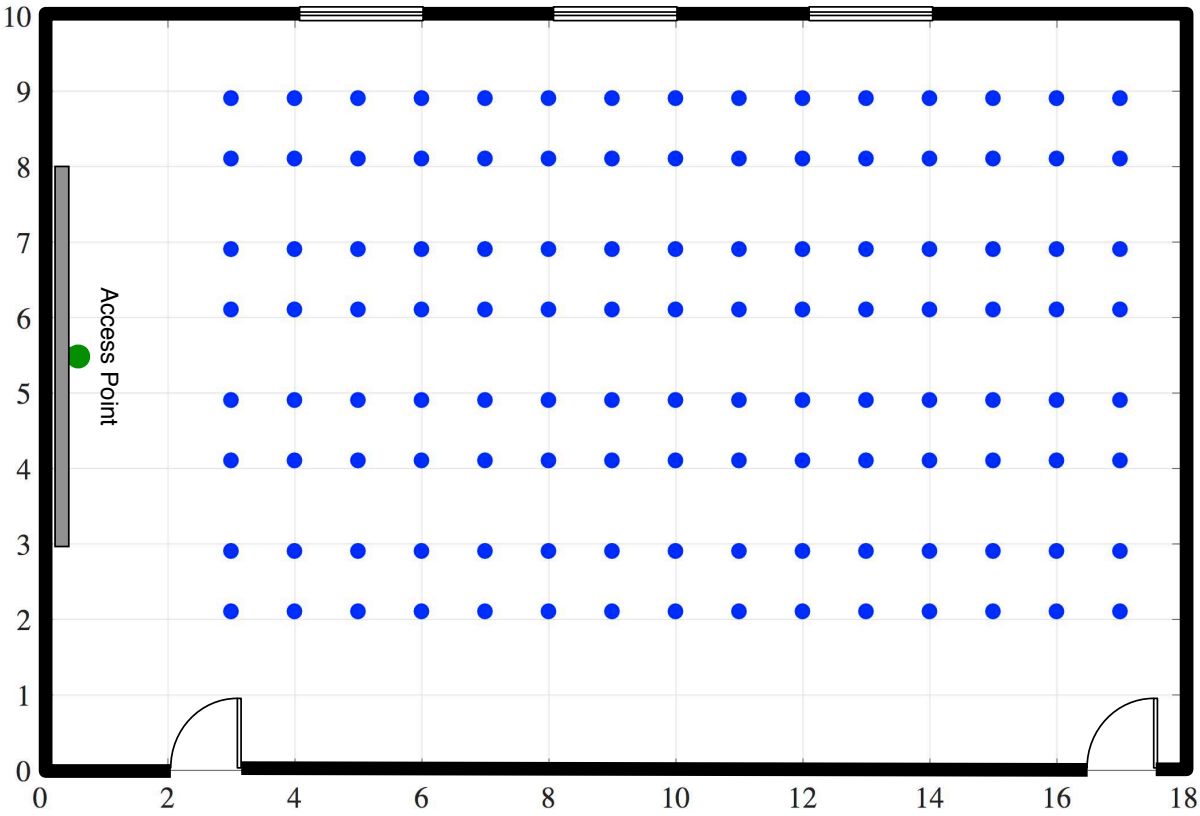

Figure 4-9: 121 nodes grid topology with full communication

4.6.2 Parameters

The system parameters are listed in TABLE 4.3. Network simulation operates on the premise that the intermediate node can transmit and receive the data packets simultaneously without self-interference.

In TABLE 4.3, the CST is follow CST index table 2 to adjust its corresponding dBm value. Here, the mmWave is used for wireless UDNs, thus, the frequency is set as 60 GHz. Channel bandwidth is set as 100 MHz for common. The unlicensed band at 60 GHz provides additional bandwidth, around 7 GHz, offering an opportunity for coexistence with unlicensed use, e.g. by using a WiFi coexistence mode.

The intent to deploy wireless UDNs in the millimeter-wave band follows trends in other systems, e.g., IEEE 802.11ad, that specify short range high-bandwidth connectivity in the unlicensed band at 60 GHz. The wireless UDNs aim for tight integration with an overlaid cellular network and will support mobility both locally and with the overlaid network. While the wireless UDN can be deployed in the unlicensed 60 GHz band, it will generally

Table 4.3: Parameters for simulation

Parameter	Value
Minimum distance between nodes (d_0)	1 m
Frequency (f)	60 GHz
Distance power loss coefficient (α)	22
Floor penetration loss factor (L_f)	0
Maximum transmit power (P_{max})	0.1 Watt
Minimum transmit power (P_{min})	1×10^{-7} Watt
Noise level (η)	–174 dBm
Channel bandwidth (B)	100 MHz
Value depends on the choice of coding and modulation parameters, and the BER requirement (Γ)	1
Maximum CST (CST_{max})	–30 dBm
Minimum CST (CST_{min})	–108 dBm
CST interval	3 dBm
Consensus coefficient (C)	Variable

support a variety of spectrum bands and regulatory regimes [82]. Transmit power levels UEs in wireless UDNs is normally set as 10 dBm (0.01 watt), thus, for evaluation of proposed approach, the maximum transmit power is set as 20 dBm (0.1 watt). Noise level is set as -174 dBm due to the indoor environment.

4.6.3 Simulation Results of 6 nodes Chain Topology

Single hop Transmission

Figure 4-10 shows user experienced data rate and transmit power versus number of iterations with single-hop transmission. Single hop is because the DACST is fixed for a static value, and all the nodes are transmitting their packets to the same destination

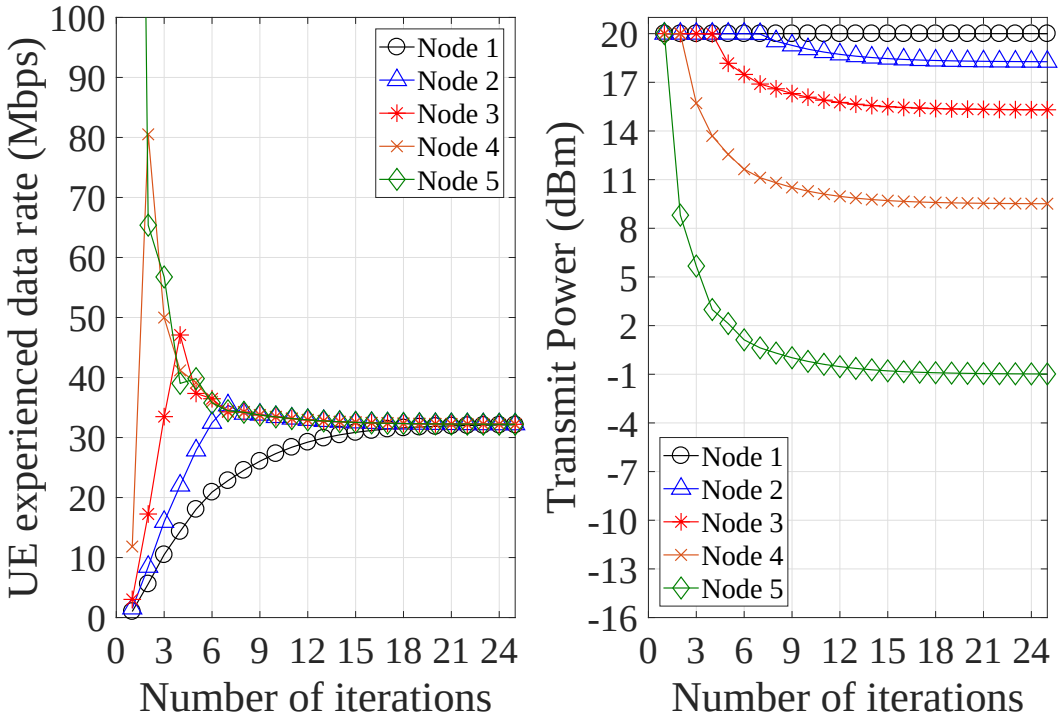

Figure 4-10: User experienced data rate and transmit power versus number of iterations with single-hop transmission

simultaneously. There is a great gap of user experienced data rate among each node. At iteration of "0", user experienced data rate of node 5 is around 300 Mbps, constantly, node 1, node 2 and node 3 are all less than 5 Mbps. Under the proposed DATPC scheme, the user experienced data rate of node 1, 2 and 3 is increase to more than 20 Mbps. Also, as iteration proceeds, the transmit power of node 5, 4 and 3 decreased dramatically to mitigate their interference.

Multihop Transmission

Figure 4-11 shows user experienced data rate and transmit power versus number of iterations with multihop transmission. Multihop is because the DACST is dynamic change the network topology, which means the packets from node 1 to node 6 cannot be directly delivered. Through the CST topology control, the nodes can only communicate with their neighbor nodes. Here, the ϵ of each link is different. There is only one flow shared the link_{12}, and 5 flows shared the $link_{56}$. There is a gap of user experienced data rate among each node. At iteration of "0", user experienced data rate of node 5 is around

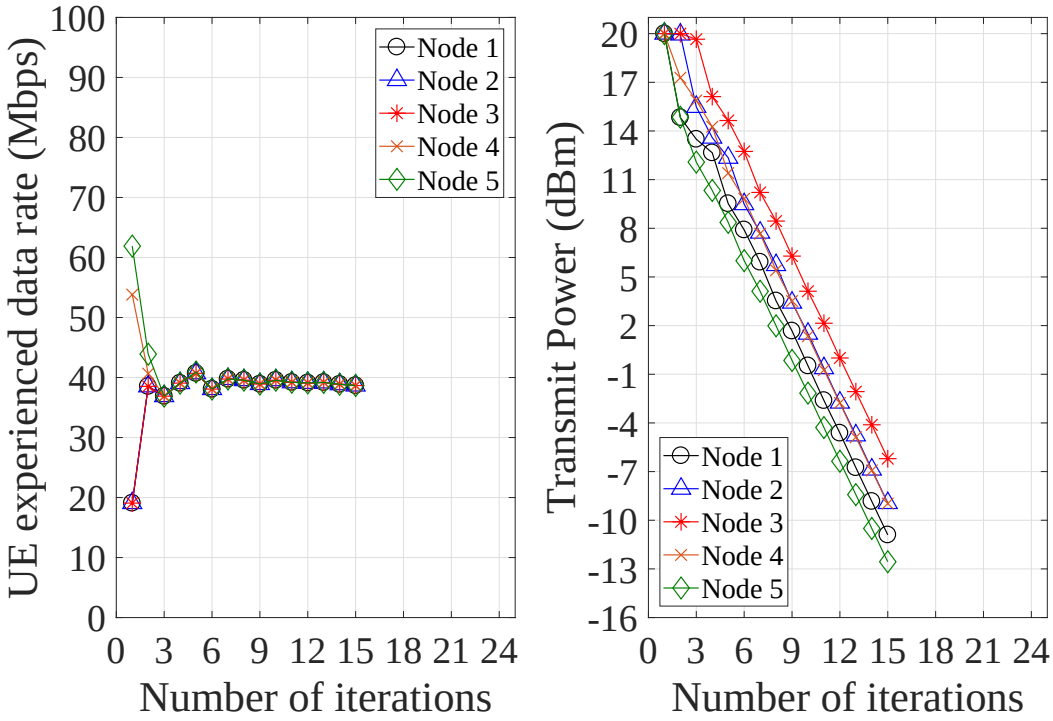

Figure 4-11: User experienced data rate and transmit power versus number of iterations with multihop transmission

60 Mbps, constantly, node 1, node 2 and node 3 are all less than 20 Mbps. Then the proposed DATPC works, thus, the user experienced data rate of all nodes are converged to around 40 Mbps. Also, as iteration proceeds, the transmit power of all nodes decreased to mitigate their interference. Here, it can be noticed that the proposed DACST scheme can prevent the cross talking, and multihop fashion can dramatically increase the user experienced data rate and decrease the total transmit power.

Performance of Energy Efficiency

Figure 4-12 shows the energy efficiency versus number of iterations. The black triangle line is the single-hop transmission, which means fixed CST value, and the red square line is the multihop transmission, which employs the DACST scheme. Before the iterations of "8", there is no much difference between them, that's because all of the two fashions are worked under the proposed DATPC scheme. However, for single-hop transmission, the node 1 and node 2 is far away the destination node. Thus, the have to maintain there transmit power to achieve higher user experienced data rate (see Fig. 4-10). For

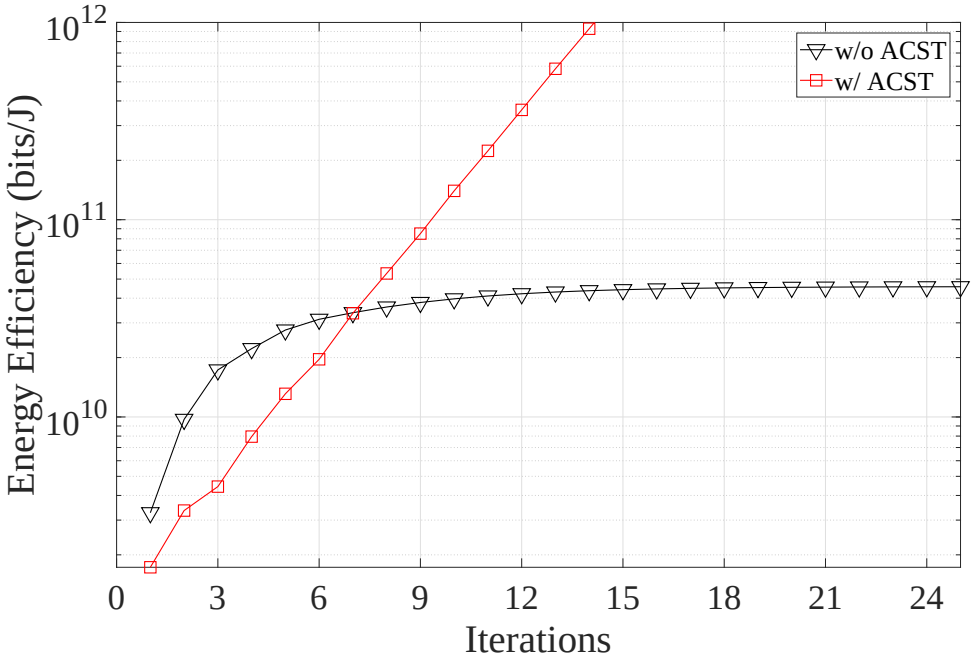

Figure 4-12: Energy efficiency versus Number of iterations for 6 nodes scenario

multihop transmission, after 3 times iterations, the nodes already converge to the balance. Due to the dense environment, the noise is too less (changed with temperature). Thus, the $SINR$ is similar to SIR. When they find the balance point, all of the nodes can decrease their transmit power together without influence on user experienced data rate. Also, if the interference level is near to the noise level, the balance would be break. Form this figure, we notice that the dramatic advantages can be achieved from proposed DACST and DATPC cooperation for high performance communication.

Influence of Consensus Coefficient

Figure 4-13 shows the number of iterations versus consensus coefficient. The black triangle line is the single-hop transmission, which means fixed CST value, and the red square line is the multihop transmission, which employs the DACST scheme. As we analyzed in Chapter 3, adjustment of the consensus coefficient can achieve the margin of user experienced data rate. For ultra dense environment, besides of that, adjustment of the consensus coefficient also can accelerate the convergence faster. For single-hop, due to the great gap among nodes, consensus coefficient should be less than 1. If the value of consensus coefficient is greater than 1, the gap among nodes cannot be eliminated, thus, the user experienced

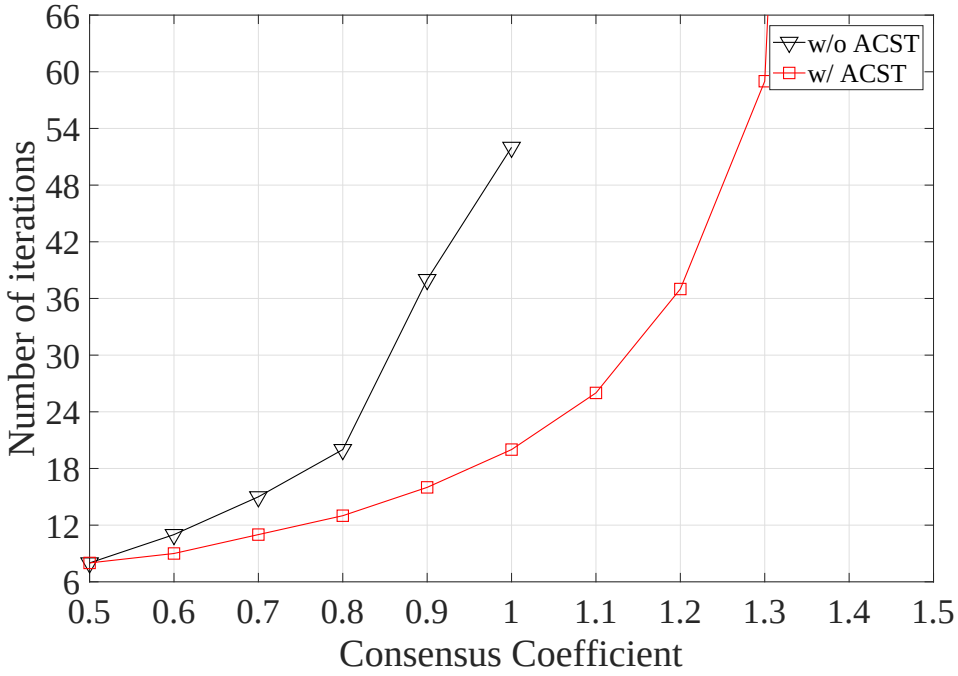

Figure 4-13: Number of iterations versus consensus coefficient for 6 nodes scenario

data rate cannot converge with the same value. Similarly, the value should less than 1 for multihop transmission to accelerate the convergence efficiently. With DACST scheme, the number of iteration are much less due to the DACST also need iterations to converge. Thus, the decreased consensus coefficient can accelerate the convergence faster.

4.6.4 Simulation Results of 121 nodes Grid Topology

Performance of proposed CTPC and ACST

Figure 4-14 shows UE experienced data rate in Mbps with or without proposed CTPC and ACST algorithms. Here, box plot is used due to there are 112 transmitting nodes. For the first column, which means without two proposed algorithms, most of the UE experienced data rate is less than 1.5 Mbps, and the average is only 0.4 Mbps. With proposed CTPC algorithm only, the UE experienced data rates converge to 1.68 Mbps. With proposed ACST algorithm only, the UE experienced data rates are less than 1.67 Mbps, and average is almost 1.4 Mbps. With proposed CTPC and ACST algorithms, the UE experienced data rates converge to 1.71 Mbps. From the UE experienced data rate, it can be demonstrated that the proposed CTPC algorithm can increase the UE experienced

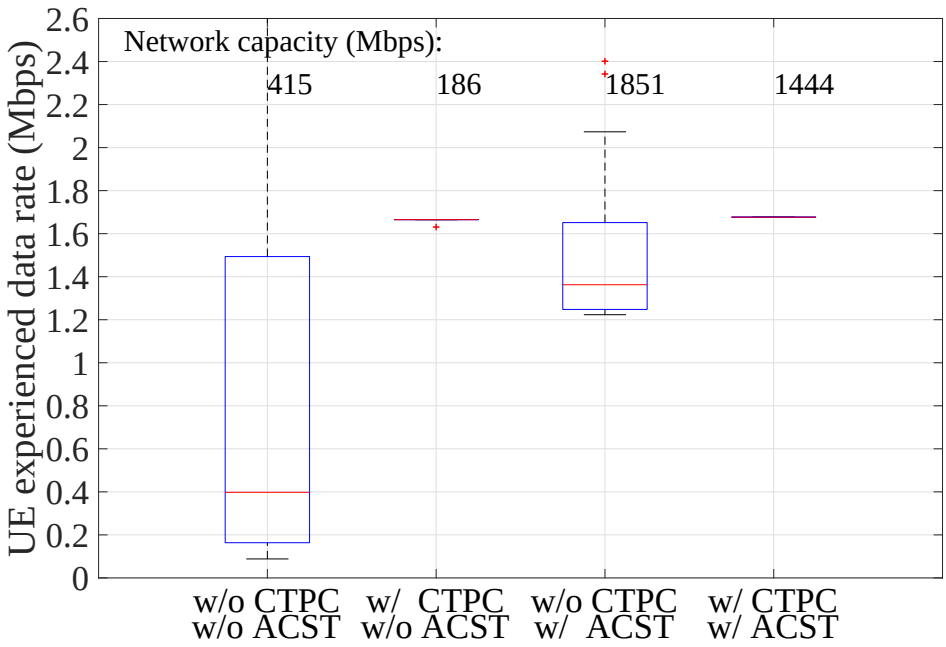

Figure 4-14: Comparison of CTPC and ACST on UE experienced data rate

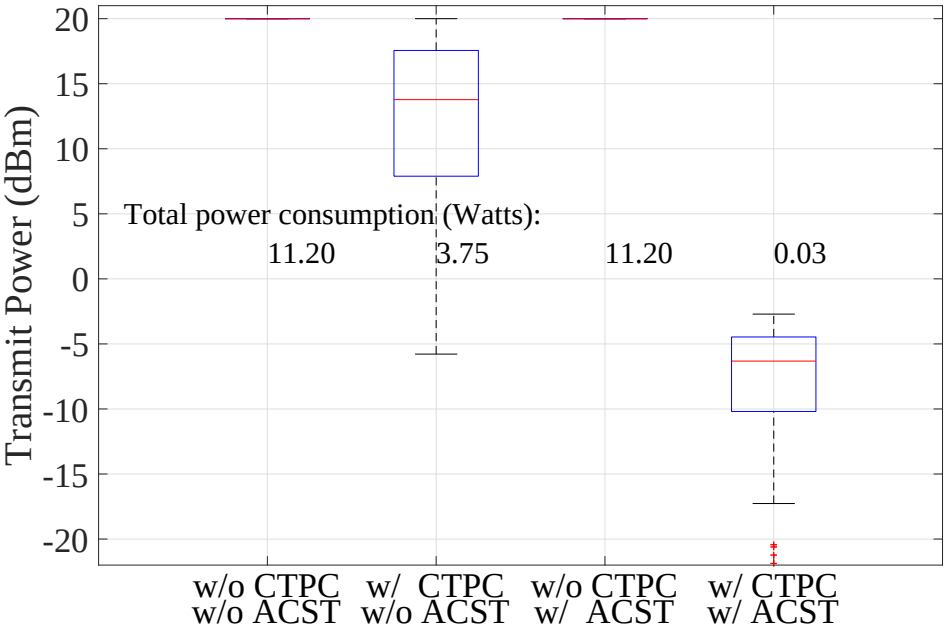

Figure 4-15: Comparison of CTPC and ACST on transmit power

data efficiently.

Figure 4-15 shows transmit power in dBm with or without proposed CTPC and ACST algorithms. Here, box plot is used due to there are 112 transmitting nodes. For the first

column, which means without two proposed algorithms, all of the transmit power are 20 dBm. With proposed CTPC algorithm only, most of the transmit power decreased. Some nodes are far away the destination nodes, thus, they maintain their transmit power as original to achieve best UE experienced data rate. The average of the transmit power is less than 15 dBm. With proposed ACST algorithm only, the transmit power of all nodes maintain the original (20 dBm). With proposed CTPC and ACST algorithms, the transmit power decrease sharply. Due to the performance of ACST algorithm, the single hop transmission is changed to multihop transmission, the CTPC algorithm can achieve better performance.

Form these two figures, it can be demonstrated that the best (4.18×) UE experienced data rate can be achieved with minimum (0.27%) power consumption with proposed CTPC and ACST algorithms.

Performance of Energy Efficiency

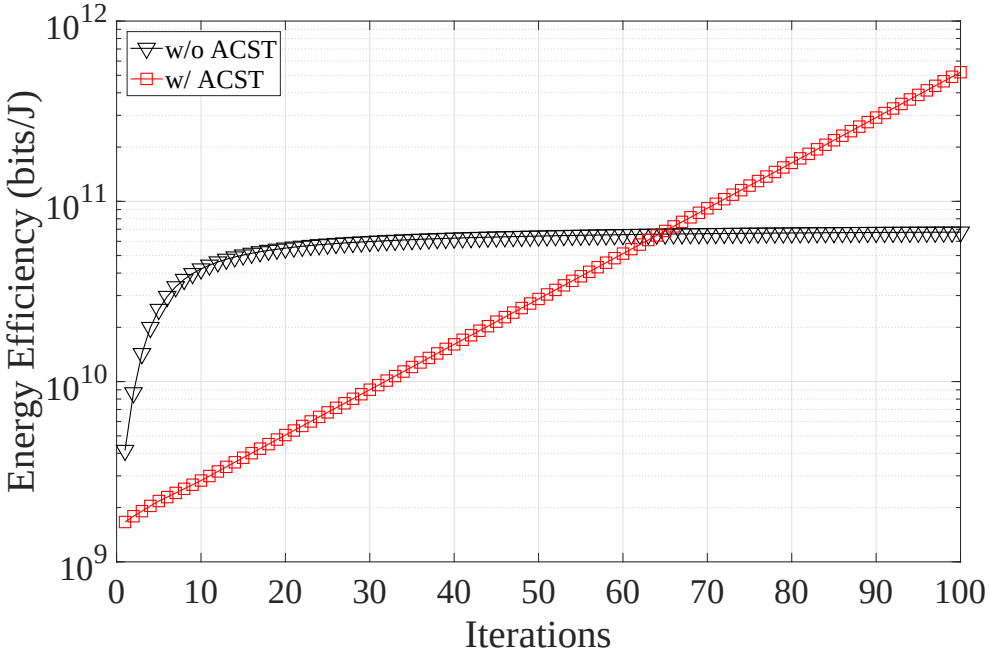

Figure 4-16: Energy efficiency versus Number of iterations for 121 nodes scenarios

Figure 4-16 indicates that with ACST algorithm, the CTPC algorithm can achieve best energy efficiency. With CTPC algorithm only, the energy efficiency also can be improved. Due to wireless UDNs environment, the noise level is much smaller than the

interference level. The performance on energy efficiency with proposed CTPC and ACST also would converge when the interference level is similar with noise level.

Influence of Consensus Coefficient

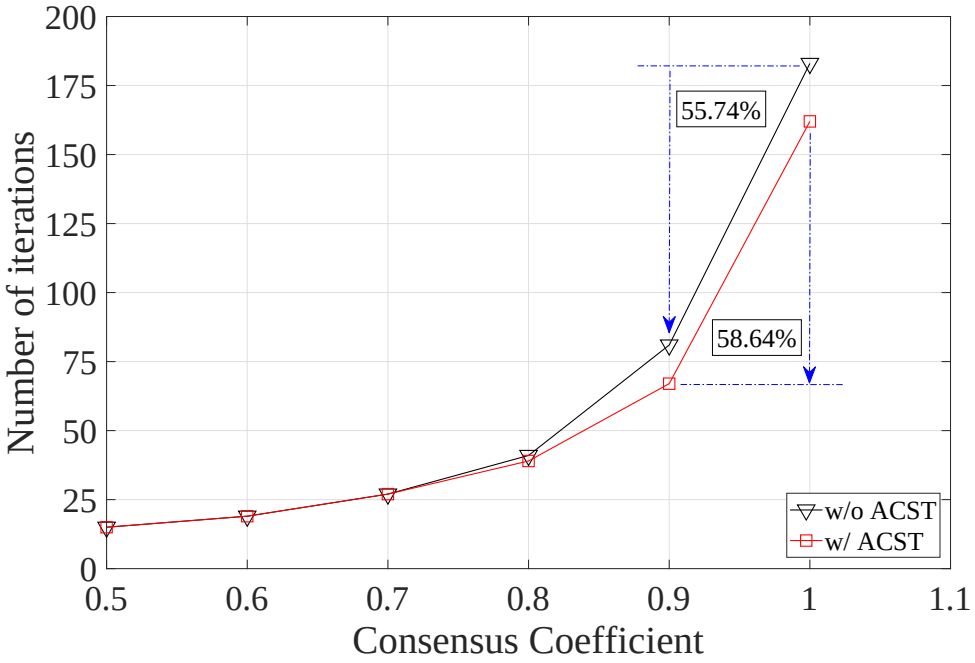

Figure 4-17: Number of iterations versus consensus coefficient for 121 nodes scenarios

Figure 4-17 indicates that the number of iterations versus consensus coefficient for 121 nodes scenarios. The black triangle line is the results without DACST scheme, and the red square line is the results that employs with DACST scheme. Adjustment of the consensus coefficient can accelerate the convergence faster. Compare with the results of 6 nodes scenarios, the number of iterations is much longer due to there are more transmitting nodes. For these kind of complete scenarios, the consensus coefficient play an important role. Only change the value of consensus coefficient from "1" to "0.9", both of the iterations decrease more than 55%. Less consensus coefficient can accelerate the convergence faster. Higher than "1" cannot lead the UE experienced data rate converge.

4.7 Emulation testbed

Not only network simulation, but also network emulation are used for evaluation in this chapter.

For the emulation environment, advanced wmediumd emulator is implemented on StarBED. StarBED is a large-scale wired-network testbed managed by the National Institute of Information and Communications Technology of Japan at the Hokuriku StarBED Technology Center located in Ishikawa prefecture, Japan [62]. The core of StarBED consists of a cluster of around 1100 standard PCs, the *experiment nodes*, which have redundant full connectivity by means of a switch cluster. Virtualization techniques such as VMware can be employed to increase the number of logical experiment nodes. QEMU is used for Starmesh emulator architecture. In addition to the core experiment network, there is a dedicated management network that controls and monitors node and switch activity. Nodes can be loaded with the appropriate software, controlled, and monitored by using the management network, thus not affecting the experiments [83].

4.7.1 StarBED

First of all, let me introduce some basic knowledge about the StarBED testbed.

StarBED is a large-scale network experiment environment designed and managed by the Hokuriku Research Center of the National Institute of Information and Communications Technology (NICT), located in Ishikawa prefecture, Japan. StarBED development started in 2002 with the goal of creating a testbed on which researchers can evaluate network technologies in realistic situations similar to those in the Internet. In 2006, the focus of StarBED changed during its second phase. The coverage area of StarBED widened to include more network technologies, such as ad hoc networks, mobile networks, home networks, and sensor networks, all of them being included under the name of "ubiquitous networks". Then, in 2011, StarBED commenced the 3rd Phase "StarBED^3". The mission scope was expanded to include research and development of new-generation networks and their security and services as well as planning the expansion of methods to deal with various mixed wired and wireless networks and cyber physical systems. Moreover, StarBED are providing testbeds capable of experimenting and verifying at the software implementation level as the large scale emulation testbed, and supporting network research and

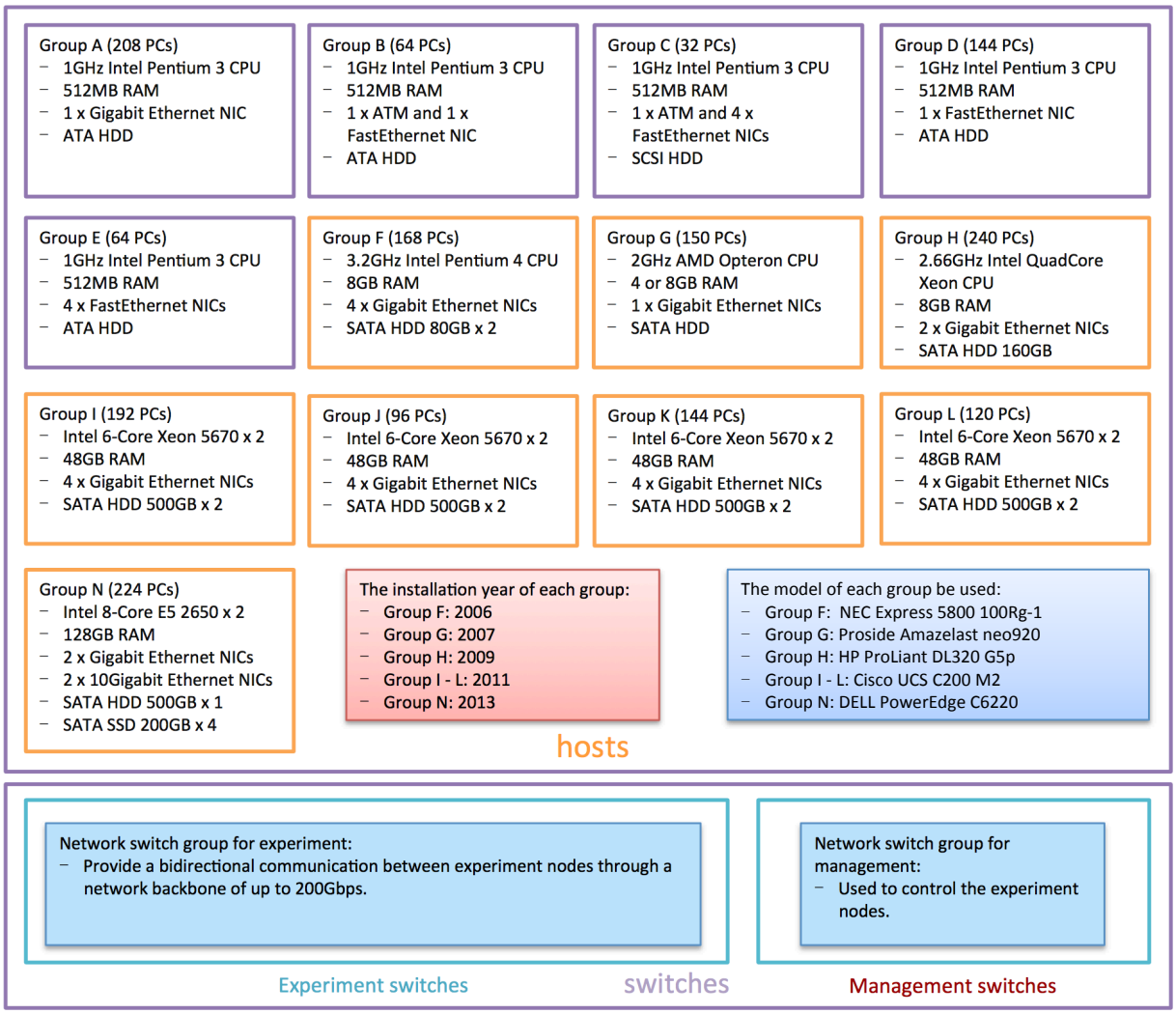

Figure 4-18: StarBED hosts and switches

development. StarBED is composed of both hardware and software components that work together to help users achieve the above mentioned goals.

- Hardware: More than 1100 PCs and more than a dozen switches make up the physical infrastructure of the testbed, we can se more details in Figure 4-18.

- Software: Two main sets of tools, called SpringOS and RUNE, were developed to enable experiments on the testbed.

In the figure I should mention that, Group A E is already belong to “Past experiment node groups" which have been used from 2002 to 2011. Now from Group F to N are used for experiment. As of August 2013, the 1,334 experiment nodes were divided into seven

groups as shown in the **Fig. 4-18**. We also can see the three groups of StarBED, as experiment node group, network switch group for management, and network switch group for experiment. The experiment network connects the experiment nodes via experiment switches, creating an environment which is independent from other networks and that makes possible highly-dependable network experiments and verification.

For this time, I used ten nodes of group K to evaluate the proposed DATPC scheme. The main specification of Group K nodes are list in **Fig. 4-19**.

Model	Cisco UCS C200 M2	
Chipset	Intel® 5520 (Tylersburg) chipset	
CPU	Intel 6-Core Xeon X5670 x 2	
Memory	48GB	
HDD	SATA 500GB x 2	
Optical Drive	DVD-ROM Drive	
NIC	(on-board) single Management Interface	for ipmi ×1
	(on-board) double GigabitEthernet Intel Gigabit Ethernet Adopter	for management ×1
		empty×1
	(extend) quad GigabitEthernet Broadcom 5709 Quad Port 10/100/1GB NIC w/TOE iSCSI	for experiment ×4

Figure 4-19: The parameters of group K

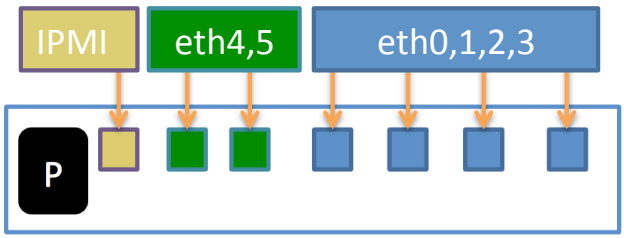

Figure 4-20: The interfaces of each real node in StarBED

For each node of Group I, we can se the interfaces of each real node in StarBED. I create an image of each real node's interfaces in **Fig. 4-20**. As we see, there are seven interfaces. The black one means the power ports. The yellow one is IPMI Gigabit Ethernet port, which is take charge of KVM console during the experiment. The nodes of Group I are assigned with IP address range 172.16.31.x/24. The two green ports are management Gigabit Ethernet ports, which are the real network interfaces of each node in the hole network. The nodes of Group I are assigned with IP address range 172.16.21.x/24. Now, only one of them is used to assign the IP address in the network, such as "eth4".

Another one is reserved, such as “eth5". The four dark blue ports are Gigabit Ethernet ports (mapped to “eth0", “eth1", “eth2", “eth3"), can be used by users or developers to configure, test, and emulate user's own network topology, and of course, can be assigned any IP addresses.

4.7.2 Starmesh Emulator

The purpose of StarMesh architecture is to design a station (STA) instance as a duplicable copy to create the same STA instance, so that the large-scale of STA instances can be emulated over the StarBED facilities. The objectives of design are to minimize the coding load of a researcher in order to enable many STA instances interact with among themselves and to link the STA instance in a quick way using the StarBED OS under the OS environment of Ubuntu.

Figure 4-21 depicts the Starmesh emulator architecture. Wmediumd is developed by Javier Lopez and Javier Cardona, cozybit Inc. It only supports that multiple experiment nodes emulated on one host. The advanced wmediumd adds new modules of communication, control, etc. Communication module supports experiment nodes communicate with others that are implemented on other hosts. Channel control module collects information of each experiment nodes and gives instructions to them. Mhop module is a user space module. The functions, such as multihop fashion and TPC algorithm, are implemented in this module. The emulation architecture environment is implemented on StarBED facilities. For each experiment node, it acts as an independent wireless node base on different QEMU. Due to this novel architecture, the use of real hosts leads it possible to realistically emulate wireless network environments. This emulator can employ the proposed DATPC scheme, but due to the usage of real equipment, the CST value has their own specification. Thus, the sparse scenarios are selected for the evaluation.

4.7.3 Emulation Results

In this subsection, a comparison between simulation and emulation is done with the 25 nodes scenario.

Because of limited source of StarBED nodes (10 experiment nodes only available for this evaluation), and on each experiment node, we only run 2 qemu for more realistic

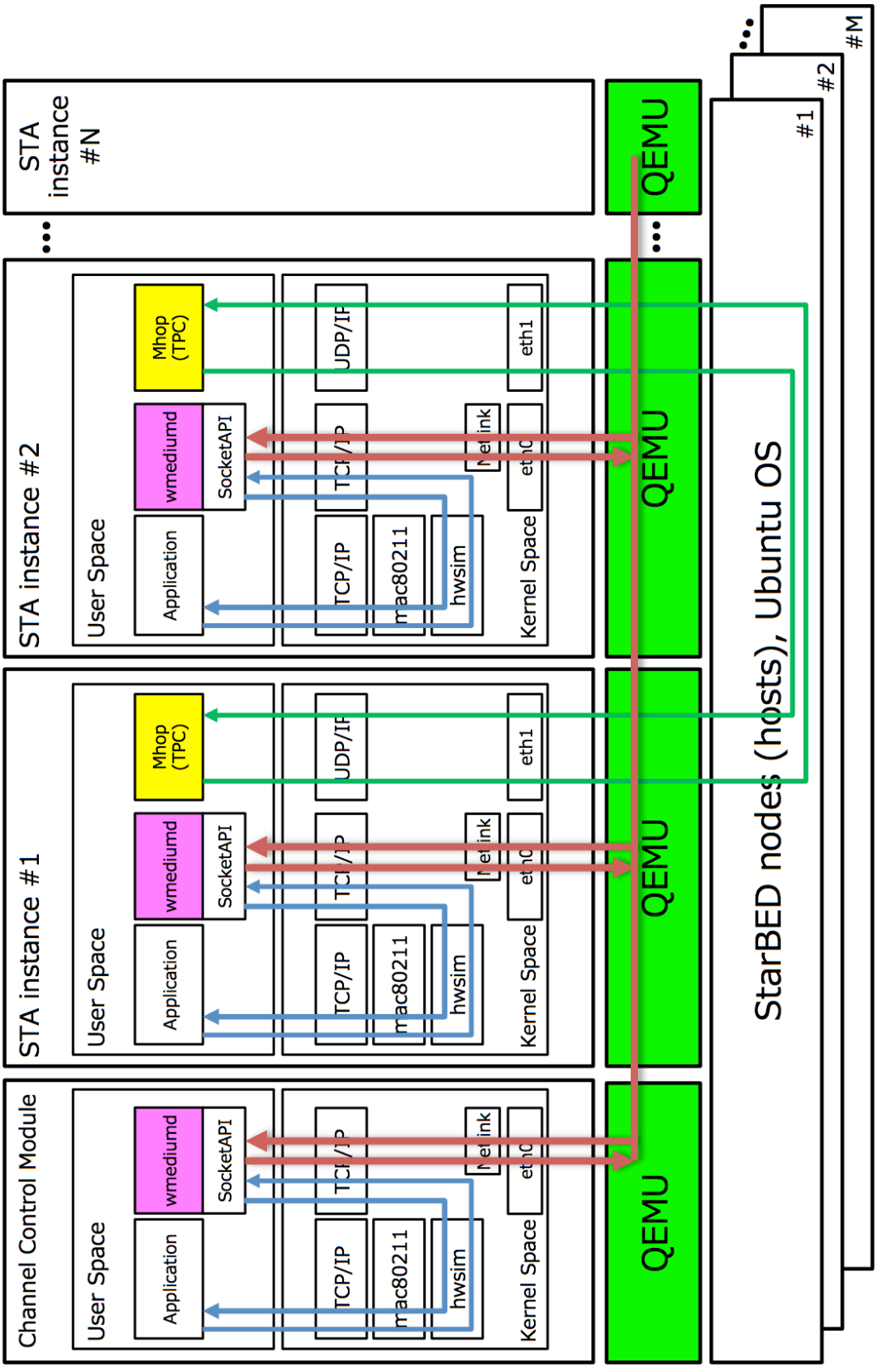

Figure 4-21: Starmesh architecture for multihop wireless network emulation

25 nodes scenario		Emulation	
		Flows (1, 3, 5)	Flows (2, 4, 6)
P (dBm)	No TPC	20	20
	CTPC	13.47	11.84
	Proportion	22.23%	15.28%
Average		18.76%	
U (Mbps)	No TPC	2.05	2.73
	CTPC	2.79	2.01
	Proportion	136.10%	73.63%
Average		104.86%	
EE(bits/Joule)	No TCP	2.05×10^4	2.73×10^4
	TCP	1.26×10^5	1.32×10^5

P: average transmit power; U: average end-to-end throughput; EE: energy efficiency;
Proportion of P: CTPC (watts)/No TPC (watts) ×100%; Proportion of U: CTPC (bps)/No TPC (bps) ×100%;

Figure 4-22: Comparison results of 25 nodes scenario with proposed DACST and DATPC

results, the flows are separated into two groups, Flow 1, 3, 5 as group one, and Flow 2, 4, 6 as group two. The results is divided into two independent column (each group run 5 times). Emulation results show that, only with 18.76% average transmit power, the network throughput can achieve 1.05 times than no TPC cases. More detail is showed in Table 4-22.

It can be concluded as emulation results show that proposed CTPC only has little progress on UE experienced data rate due to the ACST algorithm cannot be implemented with current equipment specification. But the power consumption is significantly reduced.

4.8 Summary

In this chapter, the cooperated DATPC and DACST scheme had been evaluated through both simulation and emulation in D2D communication networks with multihop fashion. The simulation results reveal that DATPC scheme can improve end-to-end throughput and can reduce the total power consumption. With the current hardware specifications of the transmit power and the CST, the only DATPC scheme does not work well in wireless UDNs. However, the DATPC and DACST scheme cooperation do enable all data flows to

accomplish the maximum end-to-end throughput when the values of the transmit power and the CST are further reduced beyond the hardware specification setting. On the other hand, the emulation results also depict the advantage of proposed DATPC scheme, because emulation use real devices for the evaluation, the DACST with current hardware specification can not be evaluated. Future research work will be conducted to investigate the performance of DATPC and DACST schemes with different kind of network topologies (i.e., grid and random) in both sparse and dense environments.

Chapter 5

Dense-aware Low-Latency Communication Control Scheme

In this chapter, the dense-aware low-latency communication control scheme in LTE and WiFi using spatial diversity and encoding redundancy is discussed. In mobile and wireless networks, controlling data delivery latency is one of open problems due to the stochastic nature of wireless channels, which are inherently unreliable. This scheme opens an opportunity to explore how the current best-effort throughput-oriented wireless services could be evolved into latency-sensitive enablers of new mobile applications such as remote three-dimensional (3D) graphical rendering for interactive virtual/augmented-reality overlay. Assuming that the signal propagation delay and achievable throughput meet the standard latency requirements of the user application, we examine the idea of trading excess/federated bandwidth for the elimination of non-negligible delays of data re-ordering, caused by temporal transmission failures and buffer overflows. The general scheme design is based on (i) spatially diverse data delivery over multiple paths with uncorrelated outage likelihoods; and (ii) forward packet-loss protection (FPP), creating encoding redundancy for proactive recovery of intolerably delayed data without end-to-end retransmissions. Analysis and evaluation are based on traces of real life traffic, which is measured in live carrier-grade long term evolution (LTE) networks and campus WiFi networks, due to no such system/environment yet to verify the importance of spatial diversity and encoding redundancy. Analysis and evaluation reveal the seriousness of the latency problem and that the proposed FPP with spatial diversity and encoding redundancy can minimize

the delay of re-ordering. Moreover, a novel FPP effectiveness coefficient is proposed to explicitly represent the effectiveness of FPP implementation.

5.1 Introduction

Nowadays, wireless networks and associated technologies are playing more important role in human daily life. Two frequently used wireless networks are cellular networks and wireless local area network (WLAN). On one hand, the first and second generations of cellular networks for mobile communications provided users with basic connectivity using analog and digital technology, respectively. The third generation networks, such as the code division multiple access (CDMA) based high speed packet access (HSPA) systems, enabled mobile Internet access in addition to wireless voice telephony. The fourth generation is represented by the current orthogonal frequency-division multiple access (OFDMA) based LTE systems that has emerged to be a true mobile broadband solution for heterogeneous traffic consisting of voice, video, and Internet data with higher deployment and maintenance costs. On the other hand, the WLAN specified by the Institute of Electrical and Electronics Engineers (IEEE) 802.11 protocol family (WiFi) is being deployed continuously. The 802.11 family consists of a series of half-duplex over-the-air modulation techniques that use the same basic protocol. 802.11-1997 was the first wireless networking standard in the family, but 802.11b was the first widely accepted one, followed by 802.11a, 802.11g, 802.11n, and 802.11ac. 802.11b and 802.11a works in the 2.4 GHz band with direct-sequence spread spectrum (DSSS) based transmission scheme and in the 5 GHz band with orthogonal frequency-division multiplexing (OFDM), respectively. 802.11g is the third modulation standard that works in the 2.4 GHz band with OFDM. 802.11n is an amendment that improves upon 802.11 standards by adding multiple-input multiple-output antennas (MIMO), operates on both the 2.4 GHz and the 5 GHz bands. The latest amendment is 802.11ac which supports wider channels in the 5 GHz band, more spatial streams, higher-order modulation, and the addition of Multi-user MIMO (MU-MIMO). Different to cellular networks, WiFi only provides excellent communication quality for users at low deployment costs in small coverage area.

Modern mobile devices, such as smart phones and tablets, already support multi-technology multi-band networking: they are commonly equipped with multiple LTE, WiFi

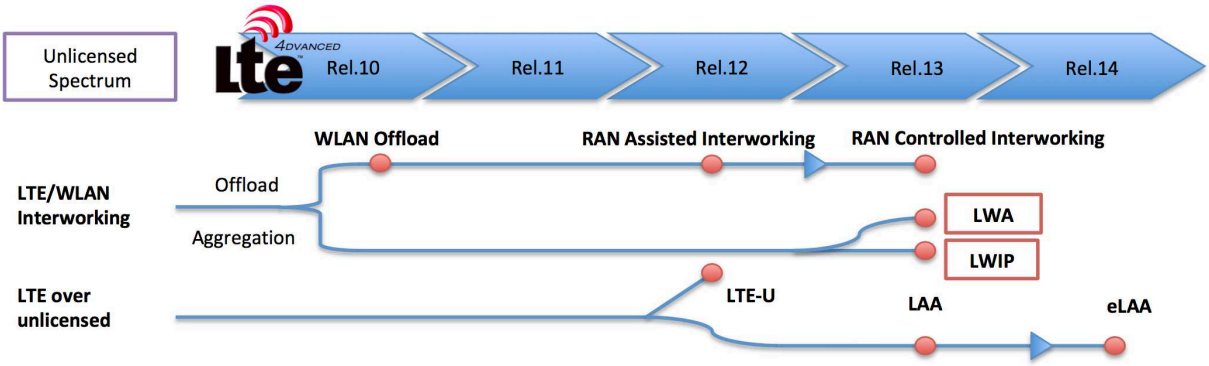

Figure 5-1: LTE-WLAN aggregation works from 3GPP.

transceivers operational in multiple licensed and unlicensed frequency bands. However, users only utilize one of the technologies at a time, either by user choice or by device control mechanisms. They have one aspect in common: best-effort data delivery, but without any quality of service (QoS) guaranteed by the network [84]. Opening gap between the growths of revenue and mobile data traffic [1, 85] brought general interest to enable new latency-sensitive applications such as steering and control of real and virtual objects (Tactile Internet), remote 3D graphical rendering for virtual/augmented-reality overlay, remote traffic control of self-driving cars and drones, closed loop control of industrial processes, and gaming [86, 87]. To overcome these challenges, third generation partnership project (3GPP) radio access network (RAN) presented to the IEEE 802.11 wireless next generation standing committee (see Fig. 5-1), briefing them on the 3GPP work done in Rel-13 for LTE-WLAN aggregation (LWA) and LTE WLAN radio level integration with IPsec tunnel (LWIP) [88]. For a user, LWA offers seamless usage of both LTE and WiFi networks and substantially increased performance. For a cellular operator, LWA simplifies WiFi deployment, improves system utilization, and reduces network operation and management costs. Yet, LWA is still under developing phase, and there is no real environment to evaluate these multi-path technologies. This research uses real life traffic to show the the importance of switching in spatial diversity. The real life traffic consist of three parts: LTE Macrocell (MC) data, LTE Small cell (SC) data, and WiFi data. In this research, the SC encompasses both femtocell and picocell.

Data transmission among wireless mobile devices via WiFi or LTE networks is handled by transport layer protocols and the most widely used is transmission control protocol

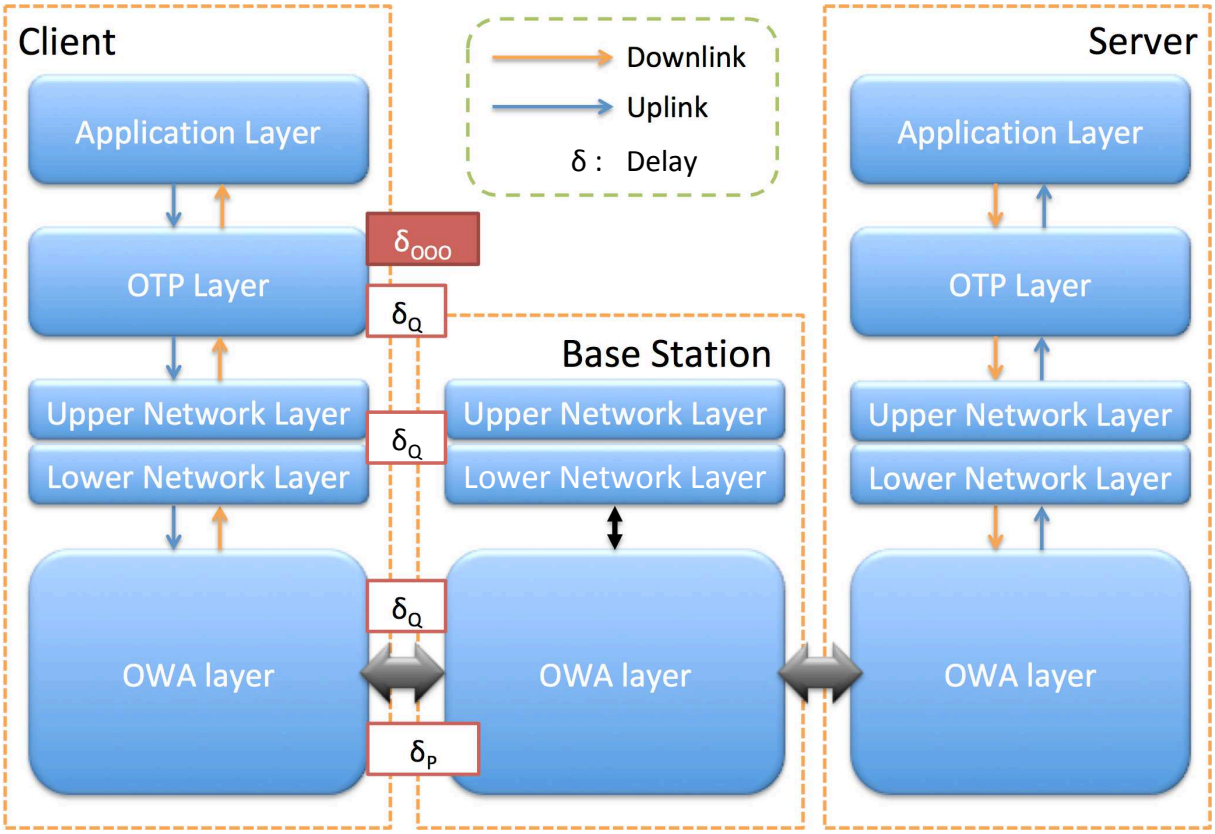

Figure 5-2: Delays on each network layer.

(TCP). In fact, there are severe limitations on the performance of TCP usage over wireless networks. Assuming that the fundamental propagation delay of the infrastructure due to non-zero physical signal propagation and transmission duration is within the user application tolerance, the objective of this scheme is to define and evaluate a mechanism for minimizing delays of data re-ordering in OTP layer (transport layer), as shown of δ_{ooo} in Fig 5-2. Re-ordering event is defined as a time-wise contiguous sequence of out-of-order packets (not in-order packets) excluding any in-order packets (the sequence number is contiguous vary with time). These are caused by retransmissions after buffer overflows and failures of basic transmission processes (decoding, integrity checks, error recovery, and segment reassembly). Our focus is precisely on LTE and WiFi networks, whose channel quality reporting targets block error rate of 10% at the physical layer, thus implying a strong default dependence on retransmissions for error-free data transfer.

5.1.1 Contributions

The contributions are: (i) Yet there is no real system/environment to evaluate the multi-path technologies. This research initiated the harbinger by tracing real life traffic to verify the importance of the spatial diversity and the encoding redundancy for low-latency communication; (ii) The severity of the delay imposed by re-ordering is intuitively understood by analyzing real life traffic; (iii) The proposed FPP thoroughly enables encoding redundancy for proactive recovery of intolerably delayed data without end-to-end retransmissions. With the spatial diversity, the FPP on secondary link minimizes the end-to-end retransmission overhead of the primary link. Moreover, FPP shows significant gain when buffer overflows are prevented; and (iv) The novel FPP effectiveness coefficient is proposed to explicitly represent the effectiveness of FPP implementation, which expressed in terms of a combination of spatial diversity and the variation of encoding redundancy with different audio and video requirements.

To our best knowledge, this is the first practical study on the latency-sensitive services by using real LTE and WiFi data traffic traces. Examples of solutions for proprietary networks include [89, 90]. Within the domain of standardized system, potential latency reduction gains assuming fundamental modifications of the LTE physical layer are studied in [91]. In the medium access, encoding redundancy is used to create novel LTE hybrid automatic repeat request (HARQ) mechanisms in [92–94]. On the network and transport layers, [95] examines opportunistic injections of encoded data into single-path WiFi transmissions. Novel TCP implementation using encoding redundancy principles with delayed block-level decoding is defined in [96]. A faster but difficult-to-configure scheme for proactive TCP retransmissions of unacknowledged data is discussed in [97].

5.2 Background and Motivation

5.2.1 Background

Controlling data delivery latency is one of the open problems in mobile and wireless networks. Network latency is a term that is used to indicate any kind of delay that happens in data communication over a network, including propagation delay in the physical layer, queuing delay in the data link layer and the network layer, and delay of re-ordering in the

transport layer. Propagation delay and queuing delay occur due to the limited speed of signal propagation and waiting time in limited buffer size, respectively. Compared to these delays that can be minimized through the hardware upgrade, the delay of re-ordering is the main issue that has to be minimized for latency-sensitive communication.

The end-to-end connection that encounters small delays, is called low-latency communication whereas connection that suffers long delay, is called high-latency communication. For low-latency communication, the end-to-end retransmission can lead to the unpredictable fluctuation in transmission rate, which is the phenomenon seriously affecting the quality of streaming of audio and/or video. For high-latency communication, the end-to-end transmitting time of a packet due to retransmission is extremely long because of hop count increment which can lead to very low end-to-end throughput.

5.2.2 Motivation

The traditional way to solve the end-to-end retransmission problem is either increasing the transmission rate or using the data aggregation technique to recover the lost or delayed packets instead of using retransmission mechanisms. Normally, increasing the transmission rate will increase the deployment cost, and using the data aggregation technique can result longer end-to-end retransmission when losing large packet sizes. With the spatial diversity, multiple radio access technologies in parallel can increase the network performance, but the delay of re-ordering and retransmission delay still occurs. Thus, FPP with spatial diversity and encoding redundancy is proposed in this research to effectively recover the delayed or lost packets instead of end-to-end retransmission. The proposed FPP is expected to provide more reliable and stable communication for low-latency communication.

5.3 Proposed Dense-aware Low-latency Communication Control Scheme

In this section, the proposed DLLCC scheme is described (see Figure 5-3). Proposed DLLCC comprises two basic components to reduce the latency, which are Spatial diversity analyzer and encoding redundancy. More detail information of these two components is

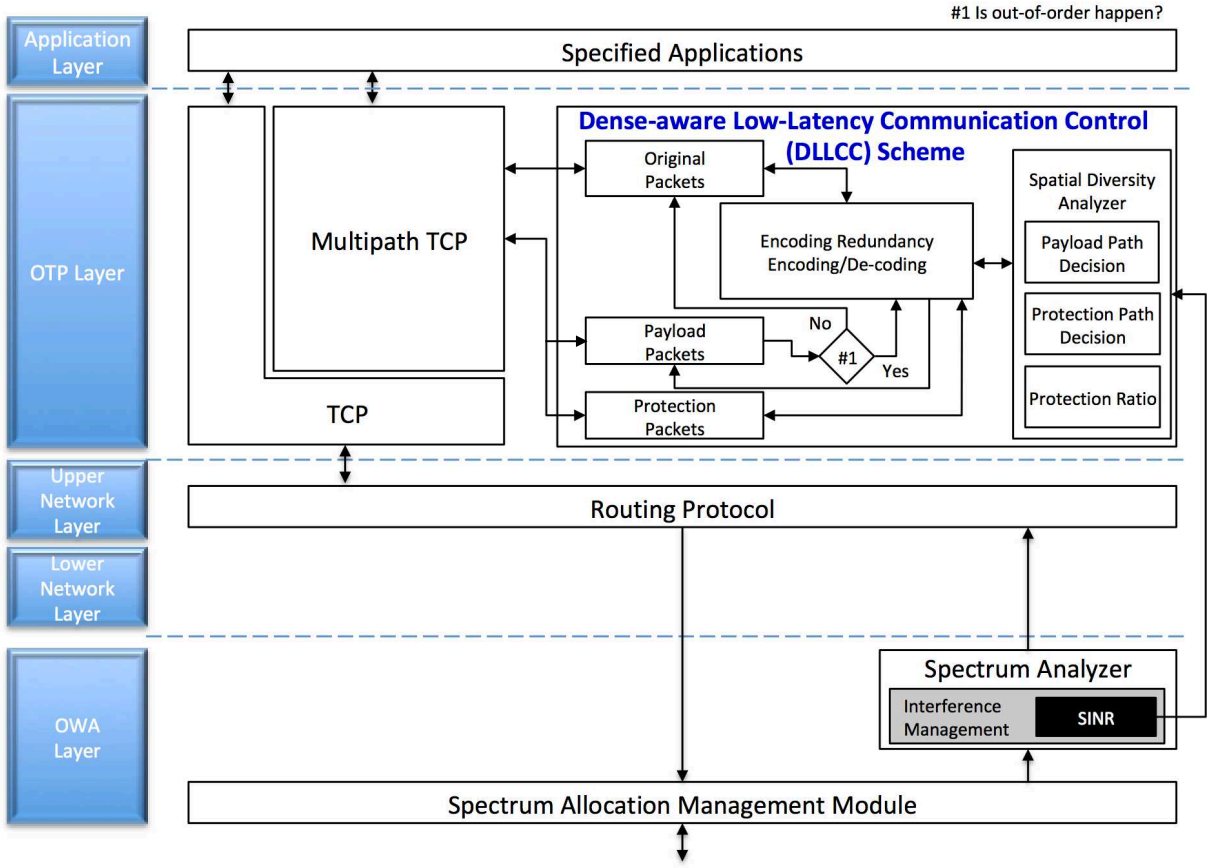

Figure 5-3: Dense-aware low-latency communication control scheme

introduced with follow subsections.

The DLLCC scheme refers the SINR value from spectrum analyzer to decide the role of each path when multi-RAT is used. The better one or more normally will be used as payload path and the others are used as protection path. Through the decision from spatial diversity, the packets is go through the encoding redundancy to output multiple packets with XOR coding. On the other hand, when packets comes, if there is no delayed packets (out-of-order packets), user can directly use them. If some of the packets delayed (out-of-order), instead of waiting for the retransmission, the delayed packets can be directly recover from the protection packets from protection path. This will lead significant low latency and high reliability.

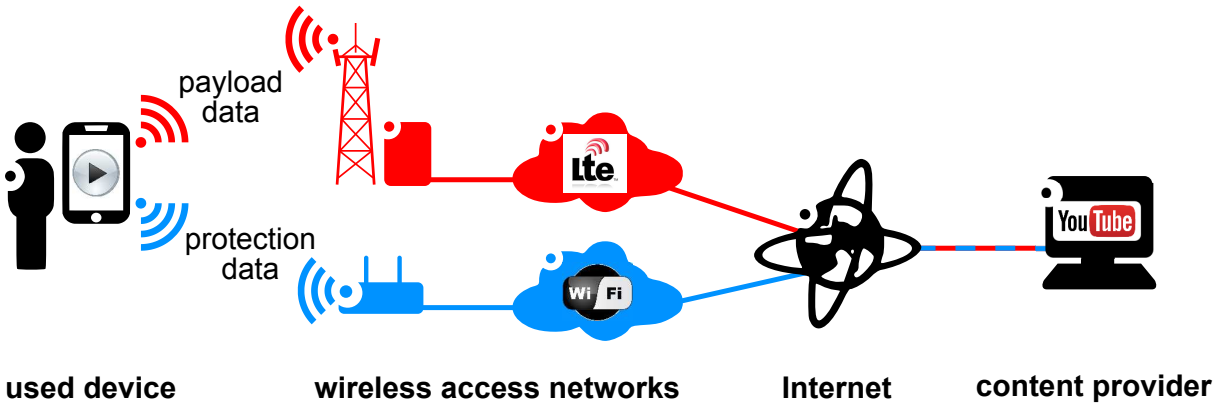

Figure 5-4: Latency-sensitive LTE-based services (primary link) are protected by using parallel WiFi connection (secondary link) for delivering FPP data.

5.3.1 Spatial Diversity

Spatial diversity refers to the delivery of a data flow over multiple radio access technologies in parallel, e.g., LWA, LWIP, etc. Hence, spatial diversity is to be understood in the transport-layer sense (YouTube video is downloaded simultaneously over LTE and WiFi whereby each wireless link represents an independent data delivery paths), not in the conventional physical-layer sense (e.g., antenna diversity of MIMO transmissions). The aggregation of multiple independent wireless links, or data delivery paths, into one logical connection theoretically allows increasing the overall throughput and reliability[1] as well as reducing latency by resource pooling – an advantageous feature when single-path connections cannot achieve the user demands. A new fifth-generation air interface as well as the allocation of new (shared) frequency bands can be expected in the near future [99], because of the global mobile data traffic will increase nearly eightfold between 2015 to 2020, from 3.7EB to 30.6EB per month [1]. Although the 4G (LTE system) has now been deployed and is reaching maturity, it is hard to meet the demands that network will face by 2020. The ongoing network densification by SC deployments improving the overall connectivity also clear motivates a study in this direction.

5.3.2 Bandwidth Aggregation

Single-path scenarios are considered as data re-ordering due to imperfect flow splitting and scheduling in multi-path scenarios can be efficiently solved assuming in-order delivery

[1]Next-generation air interfaces may be prone to outages as the user body can efficiently block the propagation of the anticipated mm-wave carriers [98].

in each path [100]. Our approach to latency control of mobile user services over a primary wireless link is based on the idea of trading latency for federated/excess bandwidth. More specifically, it is assumed that an additional wireless interface of a mobile device is seamlessly allocated for simultaneous delivery of subsequently specified FPP data over an independent secondary link (see Figure 5-4). The FPP data are used to recover lost or intolerably delayed payload data packets on a primary link before the user application can notice such events. Generalization of this atomic set-up of multiple links carrying payload and/or FPP data is straightforward. The multi-path scheduler is a source of an independent and therefore herein ignored delay of re-ordering.

It is therefore proposed to create the secondary link by using an additional wireless interface of the mobile device. As shown in Figure 5-4, for dual connectivity and carrier aggregation, when LTE framework be implemented as the primary links, because of its changeable cell size from tens of meters radius (femto- and pico-cells) up to 100 km radius MCs; also lower latency for handover and connection set-up time, WiFi could be considered as the currently best option given its ubiquitous deployment, good performance, and free-of-charge access as the secondary link. Regarding link independence, it is to be noted that WiFi access points are often back-hauled via cellular networks, especially mobile WiFi in transport vehicles.

The radio interface management in mobile devices can be done by using the network-resident service that is demonstrated in [101]. This service makes central optimized decisions based on network-wide information and operator policies. Its implementation is based on the modified multi-path TCP, a backward compatible solution for seamless transport-layer integration of networking technologies that is standardized by the Internet Engineering Task Force (IETF) [102]. Although the MPTCP working group reported five independent implementations [103], the integration of MPTCP and the proposed FPP is out of scope of this research. It can be recognized as an extension to the work after the verification of effectiveness of the proposed FPP.

5.3.3 Encoding Redundancy

Encoding redundancy is one way to compensate for the unavoidable errors or outages of wireless links by injecting an additional protection data into the actual flow of payload

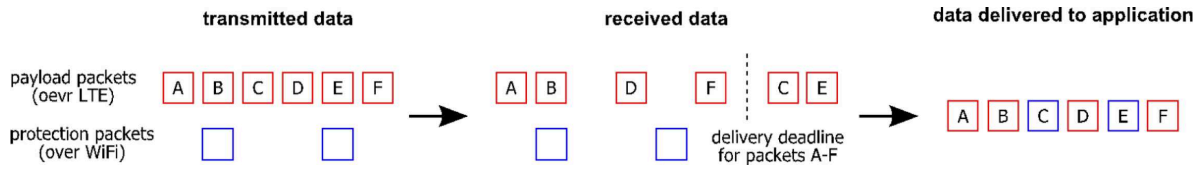

Figure 5-5: An example of encoding redundancy.

data (see Fig. 5-5). In the latency control context, the idea is to establish FPP that allows recovering lost or unacceptably delayed payload data without retransmissions before an application-required delivery deadline expires. Retransmissions minimize overhead related to missing data recovery, but they also non-negligibly increase data delivery delay by at least 1.5× of the connection round-trip time, i.e., transmission-to-acknowledgement time, as well as cause throughput drop in protocols with loss-based congestion control, e.g., sliding window protocols. The simplest example of encoding redundancy consists of a primitive replication of a data flow over multiple parallel paths; techniques more efficient in terms of the overhead are discussed subsequently.

5.3.4 Forward Packet-Loss Protection (FPP)

A naive way of protecting payload data consists of their replication over L, which is defined as the number of parallel links. The fastest link determines the overall latency at the expense of $(L-1)$-fold overhead. To compress the overhead to more reasonable levels, it is proposed to construct each FPP packet as a weighted random linear combination of n payload packets by using binary exclusive or (XOR) operation [104]. The multiplicative weights are selected at random in an identical, independent, and uniform manner [105].

Figure 5-6 visualizes the simplest protection scheme under which m FPP packets are generated for each n consecutive payload packets. In Figure 5-6, $m = 1$ and $n = 3$. As depicted by Figure 5-7, the decoding of a payload packet missing by a data delivery deadline can be done in real-time by using the received generator packets and Gaussian elimination [104, 105]. If the combining weights ensure maximum rank of the Gaussian system, one FPP packet can be used to recover one missing payload data packet or a part thereof. Thus, the protection percentage (ζ) defines the encoding protection strength of FPP , i.e.,

$$\zeta = \frac{m}{n} \times 100\% \tag{5.1}$$

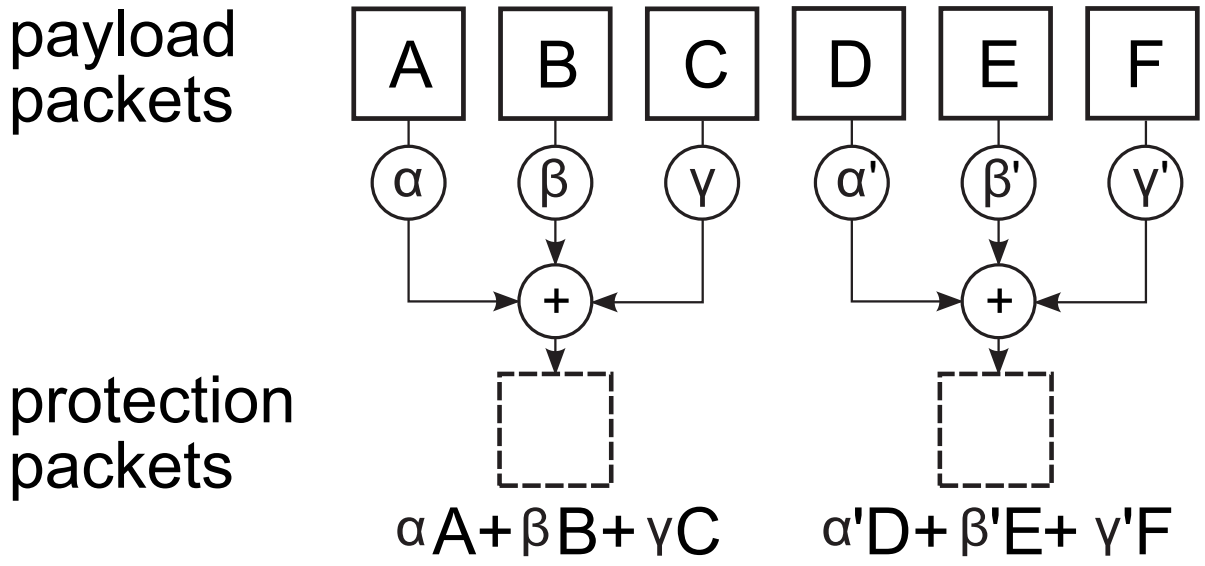

Figure 5-6: Formation of FPP packets using random linear codes.

e.g., $\zeta = 33\%$ in Fig. 5-6. Assuming that the link quality of primary link and secondary link is the same. When $\zeta = 0\%$, this means that FPP on the secondary link is not applied.

From a system point of view, one could require the protection data rate not to exceed the payload data rate, i.e., $m/n \leq 1$, as payload data duplication occurs for $\zeta = 100\%$. Yet in general, the instability of basic link characteristics such as effective throughput, delay jitter, and cross-traffic volume may justify a more complex design based on adaptive joint scheduling of FPP and payload data without an a priori primary/secondary characterization [100] but multi-path scheduling issues are out of the scope of this research contribution.

Besides the ζ factor, FPP also depends on the link quality of the primary link and secondary link. Hence, the link percentage (ρ) defines the percentage of effective transmission rate in between the secondary link (R_{sec}) and the primary link (R_{pri}), i.e.,

$$\rho = \frac{R_{sec}}{R_{pri}} \times 100\% \tag{5.2}$$

If the FPP is applied, the link quality of the secondary link cannot be zero, i.e., $R_{sec} \neq 0$. When $\rho = 100\%$, this means that the link quality of secondary link and primary link are the same.

Since FPP is depending on two factors, i.e., ζ and ρ, the FPP effectiveness coefficient

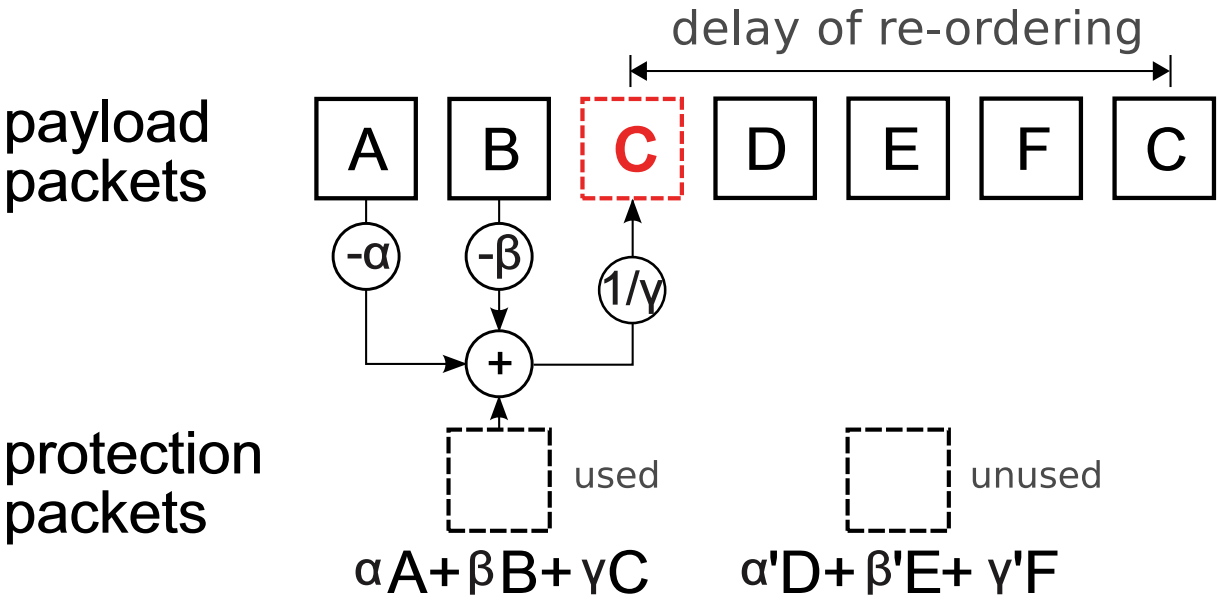

Figure 5-7: Recovery of a delayed payload packet using FPP packets to avoid the delay of re-ordering. The first FPP packet is used due to payload packet 'C' is out-of-order, second FPP packet is unused due to payload packets are in-order.

(FE) is used to indicate the effective range of the FPP implementation. It is defined as

$$FE = \frac{\zeta}{\rho} \tag{5.3}$$

where $\rho \neq 0$. FPP effectiveness coefficient can range from 0 to ∞. An effectiveness of 1 ($FE = 1$) corresponds to a complete data duplication of the FPP. An effectiveness of 0 ($FE = 0$) indicates that the FPP is not applied, whereas an effectiveness more than 1 ($FE > 1$) represents that the FPP is not appropriately implemented. Essentially, the range of $0 < FE \leq 1$ indicates that the FPP is appropriately implemented.

The above description implicitly assumes protection against data loss or delay at the transport layer of the open systems interconnection (OSI) model, typically accommodating the connection-oriented TCP and the connection-less user datagram protocol (UDP). Accordingly, random linear combinations of TCP/UDP packets are sent as the secondary FPP information, and used by the receiver for recovery of data before they are passed on to the TCP/UDP modules.

Encoding protection can be implemented to lower OSI layers as well. The advantage consists in smaller size of FPP packets and earlier correction of errors, but only shorter components of the overall end-to-end delay can be eliminated. Higher-layer errors would

not be detectable nor correctable.

5.4 Quantification of Data Re-ordering

This section describes the frequency and length of payload data re-orderings as well as the size of affected data blocks as measured in both LTE and WiFi networks. The trade off between the ζ of a secondary link and the achievable reduction of delay of re-ordering at the primary link is analyzed subsequently.

5.4.1 Definition

The following definitions that visualized in Figure 5-8 are used to capture the frequently complex re-ordering events.

Let P, T and S indicate packet, time and sequence number respectively. Considering $P(T, S)$ is a TCP packet received in time T and carrying a range $S(T) = [S_1(T), S_2(T)]$ of TCP sequence numbers. For example, a given time t, $S_1(t)$ represents the first sequence number, and $S_2(t)$ represents the last sequence number. TCP sequence numbers indicate individual bytes of ordered payload data. Packets arrive in unique times and each sequence number is received only once.

1. *In-order*

   A packet $P(T, S)$ is in-order if and only if (i) no sequence number higher than $S_2(T)$ has been received until time T (i.e., no packets expected after time T have been received); and (ii) $\cup_{\forall t<T} \arg_s p\,(t, s) = [1, S_1\,(T) - 1]$ the union of sequence numbers of all previously received packets is a contiguous range, (i.e., no packets expected before time T are missing).

2. *Out-of-order*

   A packet $P(T, S)$ is out-of-order if it is not in-order.

3. *Re-ordering event*

   A re-ordering event is defined as a time-wise contiguous sequence of out-of-order packets excluding any in-order packets. As shown in Figure 5-8, the re-ordering

event starts from an in-order packet and ends with the next consecutive in-order packet. N is the total number of packets in the re-ordering event.

4. *Ideal in-order delivery*

   Ideal in-order delivery refers to how packets would have been received if no re-ordering event happened (see Figure 5-8). Given the re-ordering event characterized by a sequence $P\left(T^i, S^i\right) \forall i \in [1, \ldots, N]$ of out-of-order packets, where $S^i(T^i) = [S_1^i(T^i), S_2^i(T^i)]$, the ideal in-order delivery is defined as a sequence of packets $P\left(T^i, \mathbb{S}^i\right)$ that are received in the original times T^i, and have monotonically increasing sequence numbers from the set $\cup_{\forall i} S^i\left(T^i\right)$, i.e., $S_2^i\left(T^i\right)+1 = S_1^{i+1}\left(T^{i+1}\right) \forall i \in [1, \ldots, N-1]$.

5. *Delayed in-order delivery*

   Delayed in-order delivery is understood as a shift of all ideally in-order delivered packets $P\left(T^i, \mathbb{S}^i\right)$ in time by the corresponding delay D^i, i.e., a packet sequence $P\left(T^i + D^i, \mathbb{S}^i\right) \forall i \in [1, \ldots, N]$, where $\mathbb{S}^i(T^i) = [\mathbb{S}_1^i(T^i), \mathbb{S}_2^i(T^i)]$.

6. *Effectively lost*

   Assuming maximum tolerable delay D_{max} and $\mathbb{S}^i = S^i$, an out-of-order packet $P\left(T^i, S^i\right)$ is effectively lost during the re-ordering event if the out-of-order packet $P\left(T^i, S^i\right)$ would have been received later than the corresponding packet $P\left(T^i + D_{max}, \mathbb{S}^i\right)$ in the ideal in-order delivery sequence delayed by D_{max}, i.e., for given i, $\arg_{T^i} P\left(T^i, S^i\right) > \arg_{T^i} P\left(T^i + D_{max}, \mathbb{S}^i\right)$.

5.4.2 Evaluation Metrics

The captured traffic traces are analyzed in terms of:

1. *Effective transmission rate* (R) – average effective transmission rate of each measured scenario. The effective transmission rate is calculated as the measured number of units of data divided by the measurement time.

2. *payload data rate* (r)– average physical data rate of the ideal in-order delivery sequence during the re-ordering event.

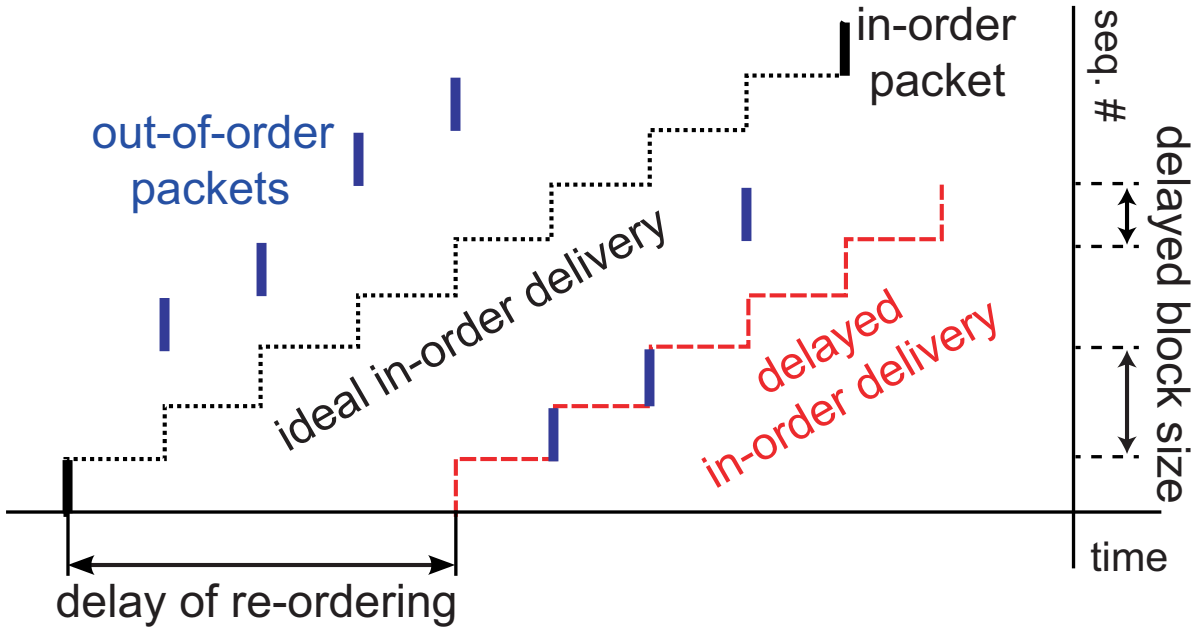

Figure 5-8: Visualization of the characteristics of a re-ordering event.

3. *delay of re-ordering* (D_r) – delay by which the ideal in-order delivery sequence $P\left(T^i + D^i, \mathbb{S}^i\right)$ of a re-ordering event must be delayed such that none of the out-of-order packets is considered effectively lost, i.e.,

$$D_r = \arg_{D^i} \max_{i \in Q} \left[\arg_{T^i} P\left(T^i + D^i, \mathbb{S}^i\right) - \arg_{T^i} P\left(T^i, S^i\right)\right] \tag{5.4}$$

for $\mathbb{S}^i = S^i$ where Q is the set of out-of-order packets when $0 < D^i \leq D_{max}$, e.g., $Q = 3$ in Figure 5-8.

4. *delayed block size* (B_d) – total number of out-of-order packets in bytes considered lost during a re-ordering event with respect to the ideal in-order delivery sequence ($D^i = 0$). It is the cardinality of the above set Q, i.e., $B_d = \sum_k B_k$, where $k \in Q$, B is the block size in bytes.

5. *average inter-event time separation* – average time interval between two consecutive re-ordering events. Assuming consecutively a limited resolution of the user in distinguishing consecutive events, multiple short re-ordering events occurring within a period of 100 ms are counted only as single event.

5.5 Measurement Data

5.5.1 LTE Network

LTE re-ordering events are quantified based on TCP data captured in live LTE networks from February to March 2015 in the New York city, USA. Two kinds of tools are used to capture real life mobile data, i.e., `tcpdump` on Ubuntu (14.04.3 LTS) and Wireshark on Microsoft Windows 7. `tcpdump` is a free and common packet analyzer that runs under the command line. Wireshark is a free and open source packet analyzer that is used for network troubleshooting, analysis, software and communications protocol development. Two devices that are installed with Ubuntu and Microsoft Windows 7, respectively act as file transfer protocol (FTP) clients. One more device that is installed with Ubuntu acts as a FTP remote server. Four LTE universal serial bus (USB) modems LG VL600, Qualcomm 9630, LG G7, Huawei e3276s-150 are used in the data collocation with regular TPC. The default TCP CUBIC implementation, an optimized congestion control algorithm for high bandwidth networks with high latency, is used for the Ubuntu-based device. Repetitive large data transfers of 0.1∼1 GB are used to emulate long-lived sessions. As a result, extensive traffic traces at the order of tens of GB are obtained in the following two scenarios:

- MC scenarios (*cross mark in the following graphs*)
  Downlink only (DL): Test user equipment (UE) connects over a commercial MC network (AT&T Inc.) of a major carrier to a remote server from both outdoor and indoor locations to download data using FTP. The server is located in the physical proximity to the LTE public gateway to avoid traffic passing through the Internet. Two sub-scenarios are distinguished: (i) *Unlimited* – background download traffic is low to moderate (off-peak hours in outdoor location). (ii) *Limited* – the data rate is an operator-limited, which is 10% of the possible data rate. Background download traffic is high (peak-hour in indoor location).

- SC scenarios (*circle mark in the following graphs*)
  Downlink/Uplink (DL/UL): Test UEs for indoor environment connect over a carrier-grade SC network in a large private enterprise network to a server to download/upload data. The server connects directly to the LTE public gateway, which is located

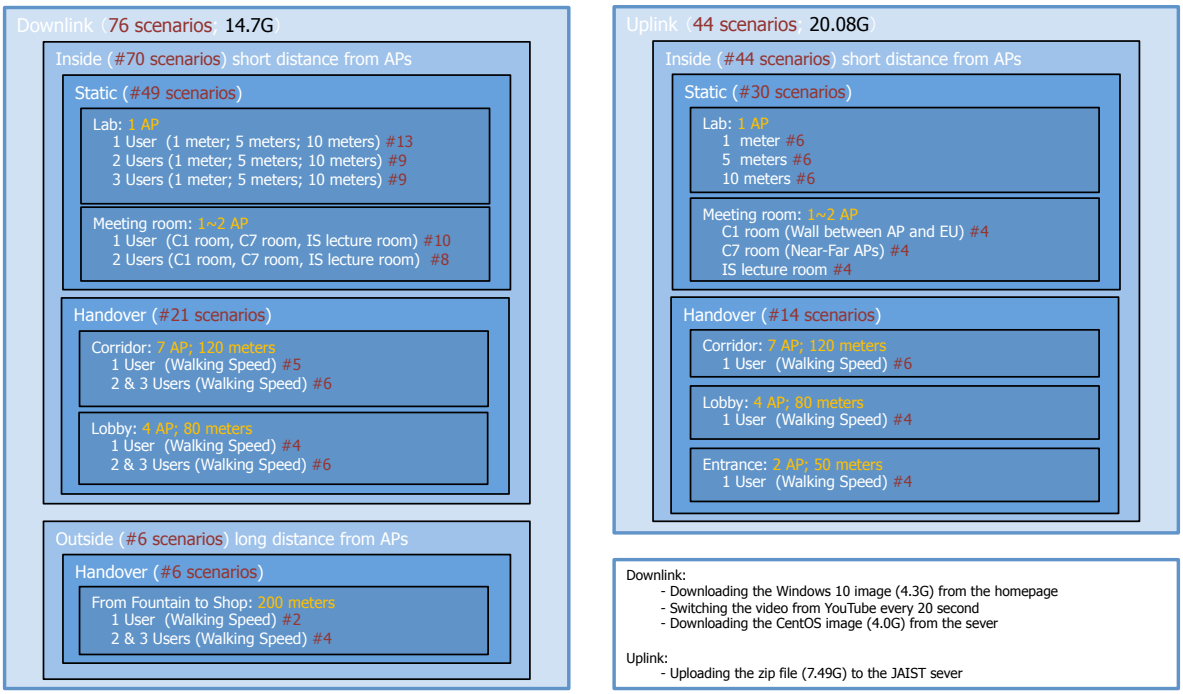

Figure 5-9: Detail of captured WiFi data.

at the enterprise site. Background traffic is low to moderate and the service LTE data rate is unlimited. Two sub-scenarios are distinguished: (i) *Static* – UEs are static. (ii) *Handovers* – UEs are moving and at least one (typically multiple) handovers occur during each session. UEs move at slow to fast walking speeds.

5.5.2 WiFi Network

WiFi re-ordering events are quantified based on regular TCP data captured from 3rd to 15th October 2015 at Japan Advanced Institute of Science and Technology (JAIST), Japan (see Fig. 5-9). For WiFi access points (APs), Cisco Aironet 1252 and 3702i are used, which support with 802.11n only and both 802.11n and 802.11ac, respectively. Two devices act as FTP clients, one is Ubuntu (15.04) with `tcpdump`, and another is Mac OS X (10.11) with Wireshark. The server based on Ubuntu (15.04) directly connects with APs through Ethernet. The distance between APs is quite different due to their location in the buildings, the average distance of APs is about 23 meters. Both download and upload data is about 5 GB. Extensive traffic traces about 35 GB are obtained in the following scenarios:

- WiFi scenarios (*triangle mark in the following graphs*)

  Downlink/Uplink (DL/UL): 76 DL scenarios for both indoor and outdoor environments and 44 UL scenarios for only indoor environment with different distance from APs are traced. Two sub-scenarios are distinguished: (i) *Static* – UEs are static. (ii) *Handovers* – UEs move at normal walking speed. For DL, at least 4 APs handovers (roaming) are occurred. For UL more than 2 APs handovers are occurred.

5.5.3 Data Analysis

In this research, it is important to note that packet losses can occur anywhere in the network and at any layer. Physical layer losses of the LTE radio link can be mostly (but not always) recovered by using Hybrid ARQ (HARQ) mechanisms in the media access control (MAC) and radio link control (RLC) layer of the LTE protocol stack. Yet buffer overflows can occur anywhere along the connections and can only be recovered by transport-layer retransmissions, resulting the re-ordering event happened at the receiver side and associated with their delays. The measurement scenarios are uncooperative, e.g., UE is either "static" or "handover". In our measurements, TCP is focused. It carries roughly 80% of Internet traffic and relies on explicit flow and congestion control in order to reduce the probability of data loss due to the congestion losses.

All of the captured real life traffic traces are analyzed under Ubuntu (15.04). The processing procedures are as follow:

1. Use `tcptrace`[2] to produce several different types of output containing information on each measurement scenario, such as elapsed time, bytes, sequence number and round trip times.

2. Use `xplot.org` command to plot the figures of `tcptrace` output files, confirm the correctness.

3. If `tcptrace` output files are correct, treat them as input files to the original MATLAB program to output the results of Section 5.4.2.

Through the data analysis, the TCP maximum transmission unit (MTU) is also calculated, i.e., 1388 bytes in LTE networks, and from 1280 to 1420 bytes (average value

[2]O., Shawn, [Online]. Available: http://www.tcptrace.org/.

is 1378 bytes) in different scenarios of WiFi. All of the measurement results (i.e., MC, SC and WiFi) are drew in the same graphs in Section 5.6 because there is no much gap difference in the TCP MTU size (i.e.,$1388 - 1378 = 10$ bytes). Since both LTE and WiFi data rate are in Megabits per second (Mbps), thus the said gap difference is negligible.

5.6 Measurement Results

The statistical measurement results of each scenario are presented in Table 5.1, including average effective transmission rate, average time between two consecutive re-ordering events, average delay of re-ordering and their standard deviation (σ), respectively. A cumulative distribution functions (CDF) of measured payload data rate, delays of re-ordering, and re-ordered block sizes for each scenario are shown in Figure 5-10, 5-12 and 5-11, respectively. The average time between two consecutive re-ordering events are presented in Table 5.1.

5.6.1 Statistical Measurement Results

Table 5.1: Statistical measurement results of each scenario.

Scenarios			Effective Transmission Rate (Mbps)		Inter-event Time Separation (s)		Delay of Re-ordering (s)	
			mean	σ	mean	σ	mean	σ
MC	DL	Unlimited	4.54	2.25	34.01	69.26	1.13	4.47
		Limited	0.39	0.18	78.88	69.30	12.84	30.21
SC		Static	21.39	11.06	7.02	10.03	0.30	0.36
		Handovers	30.85	12.30	10.90	18.18	0.26	0.56
WiFi		Static	41.46	44.85	3.60	4.27	0.04	0.06
		Handovers	34.79	33.19	1.35	1.30	0.26	1.48
SC	UL	Static	9.65	5.43	1.84	0.83	0.09	0.18
		Handovers	12.37	4.85	16.68	20.64	0.23	0.17
WiFi		Static	141.14	28.40	26.60	28.11	0.05	0.01
		Handovers	55.38	17.00	23.75	40.15	6.65	6.36

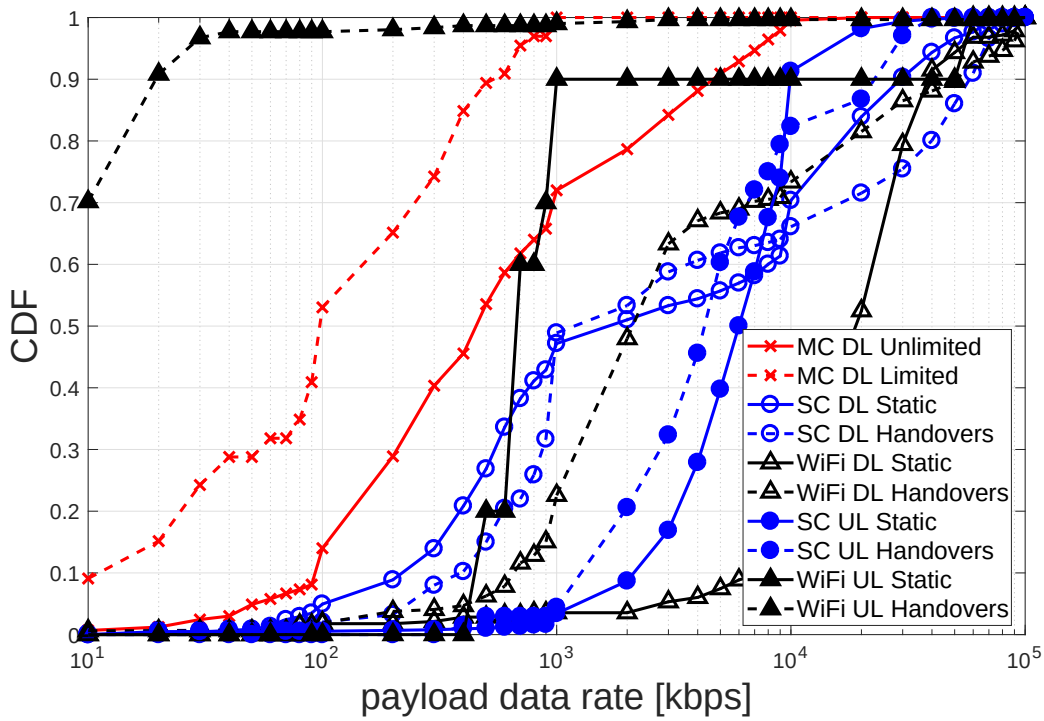

Figure 5-10: Cumulative distribution function of payload data rate.

5.6.2 Payload Date Rate

A wide range of data rates are used for the measurements. For WiFi, IEEE 802.11n (maximum data rate is 300 Mbps) and IEEE 802.11ac (maximum data rate is 1300 Mbps) based APs are used. For LTE, maximum data rate is close to 300 Mbps for SC, and only 150 Mbps for MC. The results of average effective transmission rate in Table 5.1 also confirm the reliability of the measured data. Here, the σ of effective transmission rate on "WiFi DL Static" is large due to using IEEE 802.11n or 802.11ac traces as "WiFi" scenarios. Table 5.1 presents that high average effective transmission rate implies more frequent re-ordering events happening in DL scenarios. Especially in SC/WiFi, the re-ordering event time separation is reduced to only a few seconds, and the delay of re-ordering is not as serious as MC DL scenarios, which can be easily recovered with the proposed FPP. With limited effective transmission rate, MC DL scenarios have longer inter-event time separation, but also have intolerably delay of re-ordering. Although WiFi handover scenarios have great effective transmission rate, the delay of re-ordering is much worse than in static scenarios. The σ results of delay of re-ordering obviously indicate how serious the problem of re-ordering event.

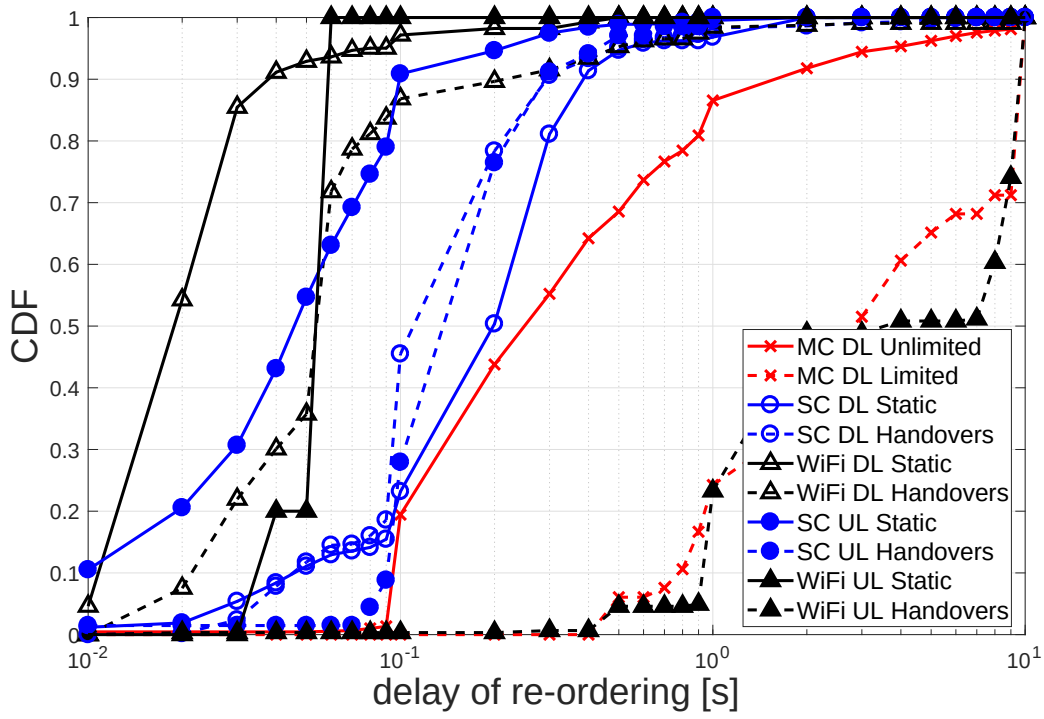

Figure 5-11: Cumulative distribution function of delays of data re-ordering.

As we can observe from Fig. 5-10 to Fig. 5-12, the lines are crossed with each others and their performances of data transmission are randomly changed. The main reasons for these phenomena are that the effective transmission rates of each scenario are different and how the TCP mechanism works during the data measurements. From Fig. 5-10, it can be seen that the overall payload data rate of the 4 scenarios ("WiFi UL Handovers", "MC DL Limited", "WiFi UL Static", and "MC DL Unlimited") is less than 1 Mbps. The corresponding payload of the other 6 scenarios are all greater than 1 Mbps. The fastest one is the "WiFi DL Static", which has 80% more than 10 Mbps, and the lowest one is the "WiFi UL Handovers", which has 90% less than 0.02 Mbps. The results of MC scenarios indicate that by reducing the DL payload data rate to approximately 10% of the achievable payload data rate ("MC DL Unlimited" vs "MC DL Limited"), the re-ordering event period reduces from 79 s to 34 s, while the delay of re-ordering reduces by almost 10-times. Thus, if the re-ordering delay can be minimized by the proposed FPP, the effective transmission rate would be further improved.

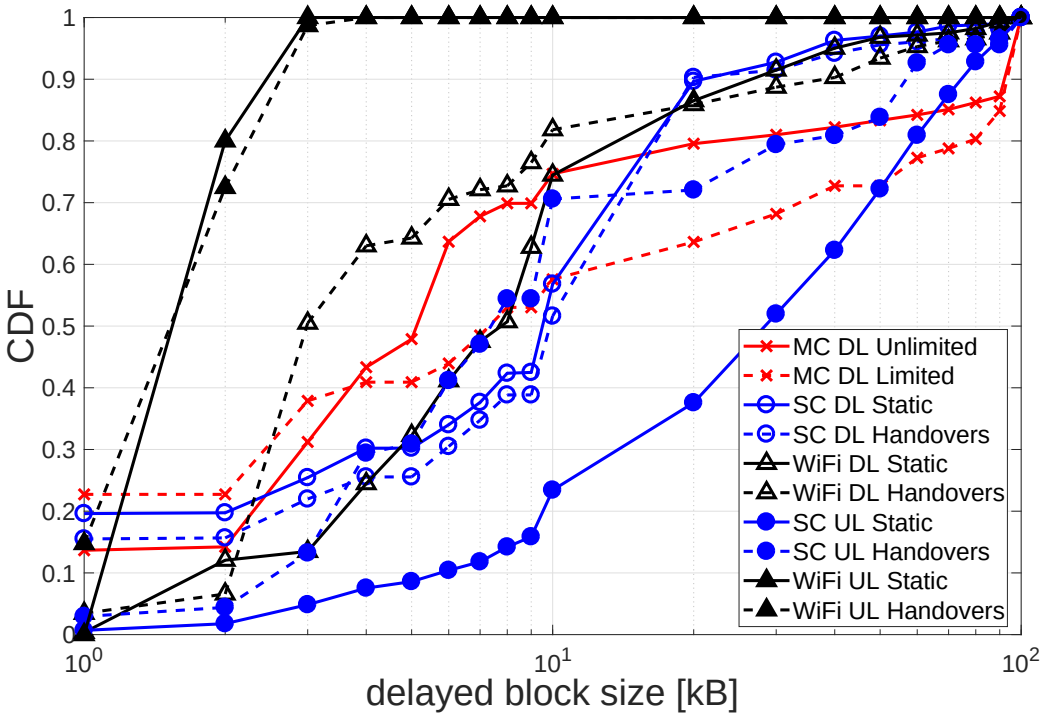

Figure 5-12: Cumulative distribution function of delayed data block sizes.

5.6.3 Delay of Re-Ordering

It can be seen in Figure 5-11 that most of the scenarios have less than 400 ms overall delay of re-ordering, and only "MC DL Limited" and "WiFi UL Handovers" have intolerable delay of re-ordering (more than 70% worse than 1 s). Thus, referring to Figure 5-10, it can be observed that high payload data rate normally leads low delay of re-ordering. E.g., "WiFi DL Static" has the highest payload data rate, it has the lowest delay of re-ordering. If the intolerable delay is set to 100 ms (audio level), all SC scenarios except "SC UL Static" cannot meet the requirement, which can be easily solved in Section 5.7 with FPP. SC DL/UL handovers have low impact on the overall payload data rate but cause major delay of re-ordering increase. The "WiFi DL Handovers" has low delay of re-ordering due to most of the out-of-order packets has efficient lost during its bad connection period. The "WiFi UL Static" also has the same situation because of less out-of-order packets (packets are in-order with long delay caused by retransmission).

5.6.4 Delayed Block Size

Figure 5-12 indicates that the re-ordered data block size (monotonically increasing and often overlapping) refers to random, no matter with payload data rate and delay of re-ordering. Both "WiFi UL Static" and "WiFi UL Handovers" have less re-ordered block size than other scenarios due to either packets are in-order packets with long delay (re-transmission) or out-of-order packets are efficiently lost. Left-bottom part of Figure 5-12 indicates that effective losses of few packets that could be attributed to the failures of the physical/data link layers[3] account only 5-20% of all losses in all studied scenarios. Such small effective losses can be easily recovered by using low constant-rate of ζ. However, more typical losses of tens of packets either require a relatively high effective ζ for payload data recovery or simply make efficient data recovery impossible.

5.6.5 Discussion

In summary, it is observed that high average payload data rate implies more frequently re-ordering events happen, also characterized by generally short delays of re-ordering. Small effective losses can be easily recovered by using FPP with low constant-rate of ζ. Large-scale of out-of-order packets during a re-ordering event are caused by buffer overflows, which require a relatively high effective ζ for payload data recovery. Analysis also indicates that most of them are caused by the TCP congestion control algorithm. Due to the serious delay of re-ordering and frequent re-ordering events from the measurement results, it is necessary to eliminate or minimize the non-negligible delay of re-ordering.

5.7 Influence of Spatial Diversity and Encoding Redundancy

In this section, the influence of spatial diversity and encoding redundancy is analyzed to mitigate the delay of re-ordering, which means the influence of ζ and links of data rate to delay of re-ordering.

[3]LTE coding and modulation for average signal-to-interference-and-noise ratio allows transmitting thousand of bits over several units of LTE resource block.

5.7.1 Influence of ζ to Delay of Re-ordering

The influence between ζ and primary link delay of re-ordering consists in the fact that the replication of primary link data to the secondary link ($\zeta = 100\%$) minimizes the delay of re-ordering, while no FPP ($\zeta = 0\%$) implies inactive latency control. In this subsection, ρ is set to 100% to show the influence of ζ only, which means there is no influence on the effective transmission rate of the secondary link. Since $\rho = 100\%$, the FE is equal to ζ. E.g., $\zeta = 100\%$ leads to $FE = 1$, which corresponds to a complete data duplication of the FPP.

To examine how data streams benefit from the FPP, let examine a scheme with a given constant ζ that attempts to recover all the effectively lost packets during each re-ordering event. More accurately, a reduced delay in second (D_{min}) is computed as the minimum of (i) the delay of re-ordering D_r experienced during a re-ordering event; and (ii) time needed for the delivery of FPP data size, which equals to the delayed data block size (B_d) given a data rate (R) of ζ, i.e., as

$$D_{min} = \min\left(D_r, \frac{B_d}{(\zeta/100 \cdot R)}\right) \tag{5.5}$$

where $\zeta/100 \cdot R$ can be defined either as a relative fraction of the payload data rate experienced during the re-ordering event (Figure 5-13), or in absolute terms (Figure 5-14). Using payload data rate instead of the effective transmission rate is more accurate due to the TCP's fluctuation in transmission rate.

It is observed from Figure 5-13 that scenarios characterized by low physical data rate (both "MC DL Unlimited/Limited" and "WiFi UL Handovers" scenarios) or short delays of re-ordering ("SC UL Static" and "WiFi UL Static") do not benefit from FPP. In the former case, FPP is not sufficiently available due to limited data rate of ζ, while in the latter case, reductions of delay of re-ordering in already short delays of re-ordering are negligible. The rest (SC DL scenarios, WiFi DL scenarios and "SC UL Handovers") exhibit the right balance of sufficiently high data rate and long-enough delays of re-ordering that makes the impact of FPP the most significant.

The benefits of FPP could be clearly enhanced by improving the data rate of the ζ. In this context, Figure 5-14 shows the probability that the FPP data rate of the

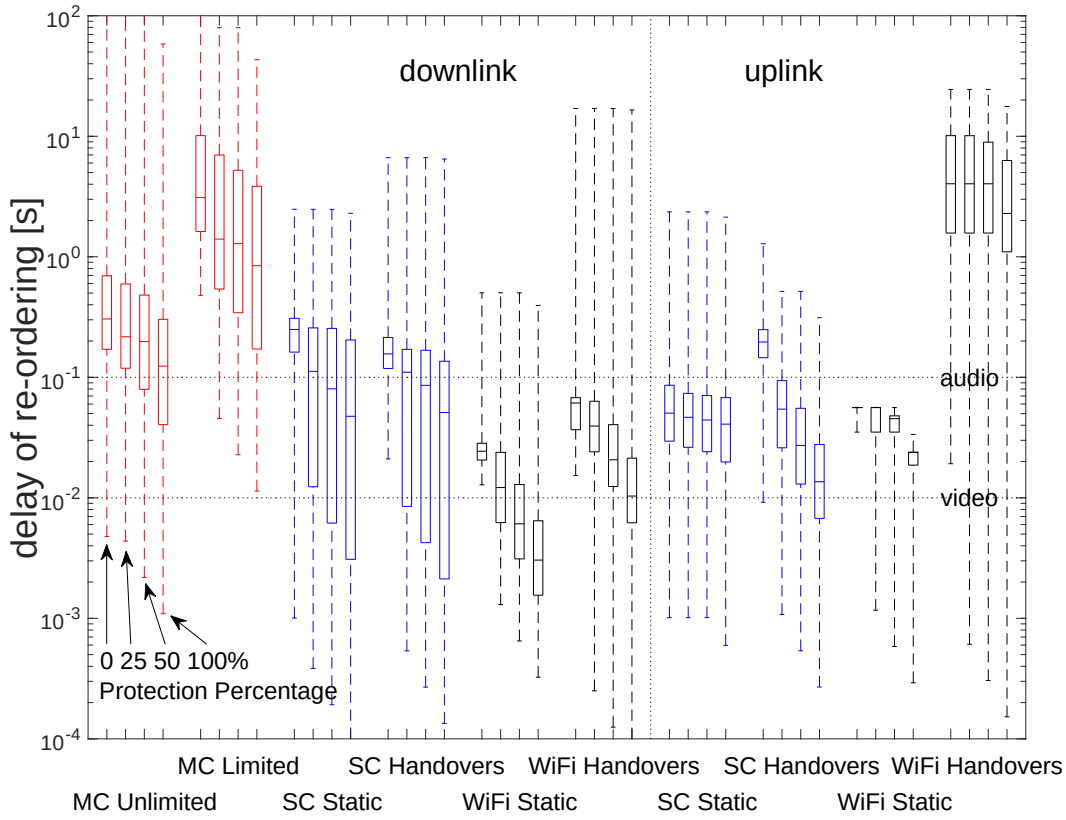

Figure 5-13: Distribution of delays of data re-ordering as function of ζ being a pre-defined fraction of the physical payload data rate. Range bars delimit the 25-th and 75-th percentiles as well as indicate the median.

secondary link is lower than the payload data rate of the primary link. Nevertheless, the notion of primary and secondary link should be revisited when high relative ζ is required (comparable data rate of primary and secondary links). Let alone when the secondary link data rate exceeds the primary one in this subsection.

We observe from right-top part of Figure 5-12 that large-scale of out-of-order packets in LTE network can be explained by the "Unacknowledged RLC Mode" which permits to drop unacknowledged data during a handover. Although it was not possible to confirm the RLC configuration in the measured commercial networks, it can be generally stated that this mode is used for broadcast over multicast control channel (MCCH) and multicast traffic channel (MTCH) using multimedia broadcast multicast service single frequency network (MBSFN) or for voice over internet protocol (VoIP). The more common TCP/IP traffic is typically handled in the RLC "Acknowledged Mode" under which unacknowledged packets are forwarded from the source E-UTRAN node B (eNodeB) to the target eNodeB

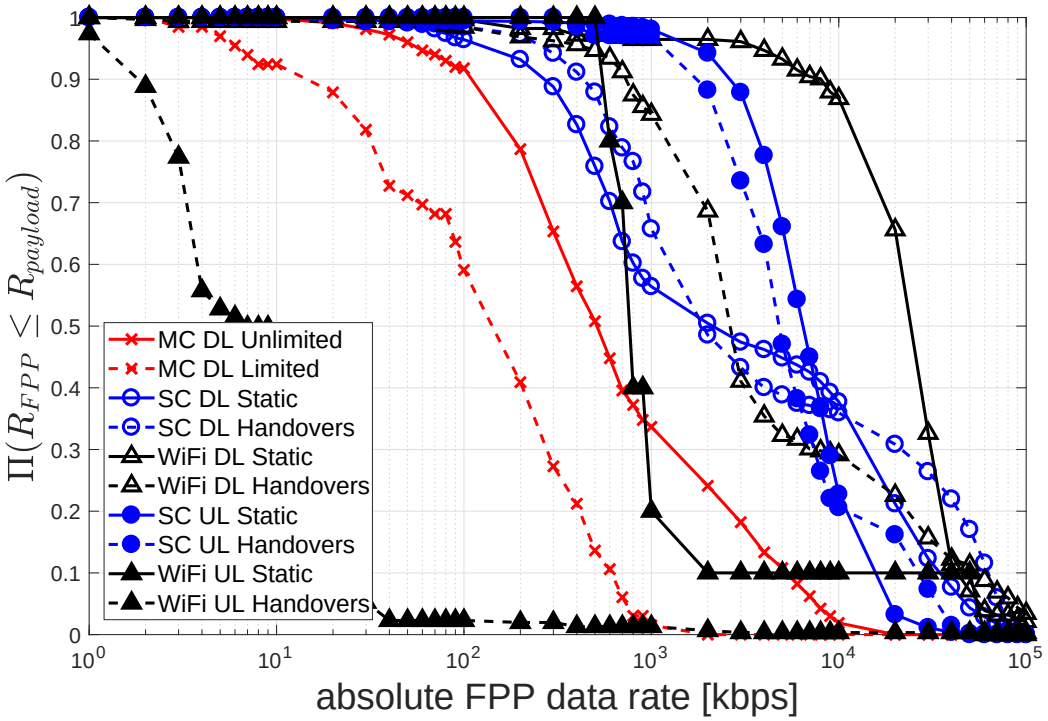

Figure 5-14: Probability that the ζ data rate of the secondary link is lower than the payload data rate of the primary link.

to ensure in collaboration with the LTE packet data convergence protocol (PDCP) layer an in-order non-duplicate data delivery processing even during handovers.

Traces of eNodeB ingress and egress traffic show that large-scale of out-of-order packets during a re-ordering event are actually caused by buffer overflows in the LTE base stations (BSs). More specifically, loss-based mechanisms for TCP congestion control systematically cause buffer overflows by progressively increasing sending data rate to detect the available channel capacity under rapidly fluctuating networking conditions.

Figure 5-15 shows that preventing buffer overflows caused by the transport layer, e.g., by using delay-based congestion control as known from TCP Vegas or TCP Compound, the efficiency of FPP-driven recovery from unavoidable data losses within the protocol stack is substantially better compared to the case with uncontrolled overflows from Figure 5-13. In particular, we observe that substantially lower ζ allows achieving major reductions of delays of re-ordering, achieving an order of magnitude in SC networks rather than WiFi networks.

More efficient way is adaptive-rate FPP schemes that proactively enhance FPP in anticipation of major data losses must be generally coupled with rate adaptation in the

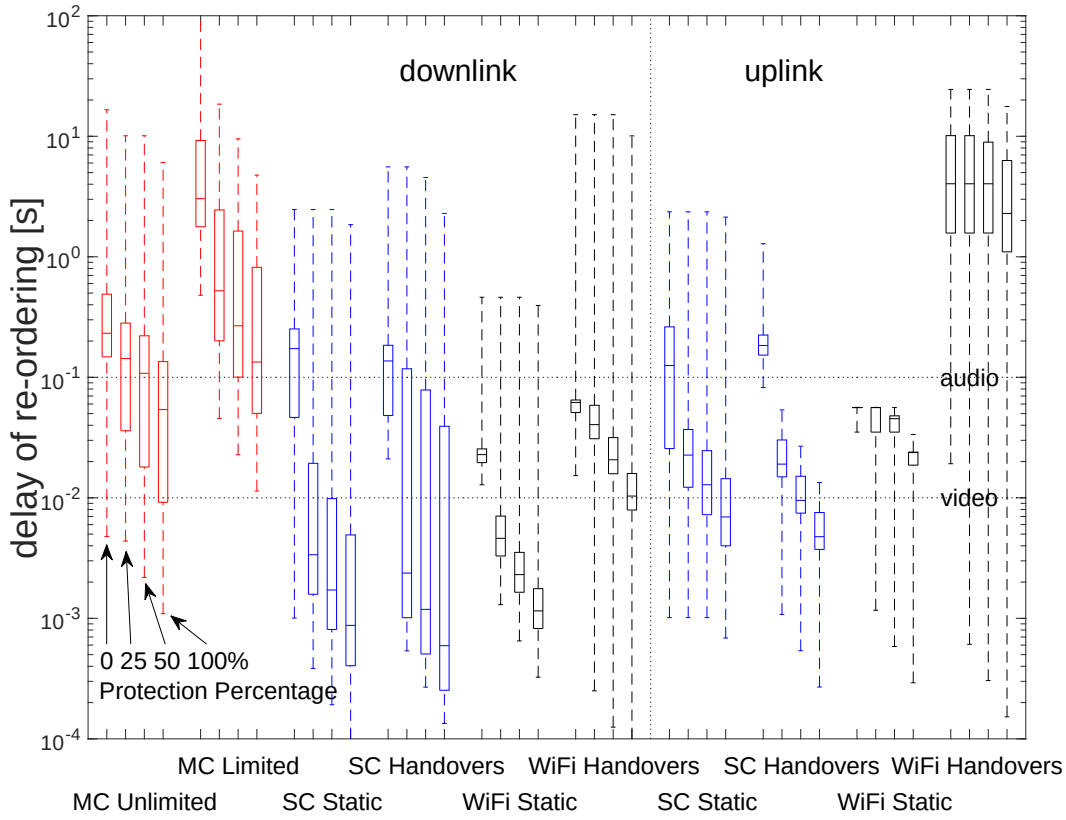

Figure 5-15: Distribution of delays of data re-ordering as function of constant-rate FPP from 5-13, assuming prevention of TCP buffer overflows. Range bars delimit the 25-th and 75-th percentiles as well as indicate the median.

transport layer. Only in this way the ζ can be minimized and the FPP performance can be maximized.

From Table 5.1 average inter-event time separation, evidence can be created by depicting the correlation between buffer overflow times, indicated by TCP Selective Acknowledgment (SACK) of out-of-order data, and round-trip time build-up under default CUBIC, a quantity directly proportional to queue occupancy in private queues typical for LTE and WiFi, e.g., see Figure 5-16. Note that in such queues, cross-traffic cannot directly contribute to buffer occupancy or delay; it only affects the serving data rate.

5.7.2 Influence of Link Percentage

In this subsection, the influence of link percentage (ρ) is discussed. The standard latency requirements (SLR) of the audio and video are 100 ms and 10 ms, respectively. Four DL

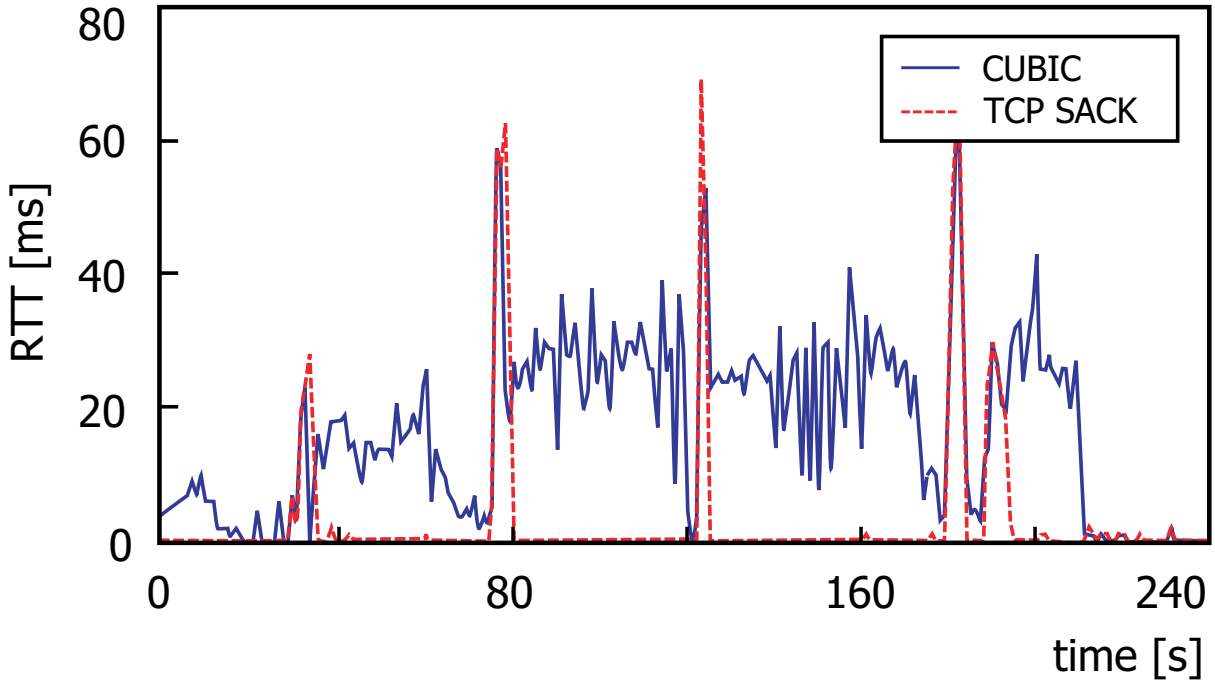

Figure 5-16: Correlation of round-trip time (RTT) under default CUBIC with re-ordering events as indicated by TCP Selective Acknowledgments (SACK) ("SC DL Static").

scenarios are selected out form the measurement data to be analyzed in pairs. "WiFi DL Static", "SC DL Static", "MC DL Unlimited", and "MC DL Limited" are selected due to the significant contrast between them. From the quantitative analysis results of Section 5.6, we observe that "WiFi DL Static" has the lowest influence when re-ordering event occurs. Thus, it is the best choice as the primary link to analyze the influence of ρ. "SC DL Static" is selected as the primary link for comparative analysis. For the secondary link, the combination the two scenarios; "MC DL Unlimited" and "MC DL Limited" show the influence of ρ on FE clearly. Since SLR of audio or video is set, ζ is found to vary with the primary link quality, i.e., $\zeta = \frac{B_d/SLR}{R_{Pri}} \times 100\%$, where B_d/SLR is the necessary effective transmission rate for FPP. The analysis results are listed in Table 5.2.

The value of FE determines whether the FPP on the secondary link is appropriately implemented or not. Table 5.2 indicates that the FE is inversely proportional to the ρ accordingly to the secondary link quality. For example, when "WiFi DL Static" acts as the primary link, "MC DL" acts as the secondary link, when the ρ of "MC DL Unlimited" is high, the FE is low and vice versa for the "MC DL Limited." FPP FE can be enhanced by increasing ρ or the quality of secondary link. Moreover, if $\rho > 100\%$, which means using high quality link as the protection link, the FE will be quite small, although it is

Table 5.2: *FE* performance for the combination of spatial diversity with audio and video requirements.

Primary Link	Secondary Link	R_{pri} (Mbps)	R_{sec} (Mbps)	ρ (%)	FE_{audio}	FE_{video}
WiFi DL Static	WiFi DL Static	41.46	41.46	100.00	0.03	0.27
	SC DL Static		21.39	51.60	0.05	0.53
	MC DL Unlimited		4.54	10.94	0.25	2.51
	MC DL Limited		0.39	0.95	2.88	28.83
SC DL Static	WiFi DL Static	21.39	41.46	193.81	0.03	0.28
	SC DL Static		21.39	100.00	0.05	0.55
	MC DL Unlimited		4.54	21.20	0.26	2.58
	MC DL Limited		0.39	1.84	2.97	29.66

a waste of network resources. That is the case when "SC DL Static" that is protected by the "WiFi DL Static" is compared to "WiFi DL Static" that is protected by the "WiFi DL Static." Low *SLR* requires high FPP *FE*, e.g., video. As we mentioned in Section 5.6, the data traffic under IEEE 802.11n/ac is traced for WiFi analysis, the performance is much greater than the normal situation by using IEEE 802.11b/g, which is unstable especially in public areas. As the secondary link, the performance of normal WiFi can be considered as similar to the analysis results of "MC DL Unlimited" and "MC DL Limited".

5.7.3 Discussion

In summary, FPP exhibits the right balance of sufficiently high data rate and long-enough delay of re-ordering to proactively recover intolerably delayed data without end-to-end retransmission. FPP with adaptive-rate scheme enhances itself proactively in anticipation of major data losses must be generally coupled with rate adaptation in the transport layer, the ζ can be minimized and the FPP performance maximized (low-latency). The effectiveness of FPP also could be clearly enhanced by improving the effective transmission rate of its implemented link, i.e., secondary link in this research. Another way is that depicting the correlation between buffer overflow times by TCP selective acknowledgement and round-trip time. Moreover, the novel FPP (*FE*) is proposed to explicitly represent the effectiveness of FPP implementation. The value of *FE* directly indicates whether the

FPP is appropriately implemented or not. Also, how to efficiently use the secondary link will be the extension work of this scheme, it will be discussed on the implementation in MPTCP environment.

For low-latency communication, the proposed FPP reduces the fluctuation of retransmission delay when packet loss occurs due to buffer overflow or transmission failures. As a result, the proposed FPP would stabilize the effective transmission rate. Moreover, for high-latency communication, the end-to-end transmitting time of a packet due to retransmission is extremely long because of the hop count increment. In that case, the FPP can significantly increase the end-to-end throughput.

5.8 Summary

The networking scenario in which payload data are delivered over a primary link while protection data are delivered in parallel over a secondary link has been discussed. The protection data is used to mitigate delay of re-ordering of the payload data without the need for lengthy reactive retransmission. Its main design characteristic is the combination of spatially diversity multi-path data delivery with redundant FPP based on random linear codes. Extensive measurements of live carrier-grade LTE networks in the New York city, targeting both SC and MC scenario deployments, and WiFi scenarios in Japan are collected for detailed performance analysis. Results revealed that the most notable reductions in delay of re-ordering are observed in SC networks. It is also shown that the transport layer largely determines the ζ versus delay of re-ordering trade off. The necessity of cross-layer design with transport layer is realized as TCP-caused buffer overflows unnecessarily degrade the achievable latency performance. FPP in combination with buffer overflow prevention, e.g., via delay-based congestion control, is proposed to achieve even order-of-magnitude reductions of delay of re-ordering for low ζ. Also, by the novel FPP *FE*, the effectiveness of FPP implementation can be explicitly represented.

Future works include the following parts: (i) In this research, processing of encoding time is not considered in the FPP due to the slight effect, this will be considered in the follow research to improve the precision of FPP performance; (ii) The FPP will be implemented and verified in MPTCP environment, and the integration between FPP and MPTCP will be discussed for the enhancement of network performance; (iii) The FPP

can be implemented on both primary and secondary links, which can offer substantially increased performance (high throughput, low latency, etc.). It depends on the development of new specifications, e.g., LWA. The design of an intelligent switching mechanism based on the latency constraint or an adaptive data rate interaction algorithm between payload and protection packets is necessary for this direction; and (iv) The evolution of TCP SACK number based on average inter-event time separation is also one of the attractive extension of this research.

Chapter 6

Conclusion

6.1 Discussion and Conclusion

In this dissertation, I developed an high performance dense communication framework base on the technologies of future 5G and beyond. With the D2D communication, multihop fashion, and multi-RAT techniques, three key schemes are proposed to solve the energy-efficient issues; interference management issues, and low-latency issues for future wireless ultra-dense networks (UDNs), respectively. Besides of that, I also proposed new components to support the framework, such as interference-based sensing in spectrum sensing scheme, concurrent transmission, sequential transmission, and mix of them for network capacity optimization in chapter 2. More detail work is recalled briefly as below.

In chapter 3, I designed a dense-aware adaptive transmit power control (DATPC) scheme to maximize end-to-end throughput with minimized the total interference power and reduce the total energy consumption. The core of the DATPC scheme is consensus transmit power control algorithm. It is the first one to supports multiple flow traffics in D2D communication with multihop fashion. This scheme would be implemented into open wireless architecture (OWA) layer for 5G and beyond. Simulation results reveal that under proposed DATPC scheme, only with less than half energy consumption, users could experience on average 2–3 times data rates. Furthermore, based on the proposed DATPC scheme, using proposed mix of concurrent and sequential transmission of spectrum sharing scheme can provides a better average network capacity. The advantage of this scheme is that different with centralized control, this framework is space-division based distributed

control scheme, thus, any devices can use proposed scheme easily.

In chapter 4, to solve the limitation of proposed DATPC scheme in ultra-dense networks, I proposed a dense-aware adaptive carrier sense threshold (DACST) scheme to cooperative with DATPC scheme. The aim of proposed scheme can achieve higher user experienced data rate with dramatic improvements of energy efficiency for UDNs. Same with DATPC scheme, proposed DACST scheme is also implemented into OWA layer and also has relationship with network layer. With the proposed DACST scheme, the cooperation between them can achieve optimized user experienced data rate with acceptable interference level, and also improve the energy-efficient significantly in UDNs. In addition, an advanced Starmesh emulator over the StarBED testbed is used to further verify the performance evaluation of the proposed DATPC and DACST schemes. Due to the real devices (hardware specification) used for the evaluation, DACST scheme cannot work well. However, the proposed DATPC scheme still shows the advantages in simulation results.

In chapter 5, I propose a dense-aware low-latency communication control (DLLCC) scheme to solve the high latency problem that are caused by retransmission. The proposed DLLCC scheme should be implemented into open transport layer based on multipath TPC. In mobile and wireless networks, controlling data delivery latency is one of open problems due to the stochastic nature of wireless channels, which are inherently unreliable. This scheme opens an opportunity to explore how the current best-effort throughput-oriented wireless services could be evolved into latency- sensitive enablers of new mobile applications such as remote three-dimensional (3D) graphical rendering for interactive virtual/augmented-reality overlay. The general system design is based on (i) spatially diverse data delivery over multiple paths with uncorrelated outage likelihoods; and (ii) forward packet-loss protection (FPP), creating encoding redundancy for proactive recovery of intolerably delayed data without end-to-end retransmissions. Analysis and evaluation are based on traces of real life traffic, which is measured in live carrier-grade long term evolution (LTE) networks and campus WiFi networks, due to no such system/environment yet to verify the importance of spatial diversity and encoding redundancy. Analysis and evaluation reveal the seriousness of the latency problem and that the proposed FPP with spatial diversity and encoding redundancy can minimize the delay

of re-ordering. Moreover, a novel FPP effectiveness coefficient is proposed to explicitly represent the effectiveness of FPP implementation.

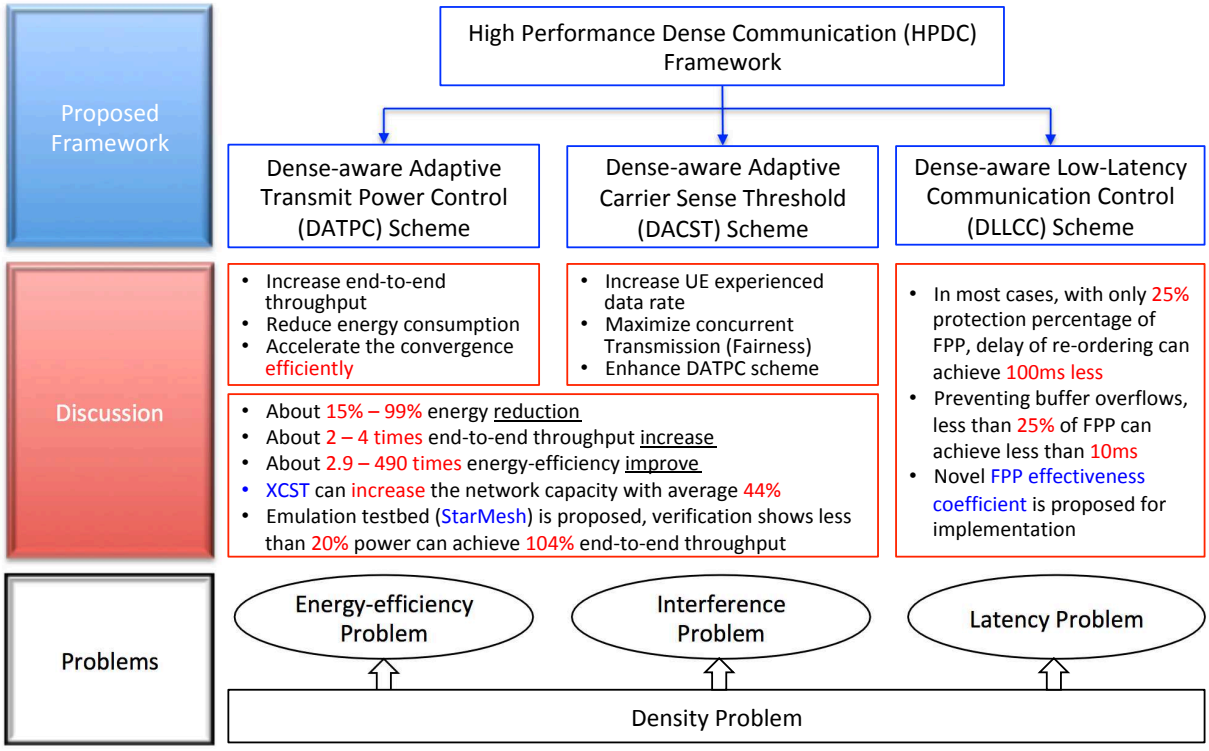

Figure 6-1: Summary of proposed framework to solve the density problems.

More clearly, the summary of proposed framework can be seen in Fig. 6-1.
The main contributions of our work are:

- Identify and revisit the problems of ultra-dense network in near future
- To deal with the dense problem, this dissertation point out three main sub-problems and contribute three different schemes to solve them
  - DATPC scheme operates a distributed manner for WUDNs that takes into account the spatial reuse and reduces the system overhead by sharing information with only adjacent nodes. Moreover, the feasibility and complexity of the DATPC scheme are well-triggered by a novel consensus coefficient.
  - DACST scheme revisits the carrier sense threshold for WUDNs and also enhances a TPC to improve the efficiency and effectiveness of power transmission by maximizing the user experienced data rate for a highly dense indoor environments.

– For DLLCC scheme, to our best knowledge, this is the first practical study on the latency-sensitive services by using real LTE and WiFi data traffic traces. In the medium access, encoding redundancy is used to create novel LTE hybrid automatic repeat request (HARQ) mechanisms. (i) Yet there is no real system/environment to evaluate the multi-path technologies. This research initiated the harbinger by tracing real life traffic to verify the importance of the spatial diversity and the encoding redundancy for low-latency communication; (ii) The severity of the delay by re-ordering is intuitively understood by analyzing real life traffic; (iii) The proposed FPP thoroughly enables encoding redundancy for proactive recovery of intolerably delayed data without end-to-end retransmissions. With the spatial diversity, the FPP on secondary link minimizes the end-to-end retransmission overhead of the primary link. Moreover, FPP shows significant gain when buffer overflows are prevented; and (iv) The novel FPP effectiveness coefficient is proposed to explicitly represent the effectiveness of FPP implementation, which expressed in terms of a combination of spatial diversity and the variation of encoding redundancy with different audio and video requirements.

– The scientific approach, spatial diversity, can be applied to the time-critical of CPS and/or IoT applications.

The contribution of this work can provide in a common portion to the requirements of the future wireless networks, especially to the future wireless ultra-dense networks on 5G or beyond. Our work can be classified into three categories: energy-efficient communications, low interference D2D communications, and high reliability, low latency communications.

6.2 Directions and Future Works

Therefore, a related future topic could be the extension of this work in creating more schemes for future 5G protocol stack. The current work applied only on open wireless architecture layer, lower network layer and open transport layer. Thus, more scheme should be proposed into the future 5G protocol stack to achieve high performance communication

for other specific situations.

For the current hardware specification of user equipment, the interference issue will greatly limited the network performance. This is also another initiative for the future mobile device makers. The best setting for the future wireless ultra-dense networks still need to be test and lead to a common decision or standard.

For more detail of this framework, future works include the following parts:

- For DATPC and DACST scheme in OWA layer:
  - The way to optimize the computation of these two scheme is a new research direction.
  - The most efficient distributed way with minimum overhead to share information with neighbors is also a challenge.
  - The way to trade the interference as useful information instead of unwanted signal is also another new area to improve the proposed high performance communication scheme.
- For DLLCC scheme in OTP layer:
  - Processing of encoding time will be considered in the FPP
  - The design of an intelligent switching mechanism based on the latency constraint or an adaptive data rate interaction algorithm between payload and protection packets is necessary.
- New functionality scheme can be approached into current HPDC framework, e.g., detecting density scheme.

Bibliography

[1] Cisco, "Cisco visual networking index: Global mobile data traffic forecast update, 2016-2021 white paper," in *Tech. Rep*, [Online]. Available: https://www.cisco.com/c /en/us/solutions/collateral/service-provider/visual-networking-index-vni /mobile-white-paper-c11-520862.html, 2017.

[2] ITU-R, *IMT Vision – Framework and overall objectives of the future development of IMT for 2020 and beyond*, 2015.

[3] A. Osseiran, F. Boccardi, V. Braun, K. Kusume, P. Marsch, M. Maternia, O. Queseth, M. Schellmann, H. Schotten, H. Taoka, *et al.*, "Scenarios for 5G mobile and wireless communications: The vision of the METIS project," *IEEE Communications Magazine*, vol. 52, no. 5, pp. 26–35, 2014.

[4] J. Zhao and A. D. Ellis, "A novel optical fast ofdm with reduced channel spacing equal to half of the symbol rate per carrier," in *Optical Fiber Communication (OFC), collocated National Fiber Optic Engineers Conference, 2010 Conference on (OFC/NFOEC)*, IEEE, 2010, pp. 1–3.

[5] F. Schaich and T. Wild, "Waveform contenders for 5G–OFDM vs. FBMC vs. UFMC," in *Communications, Control and Signal Processing (ISCCSP), 2014 6th International Symposium on*, IEEE, 2014, pp. 457–460.

[6] S. Chen, B. Ren, Q. Gao, S. Kang, S. Sun, and K. Niu, "Pattern division multiple access–a novel nonorthogonal multiple access for fifth-generation radio networks," *IEEE Transactions on Vehicular Technology*, vol. 66, no. 4, pp. 3185–3196, 2017.

[7] M. Taherzadeh, H. Nikopour, A. Bayesteh, and H. Baligh, "Scma codebook design," in *2014 IEEE 80th Vehicular Technology Conference (VTC2014-Fall)*, 2014, pp. 1–5.

[8] L. Ping, Q. Guo, and J. Tong, "The ofdm-idma approach to wireless communication systems," *IEEE Wireless Communications*, vol. 14, no. 3, 2007.

[9] J. Choi, "Low density spreading for multicarrier systems," in *Spread Spectrum Techniques and Applications, 2004 IEEE Eighth International Symposium on*, IEEE, 2004, pp. 575–578.

[10] H. Halbauer, S. Saur, J. Koppenborg, and C. Hoek, "3D beamforming: Performance improvement for cellular networks," *Bell Labs Technical Journal*, vol. 18, no. 2, pp. 37–56, 2013.

[11] K. Linehan and R. Chandrasekaran, "Active antennas: The next step in radio and antenna evolution," *Commonscope White Paper*, vol. 10, 2011.

[12] E. G. Larsson, O. Edfors, F. Tufvesson, and T. L. Marzetta, "Massive MIMO for next generation wireless systems," *IEEE Communications Magazine*, vol. 52, no. 2, pp. 186–195, 2014.

[13] S. Venkatesan, A. Lozano, and R. Valenzuela, "Network MIMO: Overcoming intercell interference in indoor wireless systems," in *Signals, Systems and Computers, 2007. ACSSC 2007. Conference Record of the Forty-First Asilomar Conference on*, IEEE, 2007, pp. 83–87.

[14] N. McKeown, "Software-defined networking," *INFOCOM keynote talk*, vol. 17, no. 2, pp. 30–32, 2009.

[15] H. Hawilo, A. Shami, M. Mirahmadi, and R. Asal, "Nfv: State of the art, challenges, and implementation in next generation mobile networks (vEPC)," *IEEE Network*, vol. 28, no. 6, pp. 18–26, 2014.

[16] A. Checko, H. L. Christiansen, Y. Yan, L. Scolari, G. Kardaras, M. S. Berger, and L. Dittmann, "Cloud RAN for mobile networks–A technology overview," *IEEE Communications surveys & tutorials*, vol. 17, no. 1, pp. 405–426, 2015.

[17] Z. Ma, Z. Zhang, Z. Ding, P. Fan, and H. Li, "Key techniques for 5g wireless communications: Network architecture, physical layer, and mac layer perspectives," *Science China Information Sciences*, vol. 58, no. 4, pp. 1–20, 2015.

[18] J. Hoydis, M. Kobayashi, and M. Debbah, "Green small-cell networks," *IEEE Vehicular Technology Magazine*, vol. 6, no. 1, pp. 37–43, 2011.

[19] M. Michalos, S. Kessanidis, and S. Nalmpantis, "Dynamic adaptive streaming over HTTP," *Journal of Engineering Science and Technology Review*, vol. 5, no. 2, pp. 30–34, 2012.

[20] D. Lecompte and F. Gabin, "Evolved multimedia broadcast/multicast service (eMBMS) in LTE-advanced: Overview and Rel-11 enhancements," *IEEE Communications Magazine*, vol. 50, no. 11, 2012.

[21] G. Wu, S. Talwar, K. Johnsson, N. Himayat, and K. D. Johnson, "M2m: From mobile to embedded internet," *IEEE Communications Magazine*, vol. 49, no. 4, 2011.

[22] M. Mukherjee, L. Shu, V. Kumar, P. Kumar, and R. Matam, "Reduced out-of-band radiation-based filter optimization for UFMC systems in 5G," in *Wireless Communications and Mobile Computing Conference (IWCMC), 2015 International*, IEEE, 2015, pp. 1150–1155.

[23] G. Fettweis, M. Krondorf, and S. Bittner, "Gfdm-generalized frequency division multiplexing," in *Vehicular Technology Conference, 2009. VTC Spring 2009. IEEE 69th*, IEEE, 2009, pp. 1–4.

[24] S. M. Yu and S.-L. Kim, "Downlink capacity and base station density in cellular networks," in *Modeling & Optimization in Mobile, Ad Hoc & Wireless Networks (WiOpt), 2013 11th International Symposium on*, IEEE, 2013, pp. 119–124.

[25] S. Stefanatos and A. Alexiou, "Access point density and bandwidth partitioning in ultra dense wireless networks," *IEEE transactions on communications*, vol. 62, no. 9, pp. 3376–3384, 2014.

[26] J. Park, S.-L. Kim, and J. Zander, "Asymptotic behavior of ultra-dense cellular networks and its economic impact," in *Global Communications Conference (GLOBECOM), 2014 IEEE*, IEEE, 2014, pp. 4941–4946.

[27] M. Ding, D. López-Pérez, G. Mao, P. Wang, and Z. Lin, "Will the area spectral efficiency monotonically grow as small cells go dense?" In *Global Communications Conference (GLOBECOM), 2015 IEEE*, IEEE, 2015, pp. 1–7.

[28] J. Liu, M. Sheng, L. Liu, and J. Li, "Network densification in 5g: From the short-range communications perspective," *IEEE Communications Magazine*, vol. 55, no. 12, pp. 96–102, 2017.

[29] B. Lannoo, "Energy consumption of ICT networks," in *TREND Final Workshop*, 2013.

[30] G. Y. Li, Z. Xu, C. Xiong, C. Yang, S. Zhang, Y. Chen, and S. Xu, "Energy-efficient wireless communications: Tutorial, survey, and open issues," *IEEE Wireless Communications*, vol. 18, no. 6, 2011.

[31] T. Chen, H. Kim, and Y. Yang, "Energy efficiency metrics for green wireless communications," in *Wireless Communications and Signal Processing (WCSP), 2010 International Conference on*, IEEE, 2010, pp. 1–6.

[32] S. Tombaz, K. W. Sung, and J. Zander, "Impact of densification on energy efficiency in wireless access networks," in *Globecom Workshops (GC Wkshps), 2012 IEEE*, IEEE, 2012, pp. 57–62.

[33] Y. C. Hu, M. Patel, D. Sabella, N. Sprecher, and V. Young, "Mobile edge computing: A key technology towards 5G," *ETSI White Paper*, vol. 11, 2015.

[34] J. Liu, N. Kato, J. Ma, and N. Kadowaki, "Device-to-device communication in LTE-advanced networks: A survey," *IEEE Communications Surveys & Tutorials*, vol. 17, no. 4, pp. 1923–1940, 2015.

[35] M. N. Tehrani, M. Uysal, and H. Yanikomeroglu, "Device-to-device communication in 5g cellular networks: Challenges, solutions, and future directions," *IEEE Communications Magazine*, vol. 52, no. 5, pp. 86–92, 2014.

[36] S. A. Hamid, H. S. Hassanein, and G. Takahara, *Routing for wireless multi-hop networks*. Springer Science & Business Media, 2013.

[37] W. W. R. Forum, "Multi-RAT Network Architecture," in *Tech. Rep*, [Online]. Available: http://www.wwrf.ch/files/wwrf/content/files/publications/outlook/Outlook9.pdf, 2013.

[38] Y. Kojima, J. Suga, T. Kawasaki, M. Okuda, and R. Takechi, "LTE-WiFi link aggregation at femtocell base station," in *WTC 2014; World Telecommunications Congress 2014; Proceedings of*, VDE, 2014, pp. 1–6.

[39] O. Galinina, A. Pyattaev, S. Andreev, M. Dohler, and Y. Koucheryavy, "5G multi-RAT LTE-WiFi ultra-dense small cells: Performance dynamics, architecture, and trends," *IEEE Journal on Selected Areas in Communications*, vol. 33, no. 6, pp. 1224–1240, 2015.

[40] W. Ni and I. B. Collings, "A new adaptive small-cell architecture," *IEEE Journal on Selected Areas in Communications*, vol. 31, no. 5, pp. 829–839, 2013.

[41] A. Orsino, G. Araniti, A. Molinaro, and A. Iera, "Effective RAT selection approach for 5G dense wireless networks," in *Vehicular Technology Conference (VTC Spring), 2015 IEEE 81st*, IEEE, 2015, pp. 1–5.

[42] J. L. Tomici and P. Chitrapu, "Multi-RAT traffic offloading solutions for the bandwidth crunch problem," in *Systems, Applications and Technology Conference (LISAT), 2011 IEEE Long Island*, IEEE, 2011, pp. 1–6.

[43] O. Galinina, S. Andreev, M. Gerasimenko, Y. Koucheryavy, N. Himayat, S.-P. Yeh, and S. Talwar, "Capturing spatial randomness of heterogeneous cellular/WLAN deployments with dynamic traffic," *IEEE Journal on Selected Areas in Communications*, vol. 32, no. 6, pp. 1083–1099, 2014.

[44] 3GPP TS 23.261, v10.1.0, "Ip flow mobility and seamless wireless local area network (WLAN) offload," in *TSG/WG, 3GPP, Tech. Rep. 23.261*, 2010.

[45] Telecommunication Technology Committee, "TTC Ad Hoc Group on Future Mobile Networking White Paper," in *Tech. Rep*, [Online]. Available: http://www.ttc.or.jp/e/topics/20150413/, 2015.

[46] T. Janevski, "5g mobile phone concept," in *Consumer Communications and Networking Conference, 2009. CCNC 2009. 6th IEEE*, IEEE, 2009, pp. 1–2.

[47] A. Gohil, H. Modi, and S. K. Patel, "5g technology of mobile communication: A survey," in *Intelligent Systems and Signal Processing (ISSP), 2013 International Conference on*, IEEE, 2013, pp. 288–292.

[48] Andrew S. Tanenbaum and David J. Wetherall, *Computer Networks*. PEARSON, 2011.

[49] Douglas E. Comer, *Internetworking With TCP/IP: Principles, protocols and Architecture*. PEARSON, 2014.

[50] W. W. Lu, "An open baseband processing architecture for future mobile terminal design," *IEEE Wireless Communications*, vol. 15, no. 2, 2008.

[51] E. Hossain, D. Niyato, and Z. Han, *Dynamic spectrum access and management in cognitive radio networks*. Cambridge university press, 2009.

[52] Qualcomm, "New 3GPP effort on NR in unlicensed spectrum expands 5G to new areas cite," Tech. Rep., May, 2017.

[53] Qualcomm, "Shared spectrum for 5G new radio," Tech. Rep., Feb., 2017.

[54] S. Max, E. Weiss, G. R. Hiertz, and B. Walke, "Capacity bounds of deployment concepts for wireless mesh networks," *Performance Evaluation*, vol. 66, no. 3, pp. 272–286, 2009.

[55] ITU-R, "Propagation data and prediction methods for the planning of indoor radiocommunication systems and radio local area networks in the frequency range 300 mhz to 100 ghz," in *Recommendation ITU-R P.1238-9*, [Online]. Available: https://www.itu.int/rec/R-REC-P.1238-9-201706-I/en, 2017.

[56] *OUTLOOK: Visions and research directions for the wireless world*. WWRF(World Wide Radio Forum), July, 2009.

[57] M. Kubisch, H. Karl, A. Wolisz, L. Zhong, and J. Rabaey, "Distributed algorithms for transmission power control in wireless sensor networks," in *Wireless Commun. and Networking, (WCNC 2003)*, IEEE, vol. 1, 2003, pp. 558–563.

[58] N. Li, J. Hou, and L. Sha, "Design and analysis of an MST-based topology control algorithm," *Wireless Commun., IEEE Transactions on*, vol. 4, no. 3, pp. 1195–1206, 2005.

[59] H.-H. Choi and J.-R. Lee, "Distributed transmit power control for maximizing end-to-end throughput in wireless multi-hop networks," *Wireless personal communications*, vol. 74, no. 3, pp. 1033–1044, 2014.

[60] V. Shrivastava, D. Agrawal, A. Mishra, S. Banerjee, and T. Nadeem, "Understanding the limitations of transmit power control for indoor wlans," in *Proc. of the 7th ACM SIGCOMM Conf. on Internet Measurement*, ser. IMC '07, San Diego, California, USA, 2007, pp. 351–364.

[61] Cozybit, *Wmediumd*, 2011.

[62] T. Miyachi, K. Chinen, and Y. Shinoda, "StarBED and SpringOS: Large-scale general purpose network testbed and supporting software," in *Proc. of the 1st int. conf. on Performance evaluation methodolgies and tools*, ACM, 2006, p. 30.

[63] J. Nakata, S. Uda, T. Miyachi, K. Masui, R. Beuran, Y. Tan, K. Chinen, and Y. Shinoda, "StarBED2: Large-scale, realistic and real-time testbed for ubiquitous networks," in *Testbeds and Research Infrastructure for the Develop. of Networks and Communities, (TridentCom 2007)*, IEEE, 2007, pp. 1–7.

[64] R. Beuran, L. T. Nguyen, K. T. Latt, J. Nakata, and Y. Shinoda, "Qomet: A versatile wlan emulator," in *Advanced Information Networking and Applications, 2007. AINA'07. 21st International Conference on*, IEEE, 2007, pp. 348–353.

[65] M. Kodialam and T. Nandagopal, "Characterizing the capacity region in multi-radio multi-channel wireless mesh networks," in *Proceedings of the 11th annual international conference on Mobile computing and networking*, ACM, 2005, pp. 73–87.

[66] G. Miao, N. Himayat, G. Y. Li, and S. Talwar, "Distributed interference-aware energy-efficient power optimization," *IEEE Transactions on Wireless Communications*, vol. 10, no. 4, pp. 1323–1333, 2011.

[67] H. C. Le, H. Guyennet, and V. Felea, "OBMAC: An overhearing based MAC protocol for wireless sensor networks," in *Sensor Technologies and Applicat., (SensorComm 2007)*, IEEE, 2007, pp. 547–553.

[68] T. S. Kim, H. Lim, and J. C. Hou, "Understanding and improving the spatial reuse in multihop wireless networks," *Mobile Computing, IEEE Transactions on*, vol. 7, no. 10, pp. 1200–1212, 2008.

[69] R. S. Karlsson, "Radio resource sharing and capacity of some multiple access methods in hierarchical cell structures," in *Vehicular Technology Conference, 1999. VTC 1999-Fall. IEEE VTS 50th*, IEEE, vol. 5, 1999, pp. 2825–2829.

[70] M Fan, M Yavuz, S Nanda, Y Tokgoz, and F Meshkati, "Interference management in femto cell deployment," in *3GPP2 femto workshop*, 2007.

[71] K. Han, Y. Choi, D. Kim, M. Na, S. Choi, and K. Han, "Optimization of femtocell network configuration under interference constraints," in *Modeling and Optimization in Mobile, Ad Hoc, and Wireless Networks, 2009. WiOPT 2009. 7th International Symposium on*, IEEE, 2009, pp. 1–7.

[72] T. Zahir, K. Arshad, Y. Ko, and K. Moessner, "A downlink power control scheme for interference avoidance in femtocells," in *Wireless Communications and Mobile Computing Conference (IWCMC), 2011 7th International*, IEEE, 2011, pp. 1222–1226.

[73] X. Li, L. Qian, and D. Kataria, "Downlink power control in co-channel macrocell femtocell overlay," in *Information Sciences and Systems, 2009. CISS 2009. 43rd Annual Conference on*, IEEE, 2009, pp. 383–388.

[74] J. Yoon, J. Lee, and H. S. Lee, "Multi-hop based network synchronization scheme for femtocell systems," in *Personal, Indoor and Mobile Radio Communications, 2009 IEEE 20th International Symposium on*, IEEE, 2009, pp. 1–5.

[75] J. G. Andrews, "Interference cancellation for cellular systems: A contemporary overview," *IEEE Wireless Communications*, vol. 12, no. 2, pp. 19–29, 2005.

[76] L. G. Trichard, J. S. Evans, and I. B. Collings, "Large system analysis of linear parallel interference cancellation," in *Communications, 2001. ICC 2001. IEEE International Conference on*, IEEE, vol. 1, 2001, pp. 26–30.

[77] F. van der Wijk, G. M. Janssen, and R. Prasad, "Groupwise successive interference cancellation in a ds/cdma system," in *Personal, Indoor and Mobile Radio Communications, 1995. PIMRC'95. Wireless: Merging onto the Information Superhighway., Sixth IEEE International Symposium on*, IEEE, vol. 2, 1995, pp. 742–746.

[78] A. Duel-Hallen, J. Holtzman, and Z. Zvonar, "Multiuser detection for cdma systems," *IEEE Personal Communications*, vol. 2, no. 2, pp. 46–58, 1995.

[79] M. Honig, U. Madhow, and S. Verdu, "Blind adaptive multiuser detection," *IEEE Transactions on Information Theory*, vol. 41, no. 4, pp. 944–960, 1995.

[80] M. Kodialam and T. Nandagopal, "Characterizing the capacity region in multi-radio multi-channel wireless mesh networks," in *Proc. of the 11th Annual Int. Conf. on Mobile Computing and Networking*, ser. MobiCom '05, Cologne, Germany, 2005, pp. 73–87.

[81] X. Guo, S. Roy, and W. Conner, "Spatial reuse in wireless ad-hoc networks," in *Vehicular Technology Conf., (VTC 2003-Fall)*, IEEE, vol. 3, 2003, pp. 1437–1442.

[82] R. Baldemair, T. Irnich, K. Balachandran, E. Dahlman, G. Mildh, Y. Selén, S. Parkvall, M. Meyer, and A. Osseiran, "Ultra-dense networks in millimeter-wave frequencies," *IEEE Communications Magazine*, vol. 53, no. 1, pp. 202–208, 2015.

[83] R. Beuran, L. T. Nguyen, T. Miyachi, J. Nakata, K. Chinen, Y. Tan, and Y. Shinoda, "QOMB: A wireless network emulation testbed," in *Global Telecommun. Conf., (GLOBECOM 2009)*, IEEE, 2009, pp. 1–6.

[84] 3GPP Work Item Description, "Si: Study on latency reduction techniques for LTE," in *3GPP TSG RAN Meeting #67, RP-150465, Tech. Rep*, [Online]. Available: http://www.3gpp.org/DynaReport/TDocExMtg–RP-67–31196.htm, 2015.

[85] GSMA, "The mobile economy 2015," in *Tech. Rep*, [Online]. Available: http://www.gsmamobileeconomy.com/GSMA-Global-Mobile -Economy-report-2015.pdf, 2015.

[86] N. Nikaein, R. Knopp, A. M. Cipriano, S. Krco, I. Tomic, P. Svoboda, M. Laner, E. Larsson, Y Wu, M. G. Fuertes, *et al.*, "Low-latency in wireless communication," in *In Proc. of Vitel*, Slovenia, 2011, pp. 93–99.

[87] G. P. Fettweis, "The tactile internet: Applications and challenges," *IEEE Veh. Technol. Mag.*, vol. 9, no. 1, pp. 64–70, 2014.

[88] 3GPP, "Collaboration on LTE-WLAN intergration," in *Tech. Rep*, [Online]. Available: http://www.3gpp.org/news-events/3gpp-news/1771-wlan_lte, 2016.

[89] D. Szabo, A. Gulyas, F. H. Fitzek, and D. E. Lucani, "Towards the tactile internet: Decreasing communication latency with network coding and software defined networking," in *In Proc. of IEEE European Wireless Conf.*, Budapest, Hungary, 2015, pp. 1–6.

[90] M. Weiner, M. Jorgovanovic, A. Sahai, and B. Nikolie, "Design of a low-latency, high-reliability wireless communication system for control applications," in *In Proc. of IEEE Int. Conf. on Commun. (ICC)*, Sydney, Australia, 2014, pp. 3829–3835.

[91] Ericsson, "LTE latency improvement gains," in *Tech. Rep*, [Online]. Available: http://www.ericsson.com/research-blog/lte/lte-latency-improvement-gains, 2014.

[92] D. Vukobratovic, C. Khirallah, V. Stankovic, and J. S. Thompson, "Random network coding for multimedia delivery services in LTE/LTE-Advanced," *IEEE Trans. Multimedia*, vol. 16, no. 1, pp. 277–282, 2014.

[93] Z. Lv, K. Xu, and Y. Xu, "A practical HARQ scheme with network coding for LTE-A broadcasting system," in *In Proc. of IEEE Conf. on Wireless Commun. and Signal Process. (WCSP)*, Huangshan, China, 2012, pp. 1–6.

[94] H. Hamdoun, P. Loskot, and T. O'Farrell, "Implementation trade-offs of fountain codes in LTE and LTE-A," in *In Proc. of IEEE Conf. on Commun. and Netw. (CHINACOM)*, Kunming, China, 2012, pp. 419–424.

[95] R. Mahajan, J. Padhye, S. Agarwal, and B. Zill, "High performance vehicular connectivity with opportunistic erasure coding," in *In Proc. of Conf. on USENIX Annu. Tech. Conf. (ATC)*, Bostn, USA, 2012, pp. 237–248.

[96] Y. Cui, L. Wang, X. Wang, H. Wang, and Y. Wang, "Fmtcp: A fountain code-based multipath transmission control protocol," *IEEE/ACM Trans. Netw.*, vol. 23, no. 2, pp. 465–478, 2015.

[97] C. Paasch, "Improving multipath TCP," PhD thesis, UC Louvain, 2014.

[98] C. Gustafson and F. Tufvesson, "Characterization of 60 GHz shadowing by human bodies and simple phantoms," in *In Proc. of IEEE Europ. Conf. on Antennas and Propagation (EUCAP)*, Prague, Czech Republic, 2012, pp. 473–477.

[99] 4G Americas, "5G spectrum recommendations," in *Tech. Rep*, [Online]. Available: http://www.4gamericas.org/en/resources/white-papers, 2015.

[100] A. G. Saavedra, M. Karzand, and D. J. Leith, *Low delay random linear coding and scheduling over multiple interfaces*, [Online]. Available: http://arxiv.org/abs/1507.08499, 2015.

[101] L. Hartung and M. Milind, "Policy driven multi-band spectrum aggregation for ultra-broadband wireless networks," in *In Proc. of IEEE Dynamic Spectrum Access Networks (DySPAN)*, Stockhold, Sweden, 2015, pp. 82–93.

[102] A. Ford, C. Raiciu, M. J. Handley, O. Bonaventure, and C. Paasch, "RFC 6824: TCP extensions for multipath operation with multiple addresses," in *IETF*, [Online]. Available: https://tools.ietf.org/html/draft-ietf-mptcp-rfc6824bis-05, 2016.

[103] P. Eardley, "Survey of MPTCP implementations," in *IETF*, [Online]. Available: https://datatracker.ietf.org/doc/html/draft-eardley-mptcp-implementations -survey-02.

[104] S. Katti, H. Rahul, W. Hu, D. Katabi, M. Médard, and J. Crowcroft, "XORs in the air: Practical wireless network coding," *IEEE/ACM Trans. Netw.*, vol. 16, no. 3, pp. 497–510, 2008.

[105] M. Karzand, D. J. Leith, J. Cloud, and M. Medard, *Low delay random linear coding over a stream*, [Online]. Available: http://arxiv.org/abs/1509.00167, 2015.

Publications

Journal

[1] Y. Yu, S. Kucera, Y. Lim, and Y. Tan, "Low-Latency Communication in LTE and WiFi using Spatial Diversity and Encoding Redundancy," *IEICE Transactions on Communications*, 2018. (To be published)

[2] Y. Yu, Y. Lim, and Y. Tan, "Study of Carrier Sense Threshold and Transmit Power Control for Distributed Wireless Ultra-dense Networks," *IEICE Transactions on Fundamentals of Electronics, Communications and Computer Sciences*, 2018. (Under review)

International Conference

[3] Y. Yu, S. Shah, Y. Tan, and Y. Lim, "End-to-end throughput evaluation of consensus TPC algorithm in multihop wireless networks," *IEEE International Wireless Communications and Mobile Computing Conference (IWCMC)*, Dubrovnik, Croatia, pp. 941-946, Aug. 2015

[4] S. Kucera, Y. Yu, M. Buddhikot, and Y. Lim, "Low-Latency Communications in LTE Using Spatial Diversity and Encoding Redundancy," *IEEE 84th Vehicular Technology Conference (VTC)*, Montreal, Canada, Sep. 2016

Domestic Conference

[5] Y. Yu, Y. Lim, and Y. Tan, "Study of Carrier Sense Threshold and Transmit Power Control for Distributed Wireless Ultra-Dense Networks," *IEICE ASN Conference*, Fukuoka, Japan, IEICE Tech. Rep., vol. 117, no. 426, pp. 85-90, Jan. 2018

[6] Y. Yu, S. Shah, Y. Tan, and Y. Lim, "A study on Consensus Transmit Power Control Algorithm to Maximizing End-to-End Throughput in Dense Multihop Wireless Networks," *IEICE ASN Conference*, Tokyo, Japan, IEICE Tech. Rep., vol. 114, no. 480, pp. 153-157, Mar. 2015

[7] S. Shah, Y. Yu, Y. Tan, and Y. Lim, "Best-Response Distributed Sub-channel Selection for Minimizing Interference in Cooperative and Non-cooperative Small Cell Networks," *IEICE ASN Conference*, Tokyo, Japan, IEICE Tech. Rep., vol. 114, no. 480, pp. 159-164, Mar. 2015

[8] R. Y. Kang, Y. Yu, Y. Tan, and A. O. Lim, "Emulation Study of Transmit Power Control Algorithm in Multihop Wireless Network," *IEICE Society Conference*, Kyoto, Mar. 2015

[9] Y. Yu, R. Y. Kang, Y. Tan, and A. O. Lim, "Consensus Transmit Power Control Algorithm for Maximizing End-to-end Throughput in Multihop Wireless Networks," *IEICE ASN Conference*, Tokyo, Japan, IEICE Tech. Rep., vol. 114, no. 290, pp. 7-12, Nov. 2014

[10] A. O. Lim, Y. Yu, and R. Y. Kang, "A Study of Approximation Method for Capacity Regions of Multihop Wireless Networks," *IEICE ASN Conference*, Tokyo, Japan, IEICE Tech. Rep., vol. 114, no. 290, pp. 13-17, Nov. 2014

[11] Y. Yu, R. Beuran, Y. Tan, and A. O. Lim, "A comparison study on ORBIT and QOMET," *IEICE Society Conference*, Fukuoka, Japan, 17-20 September, 2013